

The Journal of Refractory Innovations

# bulletin

2022

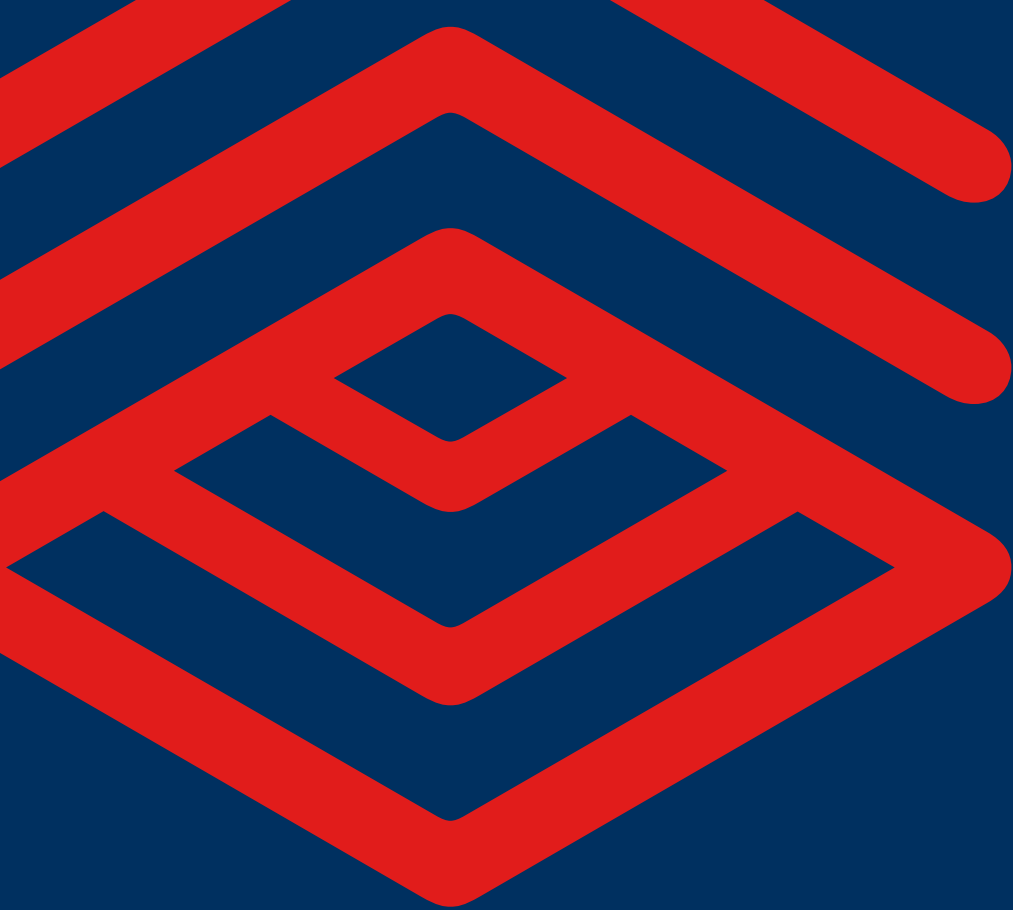
21 Refractory Waste to  
Slag Engineering Solution

29 New INTERSTOP Sealed Tundish  
Gate for Billet and Bloom Casting

47 RHI Magnesita as a Technology  
Partner and Solution Provider



RHI MAGNESITA



## Bulletin

The Journal of Refractory Innovations

2022

**Published by**  
**Chief Editor**  
**Executive Editors**

RHI Magnesita GmbH, Vienna, Austria  
Thomas Prietl

Thomas Drnek, Christoph Eglsäer, Mateus Vargas Garzon, Thomas Mathew, Felipe Nonaka,  
Ravikumar Periyasamy, Heinz Telser, Karl-Michael Zettl

**Raw Materials Expert**  
**Proofreader**  
**Project Manager**  
**Design and Typesetting**

David Wappel  
Clare McFarlane  
Michaela Hall  
Universal Druckerei GmbH, Leoben, Austria

**Contact**

Michaela Hall  
RHI Magnesita GmbH, Technology Center  
Magnesitstrasse 2  
8700 Leoben, Austria

**E-mail**

[bulletin@rhimaginesita.com](mailto:bulletin@rhimaginesita.com)

**Phone**

+43 50213 5300

**Website**

[rhimaginesita.com](http://rhimaginesita.com)

**LinkedIn**

<https://www.linkedin.com/company/rhi-magnesita>

The products, processes, technologies, or tradenames in the Bulletin may be the subject of intellectual property rights held by RHI Magnesita N.V., its affiliates, or other companies.

The texts, photographs and graphic design contained in this publication are protected by copyright. Unless indicated otherwise, the related rights of use, especially the rights of reproduction, dissemination, provision and editing, are held exclusively by RHI Magnesita N.V. Usage of this publication shall only be permitted for personal information purposes. Any type of use going beyond that, especially reproduction, editing, other usage or commercial use is subject to explicit prior written approval by RHI Magnesita N.V.

**Cover picture:** The cover illustration shows ignition of the new 122-metre tunnel kiln at the Urmitz plant in Germany. This is the first time in decades that a tunnel kiln is operating at the Urmitz plant and it will primarily be used to fire refractory bricks for various furnaces and units that are essential for the steel, glass, cement, lime, energy and chemical industries. Now ignited, the tunnel kiln will run continuously for several decades and its performance will increase the plant's capacity by approximately 25000 tonnes per year. The new tunnel kiln significantly expands the plant's nonbasic refractory product range and the design will increase the plant's energy efficiency.

# RHI Magnesita Worldwide news

## Worldwide

### CO<sub>2</sub> Transparency for All RHI Magnesita Products

With the clear commitment to take responsibility for a sustainable future, RHI Magnesita is proud as the number one company within our industry to make the CO<sub>2</sub> footprints of our around 200000 products transparent and comparable by disclosing them in our technical data sheets. All “cradle-to-gate” greenhouse gases, from raw material extraction to production and packaging, are considered in these CO<sub>2</sub> footprint calculations that are externally certified according to ISO standards. The product carbon footprint includes all scope 1 and scope 2 emissions, as well as part of the scope 3 emissions. The scope 1 emissions are direct emissions from our plants, while the scope 2 emissions are indirect emissions from the electricity we use (in a high number of plants we already have 100% green electricity or are using electricity with a very low CO<sub>2</sub> footprint). The largest share of the scope 3 emissions (all other indirect emissions) is coming from the external purchased raw materials. For these raw materials a detailed analysis was carried out. However, as only limited data was available from our suppliers, most of the values were calculated based on published results. In addition, upstream transportation and upstream fuel emissions have been included. The data will be reevaluated and recalculated on a regular basis and a short video about the topic can be accessed via [https://www.youtube.com/watch?v=u\\_NzZOU1IBE&t=4s](https://www.youtube.com/watch?v=u_NzZOU1IBE&t=4s)

## Europe

### RHI Magnesita and Horn & Co. Group Have Joined Forces to Create a Leading Recycling Platform

On May 2, 2022, RHI Magnesita and the Horn & Co. Group combined their recycling activities in Europe to increase the production, use, and supply of secondary raw materials for the European refractory industry, targeting a substantial reduction of CO<sub>2</sub> emissions. Since November 15, 2022, the newly created joint venture has been operating as MIRECO.

This partnership positions the company at the forefront of the circular economy for customers in the steel, cement, glass, and other process industries. As a result, RHI Magnesita’s ambitious plans to globally increase the recycling rate in its products from less than 3% in 2020 to more than 10% in 2025 will probably have already been achieved in 2022, marking an important step towards a targeted 15% reduction in CO<sub>2</sub> emissions by 2025.

A key feature of MIRECO is the strategic location of its main plants in and around Siegen in North Rhine-Westphalia (Germany) and Mitterdorf in Styria (Austria). Combined, these sites are ideally placed to serve customers throughout Europe.

Both partners have worked together for many years, with RHI Magnesita purchasing the majority of its secondary raw materials from Horn & Co. Group. As a result, a close and trustful relationship has evolved over time, forming an ideal basis for a joint and sustainable future. By acquiring 51% of the joint venture shares, RHI Magnesita can play a major role in developing new opportunities in the circular economy field.

---

**Worldwide**

## Successful Flow Control Webinar on Robotic Operations

RHI Magnesita invited key global steel industry customers to participate in a webinar on the topic of “Safe flow control operations through robotic automation”. The benefits for the participants included learning about safety concerns, challenges, and solutions in flow control applications as well as how to achieve maximal safety by enabling an operation without personnel needing to be in the concerned area of the continuous casting platform. The webinar offered the combination of a presentation and live demonstrations of INTERSTOP robotic mockups that are designed as an automated solution for slide gates to connect hydraulic cylinders, sensors, and/or process gases and robotic automation to secure a stable process for monotube exchange and continuous mould powder addition. After the presentation and live demonstrations by RHI Magnesita’s automation experts, the webinar was concluded with a very lively Q&A session. The webinar was received very positively by our customers and underlined the solutions RHI Magnesita Flow Control offers to remove operators from hazardous environments, thus providing safety and ensuring process stability. Customers are invited to visit the mockup installations at INTERSTOP in Switzerland or to request a webinar for their individual steel plant.

---

**Scandinavia**

## Let’s Talk About Sustainability

The European steel industry is entering a new era regarding environmental targets and so is RHI Magnesita as a refractory supplier, with sustainability on all levels having become a truly powerful force. As sustainability requires transparency, this was the core principle that guided the RHI Magnesita team at the Sustainability Meeting in Stockholm, in mid-May 2022, together with our Scandinavian customers.

In the meeting RHI Magnesita’s carbon emissions, reporting, and long-term strategy and measures to reduce them were discussed. Furthermore, there was a transparent exchange about secondary raw materials used in refractories. Several case studies on the successful implementation of refractory concepts containing CO<sub>2</sub>-neutral circular raw materials were presented and discussed. At the centre of our dialogue was RHI Magnesita’s latest sustainability initiative, namely being the first refractory supplier worldwide to make the product carbon footprint of all products fully transparent to

customers by showing the CO<sub>2</sub> values (cradle-to-gate) directly on each technical data sheet. With this information, a new type of case study was prepared. The CO<sub>2</sub> transparency of RHI Magnesita products was incorporated in a detailed analysis of different ladle refractory concepts by putting all relevant variables into context: The full carbon footprint (both indirect and direct), refractory performance, and total costs (both indirect and direct); with all the numbers aggregated over a 1-year period of ladle operation. Relating these key factors to each other brings not only transparency on the environmental impact but also enables a multi-dimensional assessment of refractory concepts and technical alternatives, and finally offers our customers an informed choice for more sustainable decisions.

RHI Magnesita is fully committed to embark on the sustainability journey together with our customers, in a transparent, customised, and local manner. Please contact us for more information ([johannes.wucher@rhimaginesita.com](mailto:johannes.wucher@rhimaginesita.com)), we would be very happy to hear from you and learn with you.

---

**Europe, North and South America**

## Digital Lining Evaluation Using 3D Scanning

The Lining Evaluation Scan (LES) was developed by RHI Magnesita to quickly determine the remaining thickness of the lining in cement rotary kilns by means of a 3D laser scanner. The measurement provides area-wide, precise information about the condition of the lining and replaces time-consuming and incomplete conventional methods. Together with the digital documentation, virtual kiln inspections can be carried out at any time from all over the world. LES enables RHI Magnesita’s customers to take fast and fact-based decisions and contributes to improving the kiln performance.

Within the last year, RHI Magnesita has invested in scanning equipment, people, and a digital platform to further extend the service in Europe, as well as North and South America. As the feedback from users of this service was outstanding, RHI Magnesita will continue investing in the scaleup so more customers around the world can be offered this service. By doing so, RHI Magnesita will be able to develop further digital products based on 3D scanning for other applications and industries and continue to accompany customers on the exciting journey to a digital future and smart industry. Further information is available at <https://www.rhimaginesita.com/industries-we-serve/cement/lining-evaluation-scan>

## Austria

### Opening of RHI Magnesita's Flow Control Training Center

In June, RHI Magnesita officially opened its state-of-the-art flow control training facilities in Leoben (Austria). Located in the same building as the Cement and Lime Training Center, the full-scale ladle and tundish models equipped with an INTERSTOP SX2 ladle gate, STG13 tundish gate, MNC-ASP nozzle changer, and SOC-H purging plug solution provide a hands-on opportunity for customers to get a deep insight into flow control technologies, refractories, and maintenance. Furthermore, there is also the opportunity to gain extensive practical knowledge about isostatically pressed products, including how to operate the INTERSTOP stopper rod and monotube changer systems. In their speeches at the opening ceremony, both CTO Luis Bittencourt and CSO Gustavo Franco emphasised the importance of the training center and its possibilities to familiarise customers with the optimal use of RHI Magnesita's refractory products.

Over the last 10 years, RHI Magnesita has developed a wide range of practical courses for customers and employees, which also include tundish training at the purpose-built facility in Veitsch (Austria) and lining trainings.

## South Africa

### INTERSTOP Ladle Slide Gate Trial at Scaw Metals

In March 2022, RHI Magnesita conducted a ladle slide gate trial at Scaw Metals (South Africa) with the aim of demonstrating improved slide gate refractory performance compared to the existing slide gate system in use. Safety and system reliability is of paramount importance to the customer and every stage of the trial planning and execution was carried out in close cooperation with the Scaw Metals' technical team. The trial was conducted using an INTERSTOP S2 ladle slide gate system and refractories from RHI Magnesita's production plants in Europe and India. RHI Magnesita provided complete trial supervision with an INTERSTOP ladle slide gate expert onsite to ensure a safe and successful trial. The results of the trial that spanned 1 ladle campaign showed that the minimum required refractory plate life of 4 heats could be safely achieved and a record performance of 7 heats was also reached for one of the plate sets. For future trials and development, the INTERSTOP SX-2 ladle slide gate will be employed, which will provide additional safety and refractory performance.

## Bahrain

### New Close Casting Record at SULB Bahrain with the INTERSTOP 13 QC

On June 10, 2022, a new record was achieved at SULB Bahrain, resulting from the continual developments and close cooperation with RHI Magnesita. A total continuous casting time of 35.05 hours over 48 ladle heats was achieved while producing 6231.9 tonnes of heavy section beam blank 2 with one submerged entry shroud (SES). Zirconia middle plates (ZETTRAL 95I T3) were used with the redesigned 4-port SES (DELTEK A721 and DELTEK Z904) in the INTERSTOP 13 QC tundish slide gate system. Based on the results and technical analysis of the used refractories, the potential exists to reach 50 heats. Considering the broad variety of steel products produced by the customer, including silicon-killed steel, aluminum-silicon-killed steel with calcium treatment, and high strength low-alloy steel (HSLA), the refractory components need to show high performance consistently under a variety of operating conditions. Such a reliable refractory performance provides the customer with confidence and flexibility.

## Egypt

### Record Close Casting Refractory Performance at Egyptian Steel IIC

In April 2022, a record total casting time of 37.5 hours, with a sequence length of 50 heats, was achieved at Egyptian Steel IIC Beni Suef after optimising the submerged entry shroud (SES) design in the INTERSTOP 33QC tundish slide gate system. Previously, a stable performance of 24 hours casting time had been reached using the standard concept of DELTEK D99 and DELTEK Z100. To achieve the new SES target life, a high-performing, wear-resistant material concept was required. Therefore, it was decided to switch to the new high-purity and high-zirconia DELTEK Z968 grade and to change the SES body material from DELTEK D99 to the highly wear-resistant DELTEK D99N.

---

**Austria**

## RHI Magnesita Opens the Dolomite Hub in Hochfilzen

After a construction period of only 2 years and an investment of more than €46 million, RHI Magnesita has transformed the traditional Hochfilzen plant (Austria) into the Dolomite Resource Center Europe, a leading innovation location of the European refractory industry. It includes an environmentally friendly conveyor tunnel, sustainable rail transport, and a new rotary kiln.

The new dolomite hub increases plant efficiency and at the same time contributes significantly to environmental protection. Moreover, the vertical integration of RHI Magnesita has been strengthened. "With the new Dolomite Resource Center we have achieved one thing above all: Independence. This will enable all our European plants to produce with 100% Hochfilzen dolomite and not have to resort to purchasing external raw materials. This is a big plus for us, but above all for the environment and our customers," said CEO Stefan Borgas.

---

**Worldwide**

## Parmod Sagar Elected President of the World Refractories Association

Parmod Sagar, President of RHI Magnesita India, West Asia and Africa, was appointed to represent the World Refractories Association (WRA) as its president and started on March 16, 2022. During the WRA Board Meeting, organised in parallel with UNITECR 2022 in Chicago (USA), board members unanimously agreed to give the reins of the association to Parmod Sagar for 30 months. He succeeds Carol Jackson, CEO and Chairman of HarbisonWalker International, who was elected as WRA president in January 2020. "I will be happy to support the WRA's efforts to the best of my abilities and I look forward to working hand-in-hand with all of you for a greener, safer, and flourishing refractory industry," Parmod said, looking forward to his time of presidency.

---

**Europe**

## Funding Approval for EU Refractory Recycling Project

RHI Magnesita is leading an EU Horizon Project for the first time. The 4-year project is called ReSoURCE and started in June 2022. The project has a total budget of €8.5 million for the consortium of 8 internationally renowned partners from research and industry, of which the ReSoURCE consortium is receiving a total funding of €6 million from the European Commission. The approval was a huge success and confirmation of RHI Magnesita's long-term commitment to refractory recycling. After the grant agreement was signed, the project started with a kick-off meeting and workshop that all members attended at RHI Magnesita's Technology Center Leoben (Austria).

ReSoURCE, short for "Refractory Sorting Using Revolutionising Classification Equipment", will innovate the full process chain of refractory recycling with an artificial intelligence supported multi-sensor sorting equipment as its core technology. Combining laser-induced breakdown spectroscopy (LIBS) and hyperspectral imaging (HSI) with optimised preprocessing and automated ejection, it will lay the foundation for a new state-of-the-art sorting of used refractory material with particle sizes down to less than 1 mm. The continuous monitoring of the economic and ecological benefits via techno-economic and life cycle assessment will ensure the green and digital transformation of the refractory recycling value chain. For more information please use the links below:

Website: <https://www.project-resource.eu/>

Twitter: <https://twitter.com/2022ReSoURCE>

LinkedIn: <https://www.linkedin.com/company/project-resource/>

---

**India**

## RHI Magnesita Strengthens Global Innovation and Opens the R&D Centre in India

At the inauguration of the new R&D facility, where the management board also participated, CEO Stefan Borgas said, “India is a strategic growth market for us. With the R&D and manufacturing hub, we are investing in expanding our capacity and capability to develop our operations for the greater region of India, the Middle East, and Africa.”

RHI Magnesita has established a phased investment plan of €42 million to increase the production capacity and automation of its existing plants in Bhiwadi (Rajasthan), Vizag (Andhra Pradesh), and Cuttack (Odisha). “We have recently scaled up the capacity of our Vizag plant by almost 30% with an investment of €6 million. We are further working on starting production of certain high-end products in the Bhiwadi facility that are currently imported,” added Stefan.

Highlighting the importance of the new R&D facility, Parmod Sagar, Managing Director and CEO of RHI Magnesita India, said, “The centre will help us to better serve local market needs and to react faster to customer requirements. This is a world-class facility that will work closely with our global R&D network for local raw material development, will provide solutions support for customer performance improvement projects, and support local manufacturing in the 3 Indian plants.”

---

**India**

## JSW Steel Dolvi Works Commissioned India’s largest BOF with RHI Magnesita’s Refractories

In 2021–2022, JSW Steel Dolvi Works commissioned its steel melting shop (SMS-II), which is part of the new integrated steel plant. With a capacity of 5 million tonnes of steel per annum, the new plant is the largest brownfield expansion in India, with a second line comprising Kanbara reactor hot metal processing, a 350-tonne basic oxygen furnace (BOF), ladle furnace, RH degasser, and twin slab caster. As the refractory project partner, RHI Magnesita’s India sales and technical team executed the job on the basis of an ongoing full line service contract for the Kanbara reactor hot metal ladle, BOF, steel ladle, and CS100 slide gate refractories, including ladle shrouds. Full refractory sets were supplied for the BOF and steel ladle and the CS100 ladle slide gate mechanism and refractory commissioning was on a 350-tonne steel ladle.

---

**Austria**

## Digital Flagship Plant Radenthein

RHI Magnesita is investing around €50 million in the modernisation, automation, and all-encompassing digitisation of its plant in Radenthein (Austria). In addition, €24.7 million are being invested in establishing new infrastructure. Besides a wireless LAN system, which connects all the machines, new robotic units and brick presses are being installed. The strategic decision in favour of Austria for this expansion and digitisation initiative means the steel, energy, chemical, nonferrous, and glass industries in Europe will continue to be reliably supplied with products from RHI Magnesita in the future.

Completing the new tunnel kiln at the Radenthein plant was another stage in the process of establishing the most modern production facility in the refractory industry. The tunnel kiln is characterised by its long service life, as it will remain in operation at 1800 °C for around 30 years before the first maintenance is required. It also contributes to a significant increase in the plant’s energy efficiency by using the excess heat from the tunnel kiln for internal processes such as drying the refractory products after impregnation. Furthermore, the employees are supported by a Manufacturing Execution System (MES), which is an intelligent and self-learning control system that is connected to all areas of the plant, communicates with them, and is controlled via a central control room. The MES is the first of its kind in the industry, and this pilot project will be rolled out to other plants worldwide in the coming years.



# A letter from our editor



It is a real pleasure to introduce the 2022 RHI Magnesita Bulletin particularly as my involvement in the publication extends over 20 years, starting with co-authoring papers and more recently taking over as the Chief Editor. During this time, I have seen how important the journal is for informing our valued readers about how RHI Magnesita is living an innovation culture to create customer value as well as presenting the new refractory products and heat management solutions that are continually under development, always with the focus on putting our clients' requirements at the centre of all our activities.

Sustainability is a key priority at RHI Magnesita and this is reflected in being the industry leader regarding the use of secondary raw materials. The long-term commitment to developing a circular economy is reflected in multiple initiatives to secure high-quality used material sources, including the recent joint venture that was set up with Horn & Co. Group (see page 3), recycling experts since 1922. We are also actively engaged in establishing the necessary technologies so that spent refractories can be effectively reapplied in new products, thereby avoiding any detrimental impact on product performance that is historically linked to the use of secondary raw materials in refractories. This is exemplified in the first two papers of this edition describing innovative aluminium carbide detection and treatment technologies to increase magnesia-carbon recycling and the favourable performance of high recycling containing magnesia-carbon bricks installed in the ladle slag zone. To save landfilling costs while simultaneously creating a positive environmental impact, RHI Magnesita also develops tailored solutions for customers to recycle refractory waste in their processes. One such case is described in the third article where multiple benefits in terms of process efficiency were achieved as the consequence of a collaboration to reuse spent MgO-containing fines as a slag forming agent in EAF steelmaking.

In response to future trends such as clean steel production and long casting sequences, INTERSTOP has developed the new Sealed Tundish Gate (STG) series and the STG 13, which is suitable for both billet and bloom applications, is presented in the next paper. This is followed by articles focusing on well filler sand and reliable ladle opening as well as how numerical simulation was used to optimise tundish refractory design, with the beneficial outcome of reducing heat losses and improving energy efficiency in the steel plant.

As a result of changing requirements from the different industries we serve, RHI Magnesita is establishing new and digital technologies that support customers "beyond refractories". In the next two papers, numerous advances are presented that are being successfully implemented worldwide, ranging from various state-of-the-art sensors to the next level of digital refractory contracts.

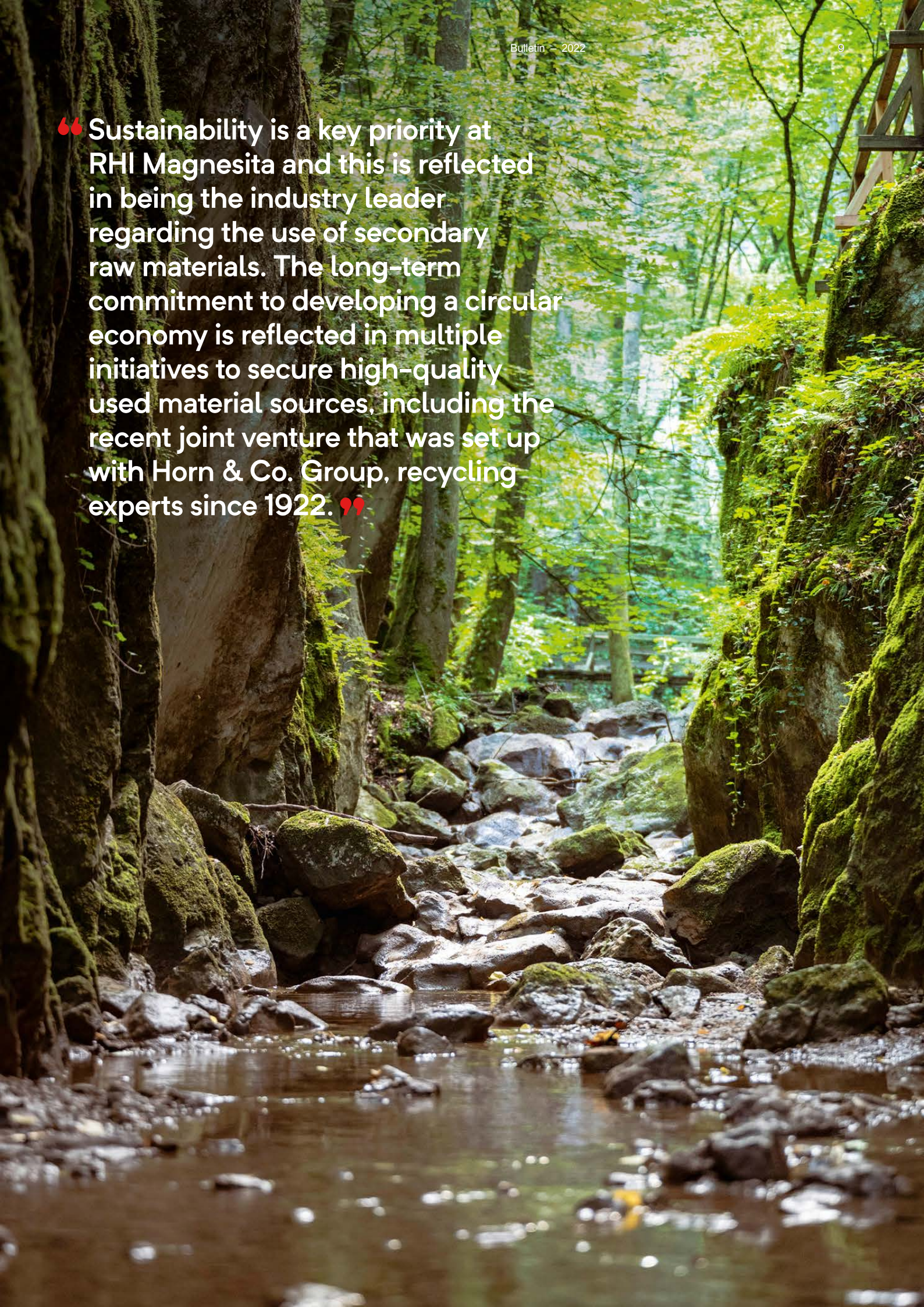
Our final article introduces the X-ray computed tomography device recently installed at RHI Magnesita's Technology Center Leoben (Austria). Offering the possibility to look inside a sample in 3D, investigations performed on flow control products are presented such as postmortem studies of a submerged entry nozzle and slide gate plate as well as how it was used to expedite complex product development.

In closing, I would like to take this opportunity to wholeheartedly thank all the authors and editorial team for their hard work and dedication to create an edition that shows how RHI Magnesita is committed to leading the refractory industry in sustainability topics and developing customer-centric technologies.

Yours sincerely

**Thomas Prietl**

Head R&D Europe, CIS and Turkey  
RHI Magnesita

A photograph of a forest stream flowing over mossy rocks. The water is clear and reflects the surrounding greenery. The rocks are covered in vibrant green moss, and the forest floor is densely packed with trees and foliage. The scene is peaceful and natural.

“ Sustainability is a key priority at RHI Magnesita and this is reflected in being the industry leader regarding the use of secondary raw materials. The long-term commitment to developing a circular economy is reflected in multiple initiatives to secure high-quality used material sources, including the recent joint venture that was set up with Horn & Co. Group, recycling experts since 1922. ”

# Contents



**21**

**Refractory Waste to Slag Engineering Solution**



**29**

**New INTERSTOP Sealed Tundish Gate for Billet and Bloom Casting**



**47**

**RHI Magnesita as a Technology Partner and Solution Provider**

- 11 Innovative Aluminium Carbide Detection and Treatment Technologies** to Increase Magnesia-Carbon Recycling
- 17 Successful Implementation** of a High Recycling Containing Magnesia-Carbon Brick in Steel Ladles
- 21 Refractory Waste to Slag Engineering Solution**—Metallurgical Consulting Supports Steel Plant's Circular Economy Strategy
- 29 New INTERSTOP Sealed Tundish Gate** for Billet and Bloom Casting
- 34 Ladle Well Filler Sands** for All Needs
- 41 Numerical Simulation as a Tool to Improve Energy Efficiency** During Operation of a Continuous Casting Tundish
- 47 RHI Magnesita as a Technology Partner and Solution Provider** for our Industrial Customers—We Thrive on Complexity
- 52 Next Level of Digital Refractory Contracts**
- 60 Material Characterisation and Product Analysis of Refractories** Using X-Ray Computed Tomography and Radioscopy

## Subscriptions Service and Contributions



We encourage you, our customers and interested readers, to relay our comments, feedback, and suggestions to improve the publication quality.

Email

[bulletin@rhimagnesita.com](mailto:bulletin@rhimagnesita.com)

Phone

**+43 50213 5300**

Stefan Heid, Alexander Leitner and Sandra Königshofer

# Innovative Aluminium Carbide Detection and Treatment Technologies to Increase Magnesia–Carbon Recycling

RHI Magnesita is dedicated to developing a more circular economy and one aspect of this initiative is increasing the recycling rate of secondary raw materials. However, because of the extreme conditions refractory products are often exposed to during use, certain components can undergo modification (e.g., chemical reactions) that complicate recycling and can result in the raw materials' intrinsic value decreasing. One example is magnesia-carbon (MgO-C) bricks, where antioxidants such as aluminium powder are added to enhance product performance. However, during application the formation of aluminium carbide ( $\text{Al}_4\text{C}_3$ ) makes recycling spent MgO-C problematic because, although only present in minor amounts, this carbide can cause severe brick cracking during heat treatment in the brick production process. This article reviews state-of-the-art processing of spent MgO-C bricks, provides insights into a novel treatment process developed by RHI Magnesita for effective  $\text{Al}_4\text{C}_3$  destruction, and highlights the importance of simultaneously developing custom-made testing techniques to achieve the company's sustainability targets.

## Introduction

Evaluating the carbon footprint of refractory products reveals high specific  $\text{CO}_2$  emissions, especially for MgO-C products that are widely used in steel applications. This is because high quantities of energy-intensive primary raw materials (e.g., dead burned magnesia and fused magnesia) as well as significant amounts of graphite are used for the production. Considering RHI Magnesita's strong commitment to establish sustainable products, the logical consequence is to massively increase the recycling share, as technologies for the environmentally friendly production of the required raw materials are currently not available.

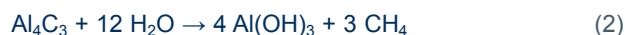
Although spent MgO-C bricks have been recycled for many decades, there is a subset of this brick type that is not straightforward to reuse, namely MgO-C bricks containing aluminium powder. With the strong focus on increasing recycling rates, it has been important to investigate strategies that enable a reliable use of this valuable secondary raw material. This article presents new technologies developed by RHI Magnesita to detect and degrade the  $\text{Al}_4\text{C}_3$  that forms during application, while ensuring the valuable raw materials are not downgraded during the treatment process.

## Formation and Hydration of $\text{Al}_4\text{C}_3$

Fine aluminium powder is incorporated into MgO-C brick formulations to increase performance by decreasing oxidation of the carbon components during application and to increase the hot modulus of rupture. At temperatures above  $700\text{ }^\circ\text{C}$  the aluminium reacts with carbon forming various phases including  $\text{Al}_4\text{C}_3$  (equation 1), which improves the brick's resistance to erosion and slag infiltration.



However, while  $\text{Al}_4\text{C}_3$  is highly refractory and beneficial during use, it drastically limits recycling of the used MgO-C because of its high hydration tendency at ambient temperatures, which is linked to a tremendous volume expansion (i.e.,  $> 100\%$ ) and methane production (equation 2) [1].



For example, if  $\text{Al}_4\text{C}_3$ -containing material is used in subsequent brick production, even extremely low amounts (i.e.,  $< 0.5\text{ wt.}\%$   $\text{Al}_4\text{C}_3$ ) can lead to critical crack formation during the tempering process (Figure 1). Therefore, it is essential to destroy any  $\text{Al}_4\text{C}_3$  in the reclaimed MgO-C bricks to stabilise this secondary raw material so it can be reliably recycled.

**Figure 1.** Tempered MgO-C bricks produced with  $\text{Al}_4\text{C}_3$ -containing secondary raw materials.



### Destruction of $\text{Al}_4\text{C}_3$ in Spent MgO-C Bricks

Although over the years various approaches have been developed to enable reuse of  $\text{Al}_4\text{C}_3$ -containing material, they are based on empirical procedures that are lengthy, uncontrolled, or energy intensive. For example, well-known options to destroy  $\text{Al}_4\text{C}_3$  are firing at high temperatures under oxidising conditions [2], long-term storage, and processes involving exposure to water or steam [3,4].

In the first case, material is crushed and fired at temperatures above 900 °C to decompose the aluminium-containing compounds, including  $\text{Al}_4\text{C}_3$  (equation 3). However, other carbon sources in the reclaimed material are also oxidised (equation 4), resulting in the loss of graphite, a valuable resource that is listed as a critical raw material [5].



The complete conversion of any carbon-containing compounds to  $\text{CO}_2$  requires a highly oxidising atmosphere in the furnace to avoid the formation of other gases (e.g.,  $\text{C}_x\text{H}_y$ ,  $\text{CO}$ , and  $\text{NO}_x$ ) in the waste stream. Furthermore, in addition to producing  $\text{CO}_2$ , the firing process generates high levels of fines and dust as well as a secondary magnesia raw material contaminated mainly with  $\text{Al}_2\text{O}_3$ ,  $\text{SiO}_2$ ,  $\text{Fe}_2\text{O}_3$ , and  $\text{CaO}$ . Although this material can be reused in MgO-C brick production, the energy-intensive firing process has the disadvantages of generating  $\text{CO}_2$  and high quantities of fines, as well as the loss of valuable carbon carriers.

Another approach to destroy  $\text{Al}_4\text{C}_3$  is storage of spent refractory material under ambient conditions, where the hydration reaction can be accelerated by regular water sprinkling. However, this process takes weeks or months and is uncontrolled because the reaction is strongly influenced by many factors such as temperature, humidity, grain size, porosity, and surface adhesions. In addition, gaseous by-products of the hydration reactions, for example ammonia, hydrogen, and methane, are directly released into the atmosphere. Considering greenhouse emissions, particularly the latter is detrimental as its contribution to global warming is 21-times higher than  $\text{CO}_2$ . Furthermore, the formation of brucite ( $\text{Mg}(\text{OH})_2$ ) and the associated destruction of coarse magnesia grains can happen, which reduces the quality and value of the material. In processes using supersaturated steam, although the reaction rate is significantly increased due to the high temperatures, similar detrimental aspects apply as described for the storage approach.

To circumvent the drawbacks of the described processes, a new technology was required to efficiently destroy the  $\text{Al}_4\text{C}_3$ , while conserving the integrity of the valuable secondary raw materials (e.g., fused magnesia, dead burned magnesia, and graphite) in spent MgO-C bricks. However, to optimise this process, it was necessary to develop equipment that could accurately measure the  $\text{Al}_4\text{C}_3$  content.

### Quantification of the $\text{Al}_4\text{C}_3$ Content in Spent MgO-C Bricks

Currently, accurate quantification of the  $\text{Al}_4\text{C}_3$  content is not possible using commercially available testing methods and there are only rudimentary options for refractories to determine whether the material has been effectively stabilised. One approach is to use a sample of the treated material for small-scale brick production and assess the bricks for cracks after tempering. However, as this type of test is time consuming, it cannot be performed at high frequency.

Another method described in the literature involves determining the carbon content of the refractory sample by combustion [6]. As the weight ratio of carbon contained in  $\text{Al}_4\text{C}_3$  is  $\frac{1}{4}$ , the  $\text{Al}_4\text{C}_3$  content can be calculated by multiplying the difference between the total carbon and free carbon by a factor of 4. However, in addition to the formation of  $\text{Al}_4\text{C}_3$  other carbon-containing phases, such as  $\text{Al}_4\text{O}_4\text{C}$ ,  $\text{Al}_{28}\text{O}_{21}\text{C}_6\text{N}_6$ ,  $\text{SiC}$ , and  $\text{Al}_4\text{SiC}_4$ , can also form in the MgO-C brick during use. As a result, the value determined by carbon combustion only indicates an upper limit, which is far from the required precision. Furthermore, due to the indirect calculation, any error is also multiplied by a factor of 4, which does not enable low levels of  $\text{Al}_4\text{C}_3$  to be determined with high accuracy. To evaluate treatment success, high accuracy is crucial, therefore this method would not be applicable.

Theoretically, X-ray diffraction measurements can detect low levels of  $\text{Al}_4\text{C}_3$ ; however, the accuracy of standard techniques is insufficient for the purpose of quality control and evaluation of treatment success [7].

From the analysis of interfacial carbides in Al(Si)/diamond composites it is known that  $\text{Al}_4\text{C}_3$  quantification can be performed by gas chromatography mass spectrometry measurements of gaseous species, in this case the methane released when  $\text{Al}_4\text{C}_3$  reacts with an aqueous NaOH solution [8]. However, since the measurement and interpretation of the results are complex, this approach is not straightforward and robust enough for a plant environment.

In summary, although there are different approaches to detect  $\text{Al}_4\text{C}_3$ , none of the options fulfil the necessary requirements of a practical and accurate testing device suitable for a plant installation. Therefore, a practical, robust, and easy to handle testing method for the quantification of  $\text{Al}_4\text{C}_3$  content was required to optimise the treatment process and rollout for quality control in the plants.

## New Solution for $\text{Al}_4\text{C}_3$ Determination and Destruction

After extensive research activities, RHI Magnesita has developed a novel custom-made plant solution for  $\text{Al}_4\text{C}_3$  detection and an efficient treatment process that ensures a source of high-quality secondary raw material. As the  $\text{Al}_4\text{C}_3$  measurement device laid the foundation to work on a new treatment process, the challenge was not only to engineer a selective analysis method but also to achieve the high precision required, with a detection limit as low as 0.01 wt.%, that can be operated efficiently in a plant environment.

### Measurement device

The measurement device is based on detecting the  $\text{CH}_4$  formed when  $\text{Al}_4\text{C}_3$  reacts with  $\text{H}_2\text{O}$  (equation 2). Although two  $\text{CH}_4$ -forming carbides exist, it is very unlikely beryllium carbide will be present in any MgO-C related refractory application, so evidence of  $\text{CH}_4$  formation from spent MgO-C bricks, identified for example by thermogravimetric analysis combined with mass spectroscopy of the gaseous emissions, can be used to determine the  $\text{Al}_4\text{C}_3$  content. This is achieved by measuring the weight/charge ratio of the ionised gas molecules while the sample is heated. As the sample must be mixed with  $\text{H}_2\text{O}$  for  $\text{Al}_4\text{C}_3$  hydration to occur,

$\text{H}_2\text{O}$  also contributes to the measured ionisation current of the respective atom mass units (AMU) in the mass spectroscopy data. The expected intensities of  $\text{CH}_4$  and  $\text{H}_2\text{O}$  based on gas fragmentation patterns are given in Table I and show that instead of using the major AMU 16 peak for  $\text{CH}_4$ , AMU 15 is a more appropriate indicator of the presence of  $\text{Al}_4\text{C}_3$ , due to the high intensity levels without the risk of severe peak misinterpretation (Figure 2).

While it was proven that there is a strong correlation between the integral of the curve and the amount of  $\text{Al}_4\text{C}_3$  present, the experimental setup is costly and not suitable to be established in standard plant quality laboratories for quantitative  $\text{Al}_4\text{C}_3$  measurements; therefore, further development steps were performed.

Due to the inhomogeneous distribution of  $\text{Al}_4\text{C}_3$  within the spent MgO-C material, it was found that a larger sample size increased the accuracy and repeatability of the testing method. By targeted digestion of 10 g samples under nonambient conditions, an innovative testing method was established by RHI Magnesita in 2021, where the  $\text{Al}_4\text{C}_3$  content can be precisely determined using an infrared sensor for  $\text{CH}_4$  detection, resulting in the measurement being completed in < 1 hour and requiring only 15 minutes of manual labour. The system is particularly well suited and

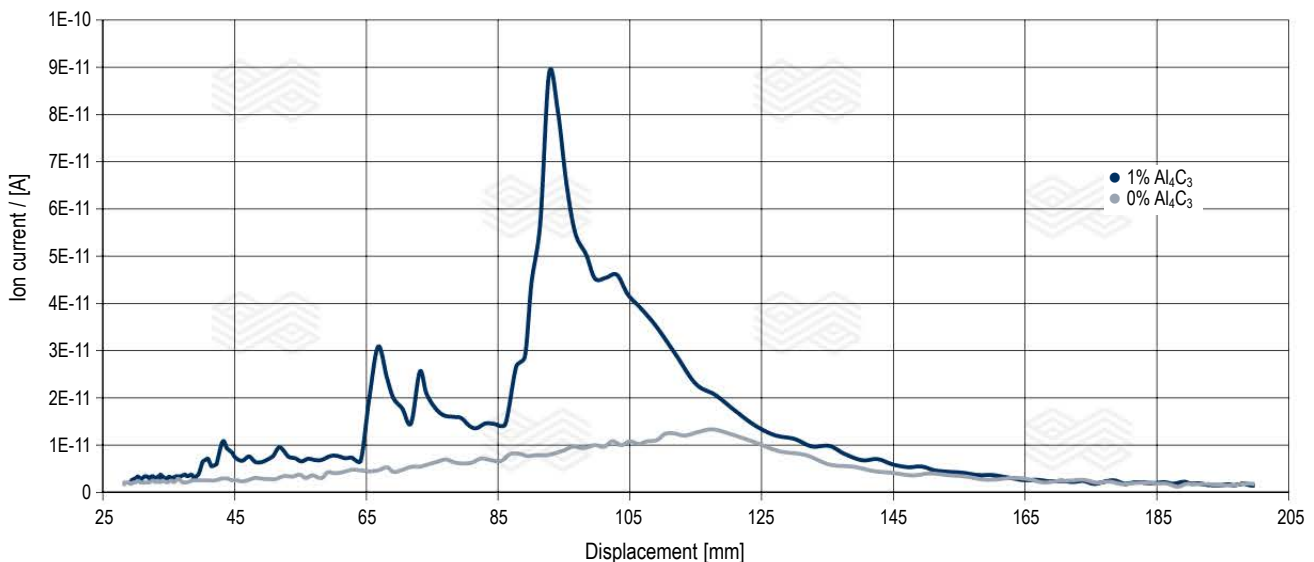
**Table I.**

Expected intensities of  $\text{CH}_4$  and  $\text{H}_2\text{O}$  for the respective AMU.

| AMU | Contribution from $\text{CH}_4$ | Intensity from $\text{CH}_4$ | Contribution from $\text{H}_2\text{O}$ | Intensity from $\text{H}_2\text{O}$ |
|-----|---------------------------------|------------------------------|--|-------------------------------------|
| 12  | $\text{C}_{12}^+$               | +                            | -                                      |                                     |
| 13  | $[\text{C}_{12}\text{H}]^+$     | +                            | -                                      |                                     |
| 14  | $[\text{C}_{12}\text{H}_2]^+$   | +                            | -                                      |                                     |
| 15  | $[\text{C}_{12}\text{H}_3]^+$   | ++++                         | -                                      |                                     |
| 16  | $[\text{C}_{12}\text{H}_4]^+$   | +++++                        | O+                                     | ++                                  |
| 17  | $[\text{C}_{13}\text{H}_4]^+$   | +                            | $[\text{HO}]^+$                        | +++                                 |
| 18  | -                               | -                            | $[\text{H}_2\text{O}]^+$               | +++++                               |

**Figure 2.**

Ion current comparison of the 15 AMU signal for an  $\text{Al}_4\text{C}_3$ -containing sample and an  $\text{Al}_4\text{C}_3$ -free sample.



accurate for  $\text{Al}_4\text{C}_3$  detection in the range of 0.01–0.50 wt.%. Validation tests with reference samples have shown a detection limit of 100 ppm  $\text{Al}_4\text{C}_3$  and a standard deviation of only +/- 0.02%.

With the new detection device it has been possible to specify limits for recycling brick production using defined amounts of  $\text{Al}_4\text{C}_3$  powder in the production lots. As cracks on the brick surface cannot be analysed quantitatively, ultrasonic measurements were used to investigate inhomogeneities or microcracks within the brick. In this case a Pundit PL-200 measurement device with an area scan, namely 8 x 4 measuring points, was used. Figure 3 shows a MgO-C brick containing 0.1–0.2 wt.%  $\text{Al}_4\text{C}_3$  with cracks visible on the surface and the corresponding ultrasonic image. For comparison, Figure 4 illustrates a MgO-C brick with < 0.1 wt.%  $\text{Al}_4\text{C}_3$  where although there were no visible surface cracks, the reduced sound velocity indicates some inhomogeneities in the brick. The visualisation and identification of microcracks or layers depends on their direction compared to the ultrasonic wave. Combined with the new  $\text{Al}_4\text{C}_3$  analysis method, specification values have been validated and will be considered in future quality inspections in the plants to optimise secondary raw material sourcing, processing, and use.

### Novel treatment process for $\text{Al}_4\text{C}_3$ destruction

When  $\text{Al}_4\text{C}_3$  is identified in sourced spent refractories, an industrial process is required to stabilise the material and make it suitable for reuse in production. Therefore, a new process was developed that guarantees efficient destruction of  $\text{Al}_4\text{C}_3$  by hydration under controlled conditions, which can be performed in an acceptable time frame without causing damage to the valuable secondary raw materials. This approach sets new standards for the recycling of antioxidant-containing MgO-C bricks in terms of sustainable recovery and streamlined logistics. Whereas previously several days or even weeks were required for such processes, the novel treatment reduces the residence time to below 12 hours, making the material almost immediately available after sourcing. In addition, emitted reaction products, especially methane, are captured and converted into emissions of less environmental concern, thereby reinforcing the commitment to truly sustainable technologies.

To optimise this process, a standardised material was required to determine  $\text{Al}_4\text{C}_3$  destruction rates at varying process conditions (e.g., time, temperature, and grain size). For this purpose, “synthetic” bricks were prepared from a standard MgO-C recipe containing 3 wt.% aluminium powder and subsequently coked at 1000 °C for 6 hours, thereby

**Figure 3.**

(a) MgO-C brick containing 0.1–0.2 wt.%  $\text{Al}_4\text{C}_3$  with cracks visible on the surface and (b) ultrasonic measurement of the brick. Measured sound velocity in the range of < 1200 m/s (red) to > 1800 m/s (dark blue).



(a)



(b)

Legend for Figure 3(b):  
 < 1200 ms<sup>-1</sup> (red), 1200–1300 ms<sup>-1</sup> (orange), 1300–1400 ms<sup>-1</sup> (yellow), 1400–1500 ms<sup>-1</sup> (light green), 1500–1600 ms<sup>-1</sup> (green), 1600–1700 ms<sup>-1</sup> (dark green), 1700–1800 ms<sup>-1</sup> (blue), > 1800 ms<sup>-1</sup> (dark blue)

**Figure 4.**

(a) MgO-C brick containing < 0.1 wt.%  $\text{Al}_4\text{C}_3$  with no cracks visible on the surface and (b) ultrasonic measurement of the brick. Measured sound velocity in the range of < 1200 m/s (red) to > 1800 m/s (dark blue).



(a)



(b)

Legend for Figure 4(b):  
 < 1200 ms<sup>-1</sup> (red), 1200–1300 ms<sup>-1</sup> (orange), 1300–1400 ms<sup>-1</sup> (yellow), 1400–1500 ms<sup>-1</sup> (light green), 1500–1600 ms<sup>-1</sup> (green), 1600–1700 ms<sup>-1</sup> (dark green), 1700–1800 ms<sup>-1</sup> (blue), > 1800 ms<sup>-1</sup> (dark blue)

promoting high levels of  $\text{Al}_4\text{C}_3$  formation. This led to an average  $\text{Al}_4\text{C}_3$  content of  $> 1$  wt.%, thereby representing a worst-case scenario compared to the real situation observed in reclaimed material, which has an inhomogeneous distribution of  $\text{Al}_4\text{C}_3$  located towards the hot face, resulting in lower but still critical levels in the spent MgO-C material (Figure 5).

To plan the full process cycle, including spent material treatment and brick production, it had to be considered that real secondary raw material would have a slightly different behaviour to the “synthetic” bricks, due to this inhomogeneous distribution in spent MgO-C materials. However, a reference material was essential to evaluate the process conditions and the resulting treatment success. The targeted hydration of  $\text{Al}_4\text{C}_3$  in a rapid time frame is challenging as the operating conditions for such processes

are within the  $\text{Mg}(\text{OH})_2$  formation field. This means the atmosphere has to be adapted to guarantee  $\text{Mg}(\text{OH})_2$  formation is either suppressed or slowed down significantly, otherwise the fused or sintered magnesia grains can be damaged. In the developed closed process, this requirement was successfully achieved for more than 12 hours, which is sufficient to destroy the  $\text{Al}_4\text{C}_3$ . Optimising the material pretreatment (e.g., preheating and crushing) and the process parameters enabled the treatment time to be further reduced below 8 hours, making a treatment cycle feasible during one regular shift.

Besides determining the complete destruction of  $\text{Al}_4\text{C}_3$ , an interesting observation during the controlled hydration treatment trials was that depending on the  $\text{Al}_4\text{C}_3$  content three different disintegration levels could be distinguished (Figure 6):

**Figure 5.**

$\text{Al}_4\text{C}_3$  distribution in “synthetic” and spent MgO-C bricks.

### Synthetic material $\neq$ spent refractory material

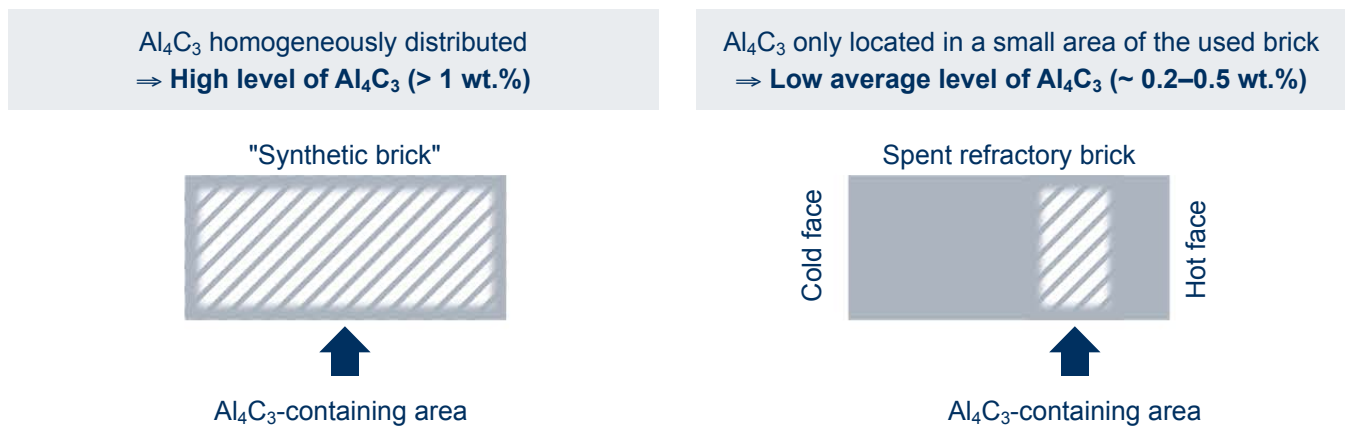


**Figure 6.**

Controlled hydration treatment of MgO-C bricks containing various amounts of  $\text{Al}_4\text{C}_3$ . (a) fully disintegrated, (b) severe cracking, and (c) minimal damage.



(a)



(b)



(c)

- A high  $\text{Al}_4\text{C}_3$  content fully disintegrates the material during the treatment process due to the high-volume expansion. Investigations of secondary raw materials (~ 30 different samples) from China, South America, and Europe showed such high levels are seldom observed and that this will not be the typical case.
- A medium  $\text{Al}_4\text{C}_3$  content leads to massive cracks, but not full disintegration of the input materials during the treatment process.
- A low amount of  $\text{Al}_4\text{C}_3$  leads to less visible damage of the input sample.

If this effect can be used to further optimise the material treatment will be further analysed after the production process has been implemented.

Starting with laboratory equipment, the proof of principle was confirmed and paved the way to procuring a 25-times bigger custom-made pilot installation, which is fully automatable and equipped with different sensors to live-track the emissions and process conditions. Besides destroying  $\text{Al}_4\text{C}_3$ , the new process is also cutting-edge in terms of emission handling. Before unloading, the vessel will be purged and any methane formed during the process will be post-combusted, thereby reducing the  $\text{CO}_2$ -equivalent emissions by 85%. Ammonia, formed by aluminium nitride hydration, will be recovered by a spray scrubber system, enabling reintroduction of the wastewater in other internal processes. Altogether, a carbon footprint of 55 kg  $\text{CO}_2$  is estimated to treat a tonne of material using the new process, which is considerably lower than the 3000 kg of  $\text{CO}_2$  emitted per tonne of primary raw materials used for MgO-C brick production.

## Conclusion

Sustainability is embedded in RHI Magnesita's business and as the global refractory leader decreasing the carbon footprint of our products and building circularity is pivotal. One area of focus is recycling and innovative technologies are being introduced to achieve the ambitious 2025 corporate targets. This article describes the recent developments that will facilitate the use of a MgO-C derived secondary raw material source that has been problematic to effectively exploit in the past. With the newly established capability of precise  $\text{Al}_4\text{C}_3$  measurement in combination with an efficient, controlled, and ecological friendly stabilisation method, the extensive use of spent MgO-C material will not only be profitable but also ensure high-quality standards are maintained to shape a far more sustainable recycling route for unfired magnesia-based refractories in the future.

## References

- [1] Schmeißer, J. *Untersuchungen zum  $\text{Al}_4\text{C}_3$ -Zerfall in Magnesita-Kohlenstoff-Recyclingmaterialien*, Ingenieursarbeit, Bergakademie Freiberg, Germany, 1991.
- [2] Fonseca de Lima, D., Lutkenhaus, M.G., Figueredo Junior, A. and Coelho Novais, C. Recycling of MgO-C Scrap from BOF with High Al Content. Proceedings of 12<sup>th</sup> Biennial Worldwide Conference on Refractories (UNITECR 2011), Kyoto, Japan, October 30–November 2, 2011, 256–259.
- [3] Tanaka, M., Yamamoto, K. and Yoshitomi, J. Recycling Technology of Carbon Containing Refractories. *Journal of the Technical Association of Refractories, Japan*. 2012, 32, 298–302.
- [4] Strawbridge, I. Recycling of Refractory Material. European Patent EP0857703B1, 1998.
- [5] "Critical Raw Materials Resilience: Charting a Path Towards Greater Security and Sustainability". Communication From the Commission to the European Parliament, the Council, the European Economic and Social Committee and the Committee of the Regions. COM(2020) 474 final.
- [6] Watanabe, S., Fujiyoshi, R. and Torigoe, A. Effects of Additives on the Hydration Resistance of MgO-C Bricks. *Journal of the Technical Association of Refractories, Japan*. 2019, 39, 91–95.
- [7] Nandy, S.K., Ghosh, N.K., Gosh, D. and Das, G.C. Hydration of Coked MgO-C-Al Refractories. *Ceramics International*. 2006, 32, 163–172.
- [8] Edtmaier, C., Segl, J., Rosenberg, E., Liedl, G., Pospichal, R. and Steiger-Thirnsfeld, A. Microstructural Characterization and Quantitative Analysis of the Interfacial Carbides in Al(Si)/Diamond Composites. *Journal of Materials Science*. 2018, 53, 15514–15529.

## Authors

Stefan Heid, RHI Magnesita, Leoben, Austria.

Alexander Leitner, RHI Magnesita, Leoben, Austria.

Sandra Königshofer, RHI Magnesita, Leoben, Austria.

**Corresponding author:** Stefan Heid, stefan.heid@rhimagnesita.com



Hartwig Kunanz, Birger Nonnen, Julia Kirowitz and Miriam Schnalzger

# Successful Implementation of a High Recycling Containing Magnesia–Carbon Brick in Steel Ladles

The progressive reduction of CO<sub>2</sub> emissions has become a fundamental target for the industrial sector, including refractory suppliers, whereby the term circular economy is drawing increasing attention. A circular economy is aiming at a zero-waste life cycle of products and hence the preservation of natural resources. Translated into the field of magnesia-carbon brick production, this implies the extensive reuse of refractory materials that have already been in operation. In this regard, the major challenge faced by product development is to design a magnesia-carbon brick with adequate chemical and physical properties mainly consisting of secondary raw materials. Furthermore, it is of crucial importance that demanded performance levels in high wear areas of steel vessels are not adversely influenced by the increased share of recycling material. For RHI Magnesita, establishing a circular economy for refractory products demands a deep understanding of product properties, the use of existing technologies in production plants, and initiation of efficient as well as economic sourcing of secondary raw materials. This article presents RHI Magnesita's approach for developing and advancing a concept of circular economy based on the successful implementation of a magnesia-carbon brick, which consists primarily of secondary raw materials. This newly developed brick is called ANCARBON C TB277-EU, contains 87 wt.% recycling material based on magnesia, and has already been successfully implemented in the slag zone of ladles at a German steel plant.

## Introduction

The term circular economy is frequently used in discussions about sustainability, whereby it is mostly understood as a resource-saving approach for raw materials. The concept is based on the idea of closing material loops by reusing spent material in the production of new goods. Hence, circular economy focuses on obtaining higher resource efficiency, which consequently increases the security of raw material supply. Additional benefits of a circular economy are the reduction of landfilling and substitution of native raw materials, with both having a positive impact on environmental issues and cost reduction.

However, the complexity of a circular economy concept becomes evident with its implementation, starting already during the process of material sourcing. The quality of secondary raw materials is often uncertain but determinant for the quality of the end product. Therefore, precise investigation of chemical and physical properties is required, especially since certain performance levels must be achieved. Taking the large selection of available secondary material sources and suppliers into account, transforms the sourcing procedure into a personnel-intensive and time-consuming process.

Another major challenge lies in the development of an efficient supply chain management, which includes additional legal aspects concerning waste transportation over borders and waste treatments that must be considered.

## Implementing a High Recycling Containing MgO-C Brick in the Ladle Slag Zone

The introduction of secondary raw materials brings along new challenges in the product development process. Limiting the influence of recycling material on the chemical and physical properties is a challenge that requires deep know-how in refractory material development. In order to fulfil a certain performance level, a new approach for counteracting these effects had to be found. This is discussed in the following case study carried out at one of our German customers. This report presents the performance results and the findings of a mineralogical postmortem investigation of the high recycling containing magnesia-carbon brick installed in the ladle slag zone.

The original lining concept of the ladle is shown in Figure 1. In the bottom and sidewall, a monolithic lining solution was installed combined with a MgO-C bricked slag zone. Before testing the high recycling containing brand, a standard magnesia-carbon brand was used in the wear lining of the ladle slag zone, which was typically changed after 75–77 heats.

With this previous lining concept, increased wear mainly occurred above the gas purging area, which resulted in residual wear lining thicknesses lower than 40 mm. In addition, cobblestoning and vertical cracking appeared in the slag zone as depicted in Figure 2. Consequently, this led in combination with the low residual thickness and high bath movement to occasionally detached bricks, especially in the purging area.

In October 2019, the first two ladle slag zones with the high recycling containing brand were tested with the trial target of eliminating cobblestoning and vertical cracking. The rest of the ladle lining concept remained unchanged.

Within each trial, the requested lifetime of over 150 heats could be achieved (including one standard slag line change in each ladle) and furthermore the vertical cracking and cobblesoning was significantly reduced, as illustrated in Figure 3.

For verification of these first positive results, the customer agreed to a follow-up trial with 10 slag zone sets in which the performance of the high recycling containing brick could be confirmed. As already shown in the first trial, cobblesoning and vertical cracks could be significantly reduced compared to the previous wear lining concept of the slag zone. The ladles using the new brand performed well with an average lifetime of 156 heats per campaign (2 slag zones) achieving the customer's targets. In addition, by reducing cobblesoning and crack formation, the gunning maintenance was decreased (Figure 4).

**Figure 1.**

Original ladle lining concept before the trial. (a) side view and (b) top view.

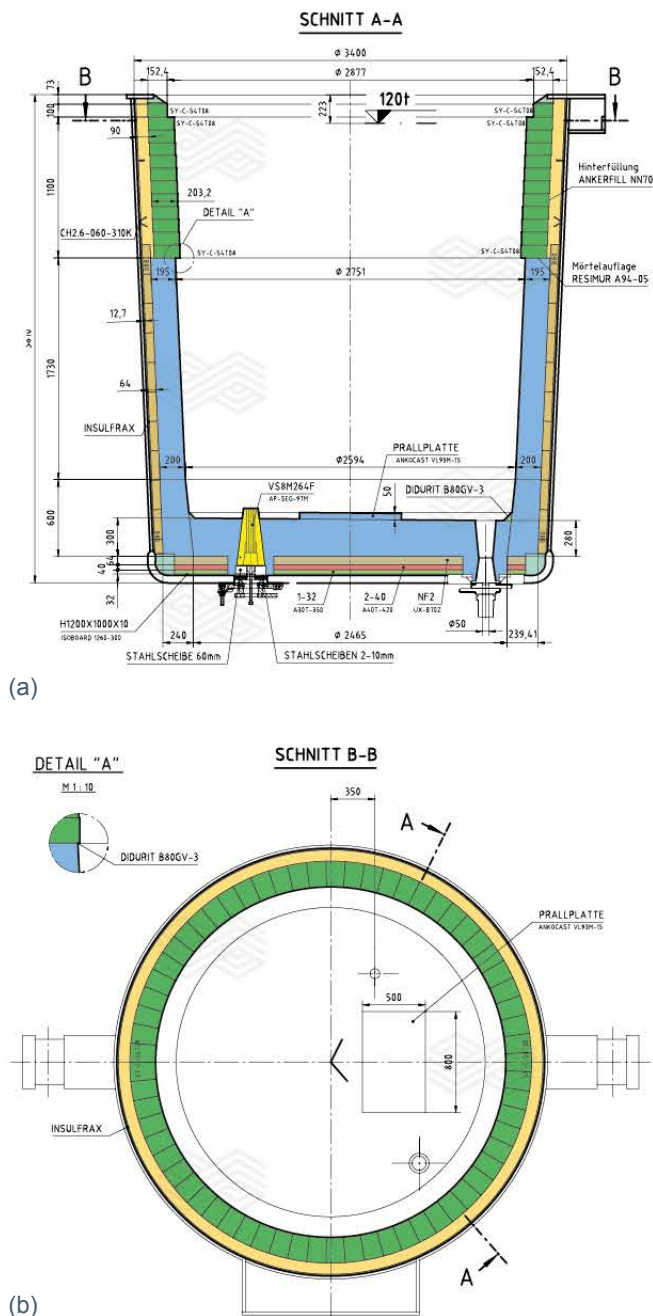


**Figure 2.**

Typical appearance of the wear lining after 43 heats with the original lining concept showing cobblesoning and vertical cracking in the slag zone.



**Figure 3.**

Typical appearance of the wear lining after 66 heats with the high recycling containing brand showing no cobblesoning and no vertical cracking in the slag zone.

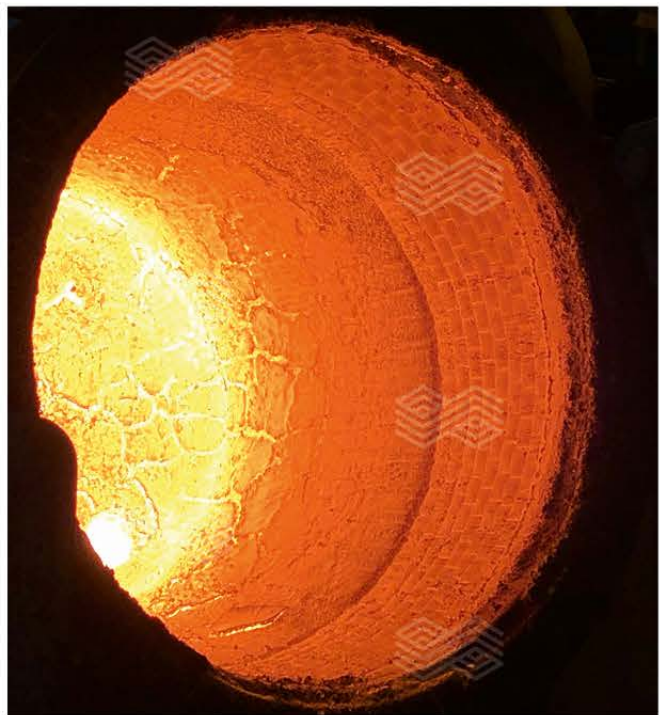


**Figure 4.**

Reduction of gunning material consumption after the high recycling containing brick MgO-C brick was installed in April 2020.



The long-term average consumption had been 0.21 kg/tonne steel; however, during the trial period only 0.13 kg/tonne steel was used. Overall, this meant a 38% reduction of refractory material use as well as a significantly lower number of gunning applications, thus reducing both time loss in production and manpower spent on maintenance.

A postmortem investigation of the high recycling containing brand was conducted at RHI Magnesita's Technology Center Leoben (Austria). Within this investigation a well-distributed graphite content, which serves as an effective protection against slag infiltration and corrosion, was found. The brick microstructure is shown in Figure 5. The grey regions are magnesia grains with different grain sizes, the light grey, almost whitish parts represent graphite, and the black spots depict particles lost during sample preparation from the fine component areas and grains.

While the overall brick performance was even improved with the 87 wt.% recycling content, various investigations showed that the addition of secondary raw materials had an influence on the bulk density, thermal conductivity, and oxidation resistance. In comparison to a standard magnesia-carbon brick, the bulk density was found to be significantly lower due to the high share of magnesia-carbon recycling material and the high carbon content.

With respect to the thermal conductivity, there are two counteracting effects that result in standard MgO-C bricks and MgO-C bricks with a high recycling content having comparable thermal conductivity levels at elevated temperatures: On the one hand the solid carbon addition increases the thermal conductivity, but on the other hand recycling material decreases it due to the inherent higher porosity compared to native raw materials. In the case of the trial brand, the thermal conductivity was within a standard range characteristic for slag zone brands (Figure 6). However, the calculated shell temperature increased to 336 °C with the "new" slag zone from 317 °C with the "original" slag zone wear lining containing less carbon.

**Figure 5.**

**Typical microstructure of the high recycling containing brand after use.**



The last aspect to be considered is the impact of recycling material on the oxidation resistance. First and foremost, high carbon containing brands are typically more susceptible to oxidation than low carbon containing brands. Therefore, the high carbon content, as well as the higher porosity of the secondary raw materials, cause a reduced oxidation resistance of the high recycling containing brick. In cases where the wear mechanism is driven by carbon burn-off, it must be noted that the performance level of the new development may suffer.

The major benefit of designing and implementing high recycling containing products is that they directly contribute to a lower carbon footprint, since a substantial amount of energy and CO<sub>2</sub> is being saved from not processing magnesite. Compared to a standard magnesia-carbon brand consisting of fused and dead burned magnesia, the carbon footprint of the high recycling containing brand is about 85% lower as shown in the following comparison:

|                                     |  |
|-------------------------------------|--|
| Standard magnesia-carbon brick      | 3.95 tonne CO <sub>2</sub> /tonne bricks |
| High recycling containing brick     | 0.55 tonne CO <sub>2</sub> /tonne bricks |
| Potential CO <sub>2</sub> reduction | 3.40 tonne CO <sub>2</sub> /tonne bricks |

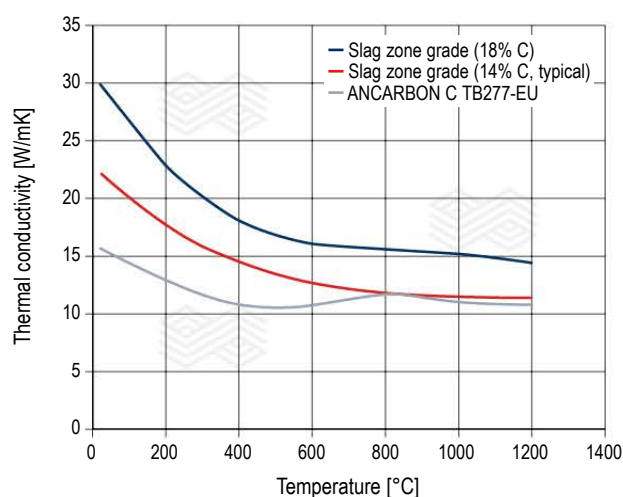
This equates to a potential CO<sub>2</sub> saving at this customer of about 2000 tonnes of CO<sub>2</sub> a year. To put this figure into context, it is the same amount of CO<sub>2</sub> that would be generated by driving a mid-range petrol car on the highway (CO<sub>2</sub> emissions of 19 kg per 100 km for 7.4 litres consumption) about 10.5 million km. This distance is equivalent to 262 times around the world.

### Circular Economy—Future Sourcing of Recycling Materials

As sourcing secondary raw materials is one of the biggest challenges in the entire circular economy process in the refractory industry, it is key to intensify the cooperation between RHI Magnesita and the steel plants. Following the example of automotive producers, where dismantling and recycling of the car is already considered during the design phase, a smart refractory recycling concept for furnaces and vessels is required.

**Figure 6.**

**Thermal conductivity comparison of various slag zone grades.**



In this regard, the starting point is at the design phase when the lining concept of a metallurgical vessel is defined. At this stage, the recycling capability of the installed brick grades already needs to be considered, meaning that the same basis for the main raw materials should be used for the total refractory lining. Taking a ladle lining concept as an example, this means that in the case of using magnesia-carbon products for the working lining, the rest of the refractory lining should also be based on magnesia raw materials. Consequently, the principal choice of the installed working lining defines the main raw material sources used for the permanent lining and unshaped products in this ladle. Simultaneously, a specific and individual dismantling and sorting concept for the refractories needs to be setup together with RHI Magnesita's customers. At this point, the described concept of having the same base raw materials in one vessel applies, since onsite sorting of the leftover materials during or after breakout becomes much easier and leads to less contamination of the resulting secondary raw materials.

After sorting, a customer-specific procedure for optimum use of each secondary raw material stream needs to be defined. In this case, the possibilities extend from recycling by producing new refractory bricks with the most valuable secondary raw materials, to using other fractions in refractory mixes or for slag conditioning. These options already show the complexity of the entire process, whereby the effort is accompanied by a required investment in crushing and sieving units, as well as establishing storage space for the sorted material streams. However, even with the current processing technology there are still materials that have no application and therefore still need to be disposed of. The goal of RHI Magnesita is to further reduce this leftover amount requiring disposal by using available recycling developments.

---

## Conclusion

This article presents an example of how to establish a circular economy concept in the refractory and steel industry. The development of a refractory product consisting mainly of secondary raw materials, which still meets the performance expectations of the customers, makes the introduction of ANCARBON C TB277-EU an economic and ecological success story.

As recycling products with significantly lower carbon footprints are already available in Europe, the next step will be achieved by further improving the secondary raw material sourcing and supply chain. The main challenge to be tackled along the way is the alignment between customer and refractory supplier on an integrated circular economy approach. This includes on the one hand that refractory concepts need to be adjusted to customer requirements, but on the other hand breakout, sorting, and reuse of installed materials must already be considered during the design phase. These progressive steps will all contribute to RHI Magnesita's strategy to provide sustainable solutions for our customers.

## Authors

Hartwig Kunanz, RHI Magnesita, Leoben, Austria.

Birger Nonnen, RHI Magnesita, Mülheim-Kärlich, Germany.

Julia Kirowitz, RHI Magnesita, Vienna, Austria.

Miriam Schnalzger, RHI Magnesita, Vienna, Austria.

**Corresponding author:** Miriam Schnalzger, [Miriam.Schnalzger@rhimagnesita.com](mailto:Miriam.Schnalzger@rhimagnesita.com)



Florian Kek, Thomas Griessacher, Christoph Bauer, Barbara Zocratto, Richard Krump and Christian Koubek

# Refractory Waste to Slag Engineering Solution—Metallurgical Consulting Supports Steel Plant’s Circular Economy Strategy

To avoid landfilling practices, the entire refractory process chain should be optimised regarding life cycle management, including sorting spent refractories for recycling in refractory production and other applications such as slag forming agents. Therefore, an industrial feasibility study was performed at Marienhütte Graz (Austria) focused on the different benefits of reusing spent MgO-containing fines as a slag forming agent in EAF steelmaking. MgO dissolution in the slag was examined using different chemical and scanning electron microscope microtextural analyses, and it was determined that typically the spent MgO fines had completely dissolved. Different quantities of spent MgO fines were injected pneumatically at different time slots during the EAF meltdown and refining periods to establish the optimum application schedule and MgO saturation level. Tracking the slag foaming behaviour was performed by recording data from an adjusted electrode regulation system. This showed an improved slag foaming due to injection of the MgO- and carbon-containing spent refractory fines compared to the standard operating procedure using dolomite. As a consequence of the close collaboration with RHI Magnesita, including a metallurgical consultancy service, multiple benefits in terms of process efficiency and sustainability were achieved during the study. Furthermore, the work highlighted that the online measurement of slag foaming behaviour opens up opportunities to investigate the incorporation of slag foaming data into machine learning tools and artificial intelligence for process optimisation.

## Introduction

Nowadays, as the life cycle of refractory products should not end when they are broken out of a furnace or vessel, it is becoming an increasingly common practice to recycle coarser high-quality material in new refractory products, substituting virgin raw material. However, the challenging task to find valuable applications for the finer spent residues remains [1,2]. To address this topic, the dissolution and slag forming potential of spent MgO-containing fines were investigated in the electric arc furnace (EAF) at Marienhütte Graz (MHG). In a series of trials, the fines were applied at different process time slots and their impact on the slag foaming behaviour was examined using data obtained from the electrode regulation system (ERS).

## Marienhütte Graz Steel Plant

MHG is a micro mill in Austria producing 410000 tonnes of reinforcement steel annually. Located in the middle of a residential area, the steel plant comprises an EAF, ladle furnace, two-strand billet caster, and a rolling mill. It operates at 40 tonnes of steel per heat and approximately 35 heats a day. The 100% scrap is charged in three buckets during one heat and its quality varies a lot depending on availability and price. Slag forming agents such as lime and dolomite are added during the meltdown phase via a specially designed hopper. The average tap-to-tap time is approximately 40 minutes and the EAF is relined 5 times a year.

Cost leadership and sustainability, such as avoiding any waste generation, are pivotal for MHG. On average, 23% of the plant’s entire energy consumption comes from renewable energy sources and the CO<sub>2</sub> emissions of the end product from “cradle to gate” are 442 kg CO<sub>2</sub> eq/tonne steel. Reprocessing metallurgical by-products such as dusts, slags, and sludge is an important part of their circular economy strategy [3,4]. For example, the EAF slag is processed into a certified artificial crushed stone used as a base course in civil engineering [5] and zinc and other components are recycled from the exhaust gas flow. Furthermore, the waste heat from the steel plant is fed into the district’s heating system and covers an entire city district demand.

In line with the steel plant’s strong commitment to sustainability, the next step was establishing the onsite reuse of generated refractory waste to avoid the environmental impact and costs associated with landfilling this material. As a solution’s provider, RHI Magnesita offered full support during the trials to determine how spent MgO-containing fines could be reused effectively for slag engineering, including metallurgical consulting, application machinery, and comprehensive slag sample analysis.

## MgO Dissolution in Slag

In steelmaking, slag conditioning with MgO is an established approach to prevent MgO dissolution from the basic lining material and reduce attack by aggressive slags [6]. MgO dissolution is driven by thermodynamic and kinetic aspects like slag chemistry, particle size, as well as the different steelmaking units and their operating conditions (e.g., temperature and tap-to-tap time). Furthermore, it plays a

crucial role in slag foaming as this behaviour is linked to the MgO saturation level. However, as refractory products, especially those containing fused MgO (i.e., periclase), are designed to withstand high-temperature corrosive environments for as long as possible, it was essential to examine in detail the solubility of MgO-containing fines in the slag. Additionally, as the slag from MHG is used for example in road construction, it was also necessary to ensure that any added MgO had completely dissolved because residual material could cause the slag to expand due to MgO hydration, making it unsuitable for this type of downstream application [5,7].

Concerns related to dissolving spent MgO fines in EAF slag have been raised in the literature [8]. Furthermore, the challenges of dissolving different MgO carriers in steelmaking slags under static laboratory conditions demonstrated that accurately determining MgO dissolution requires different chemical and scanning electron microscope (SEM) microtextural analyses, such as X-ray fluorescence (XRF), X-ray diffraction (XRD), and SEM-energy dispersive spectrometry (EDX) [9,10]. Therefore, this comprehensive approach was adopted to analyse the slag samples during the study.

## Slag Foaming

A slag foaming practice optimises the energy efficiency of the EAF process [11,12]. It protects the EAF walls, especially hot spot areas, from direct impact with the free-burning arc radiation, thus from melt down of slag bake-on and consequently from refractory wear. Shielding the arc by proper foaming enables melting with longer arc lengths also during the flat bath phase. A higher arc performance can result in both a lower specific energy requirement and a higher productivity. Carbon monoxide bubble generation and their retention in a viscous slag enable slag foaming [13] and some of the required carbon and oxygen come from the

charged materials. Nevertheless, continuous slag foaming requires an additional input of oxygen and carbon (e.g., anthracite) [11].

The effective foaminess of EAF slag is linked to its MgO and FeO contents and its basicity—B3 (equation 1) [14–18]. Furthermore, MgO saturation is essential for EAF slag foaming because secondary phase precipitations occur that serve as nucleation sites for the required carbon monoxide bubbles.

$$B3 = \frac{CaO}{SiO_2 + Al_2O_3} \quad (1)$$

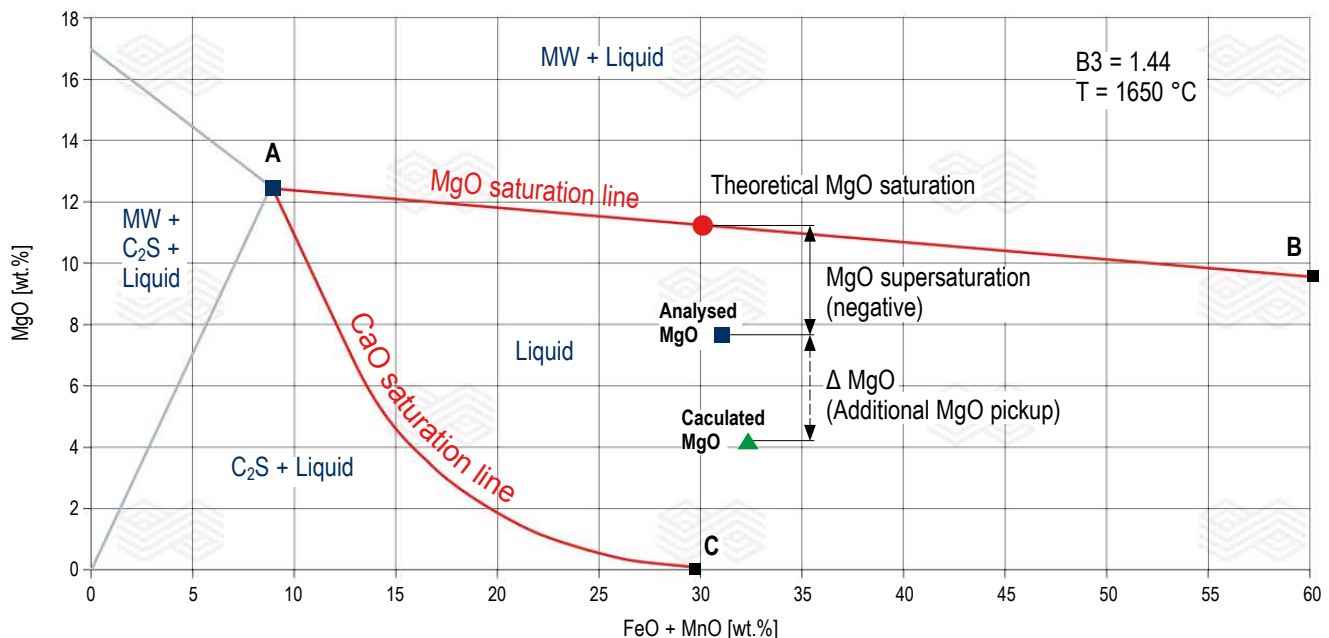
The objective of slag engineering is to find an optimised balance between applied additives, refractory wear, and slag foaming. Empirical studies and FactSage calculations carried out in the 1990s led to multiple mathematical equations that are currently used in software solutions to describe MgO saturation in FeO-rich slags [14–22]. The isothermal stability diagram (ISD) is one approach to predict MgO dissolution in relation to the FeO and CaO contents and can facilitate effective slag foaming. Throughout the trials, RHI Magnesita's e-tech software tool "Foamy Slag" [21] was used to visualise the ISD, as well as calculate the theoretical MgO saturation and other related figures.

## Isothermal Stability Diagrams

The MgO solubility dependence on the slag basicity, temperature, and the CaO-MgO-SiO<sub>2</sub>-FeO phase relationships is used to construct the ISD [15]. Figure 1 shows an ISD for slags with a B3 of 1.44 and the stability regions of the various phases at 1650 °C. Besides the liquid phase there are two stable solid mineralogical phases—MgO·FeO magnesiowüstite (MW) and dicalcium silicate (C<sub>2</sub>S). In the ISD, "A" is the point of dual saturation with

Figure 1.

Example of an ISD generated with the Foamy Slag application for slags with a B3 = 1.44 at 1650 °C.



respect to MgO (MW) and CaO (C<sub>2</sub>S) on the liquidus surface. The liquidus lines, namely saturation curves for MgO and CaO, originate from point “A” and are defined as “A–B” and “A–C”, respectively [15].

The Foamy Slag application is designed to provide insights into the slag chemistry using the ISD. The software visualises the analysed MgO value (blue square), the calculated MgO value (green triangle), and the theoretical MgO saturation point (red dot) based on input data such as slag chemistry, additions, and temperature (see Figure 1). The calculated MgO point results from the amount and chemistry of slag formers applied.

The difference between the analysed and calculated MgO values (i.e.,  $\Delta$  MgO) shows the amount of MgO pickup in the slag from the refractory brick lining and gunning mix and has to be avoided. The difference between the analysed MgO value and theoretical MgO saturation point (i.e., MgO supersaturation) indicates the slag’s affinity to dissolve MgO. The MgO supersaturation is positive or negative depending on whether the slag is over or undersaturated, respectively.

Based on the Foamy Slag application, different trial scenarios were set up and adjusted to close the gap between the analysed and calculated MgO values and to generate a slag with less affinity to dissolve MgO, thereby minimising MgO pickup from the lining and gunning mix. Furthermore, MgO saturation was targeted in the trials to enhance slag foaming.

### Foaming Slag Index

The EAF electrode current can provide information regarding the slag foaming quality. As every EAF is equipped with an accurate current measurement system to regulate the arc, called the ERS, this information can be used to determine the foaming slag index (FSI), a value derived from the current/voltage curves and total harmonic distortion [23]. A FSI of 100% indicates fully covered electrodes by an optimally foaming slag.

In the long-term trials, the ERS was adjusted to track the average FSI data over three separate time phases, at each electrode. The first phase started at the transition point between the meltdown and refining period, in which the parameters were tracked for 120 seconds. In the

subsequent 120 seconds, the second phase was recorded. This was followed by the third phase that tracked the FSI until the start of tapping. Due to the ERS adjustment to record the FSI starting at the meltdown/refining transition point, some process values had to be fixed which complicated comparing the different trial scenarios.

### Short-Term Trial Setup

To determine the process parameters that could be optimised, short-term trials were performed with two different spent MgO-containing fines and the standard MgO carrier used at MHG. The origin, chemical composition, grain size, and application method of the various MgO-containing fines are detailed in Table I.

The amount of each material applied was calculated based on the process parameters using the Foamy Slag application. At the beginning of the short-term trials, the materials were added before the first and second scrap buckets using big bags via a hopper. However, the initial trials showed that this type of application was time consuming, and not suitable for long-term trials. Therefore, a RHI Magnesita ANKERJET pressure vessel machine [24] equipped with weighing cells, a digital control panel, and semi-automated trigger was installed and connected to the EAF. An injection lance targeted the slag/steel bath through an empty pipe underneath burner no. 3 (Figure 2). Using this setup, 100 kg up to 1100 kg per heat were pneumatically injected at a maximum feeding rate of 90 kg/minute. In total 41 trials were conducted using this approach to understand the balance between the applied material and the remaining gap to the theoretical MgO saturation. Another objective was to apply MgO fines at different process time slots to clarify the impact regarding melting, lining wear, and slag foaming behaviour. The injection of spent MgO-containing fines at different time points was found to work effectively.

The EAF process is generally divided into a meltdown period in which scrap is charged and melted and a refining period to achieve the required final steel composition. The transition point between the melting and refining periods is defined by process parameters, such as the required melting energy consumption that is linked to the charged scrap weight. For the short-term trials, at least two slag samples were taken during each heat, the first sample at the refining period start

**Table I.**  
MgO-containing fines used in the short-term trials.

| Material and origin                            | MgO<br>[wt.%] | CaO<br>[wt.%] | C<br>[wt.%] | Grain size<br>[mm] | Application method                    |
|--|---------------|---------------|-------------|--------------------|---------------------------------------|
| Spent MgO-C fines<br>(Up to 60 wt.% fused MgO) | 70–80         | 5–10          | 10–15       | 0–10               | Big bag/hopper feeding<br>+ injection |
| Spent doloma fines<br>(Doloma ladle bricks)    | 30–40         | 50–60         | 2–3         | 0–70<br>0–10       | Big bag/hopper feeding<br>Injection   |
| Standard MgO-carrier<br>(Commercial dololime)  | 35–40         | 55–60         | 0           | 20–45              | Conveyor belt/hopper<br>feeding       |

and the second before tapping. Commonly, slag analyses in steel plants are performed by XRF bulk chemical analysis which does not enable the dissolution behaviour of crystalline MgO (i.e., periclase) to be determined [9,10]. Therefore, all samples were analysed at RHI Magnesita's Technology Center Leoben (TCL) by combining XRF and XRD analysis as well as optical light microscopy and SEM-EDX on selected samples.

In summary, during the short-term trials different scenarios were investigated where various materials and amounts were applied at different process time points. In total, 78 heats were monitored and 231 slag samples were taken and analysed.

### Short-Term Trial Results

XRF and XRD were performed on all the slag samples. In the very rare cases where periclase was detected by XRD, light microscopy and SEM-EDX were performed and confirmed the XRD results. In addition, those samples with high MgO concentrations were analysed microscopically, including by SEM-EDX, to clarify if the MgO had dissolved and in which phases it was incorporated. These analyses indicated that the MgO had dissolved in 98.5% of the 231 slag samples taken during the 78 heats. A SEM image of a representative sample is depicted in Figure 3a where an oversaturated MgO slag was targeted by applying spent MgO-C fines. The observed melilite matrix (CaAlMg-silicate) included different types of spinels, but no undissolved MgO was detected. The presence of undissolved periclase (Figure 3a) was only observed in 3 slag samples, which all came from heats after gunning maintenance.

**Figure 2.**

Position of the injection lance underneath burner no. 3 used to apply the MgO-containing spent fines.

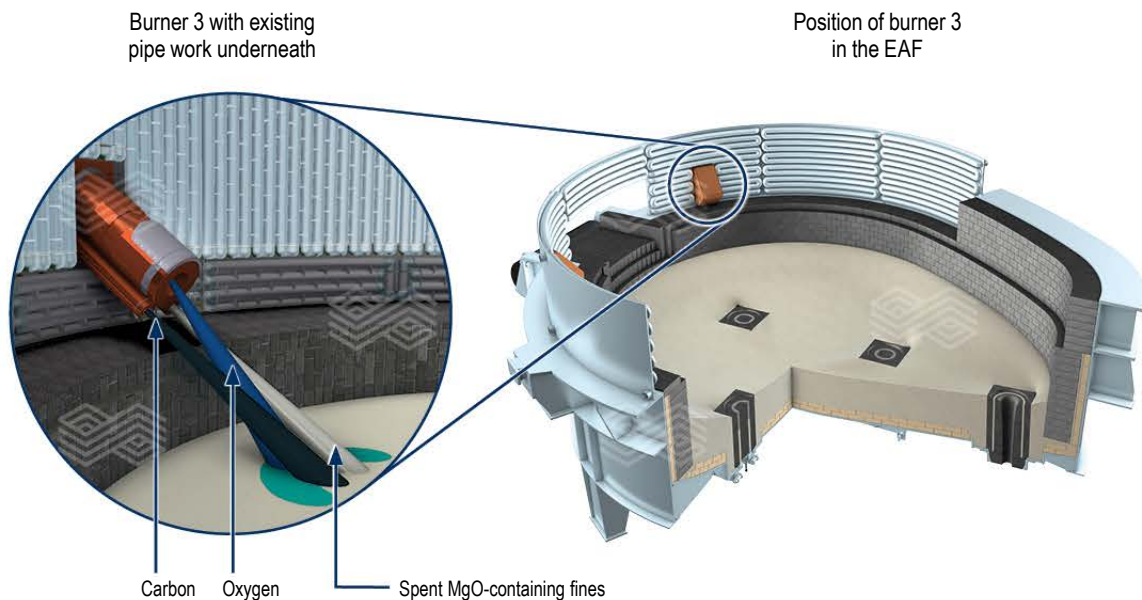
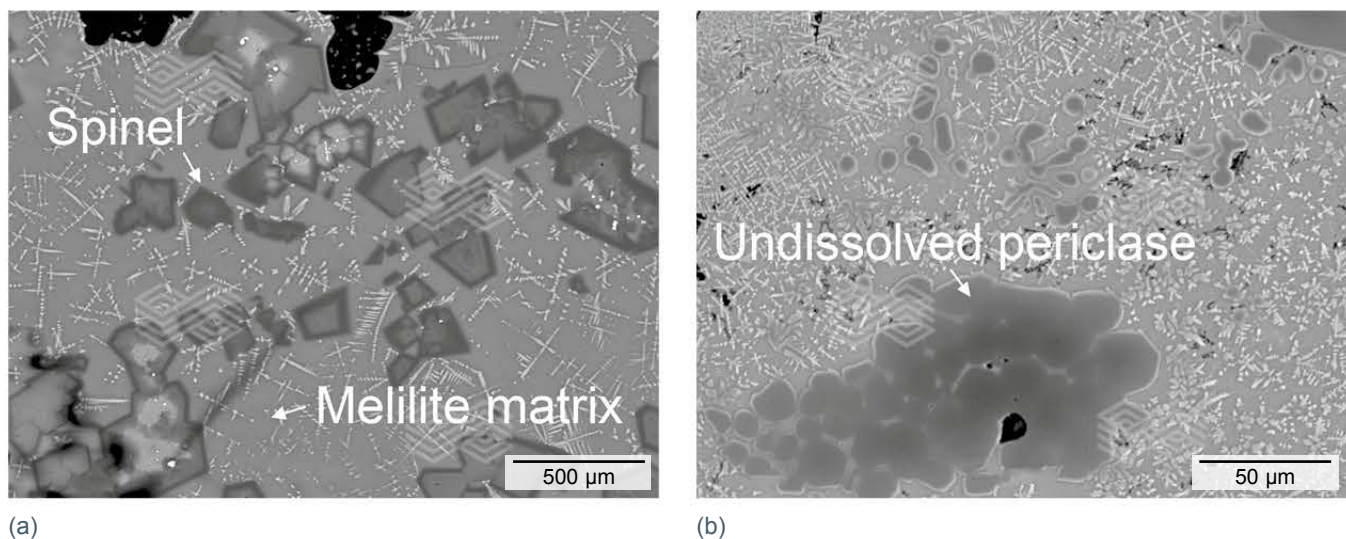


**Figure 3.**

SEM images showing (a) typical sample without any undissolved MgO and (b) very rare sample with partly undissolved periclase.



To compare the dissolution behaviour of dololime, spent MgO-C (containing up to 60 wt.% fused MgO), and spent doloma, the same MgO saturation level was targeted by adding appropriate amounts of the different MgO carriers. The average results showed that there were no significant dissolution differences between the three materials. However, a slightly decreased energy consumption was observed when the spent MgO-C material was applied during the EAF melting period. This energy decrease is assumed to be related to the carbon content in the spent fines, which supplied additional energy for dissolution and provided initial slag foaming during the melting period.

Since the method and time points of applying the MgO carrier during the EAF process can have different influences regarding MgO saturation and slag foaming [25–27], the spent fines were injected pneumatically at different set points, targeting different MgO supersaturation levels to enable deeper insights into the possible slag engineering impacts. One outcome observed was that injecting spent fines into the residual EAF slag resulted in an extraordinary slag foaming, especially with the higher carbon-containing MgO-C fines. In addition, injecting these fines during the refining period led to more slag foaming and a less noisy process. This could be caused by two reasons: An oversaturated MgO slag, which is an ideal precondition for foaming [14–18], and/or the carbon content of the spent fines reducing FeO and generating more CO bubbles [13,25,28,29]. Interestingly, in the trials it was shown that significant slag foaming also occurred under the MgO saturation point, which gives room for further investigations.

As a result of targeting different MgO supersaturations and MgO carrier addition times, slag MgO pickup from the lining and gunning mix was minimised. The conditions used to achieve this goal were then adopted for the best practice trials. The differences between 20 heats of the best practice trials (adding lime and spent refractory fines) and 30 heats of the standard operating procedure (adding lime and dololime) are shown in Table II. The low B3 values are typical for MHG and their challenging scrap conditions.

Using the XRF slag data and the Foamy Slag application results, the analysed and calculated MgO slag figures could be compared for slag samples taken immediately before tapping for the two trial scenarios. While the analysed MgO value in the slag was similar for the standard operating procedure (i.e., 6.0 wt.%) and the best practice trials (i.e., 5.9 wt.%) the  $\Delta$  MgO figures were significantly different (i.e., 3.1 wt.% and 0.8 wt.%, respectively), due to the higher MgO input in the best practice trials. These  $\Delta$  MgO values equate to the MgO pickup from the brick lining and gunning mix, namely 150 kg per heat for the standard operating procedure and 50 kg per heat in the best practice trials. Comparing the absolute amount of MgO per heat, this meant approximately 65% less MgO pickup from the brick lining and gunning mix when spent refractory fines were used.

Due to the operating practice at MHG, the slag was intentionally undersaturated. The theoretical MgO saturation level for the standard operating procedure was 15.1 wt.% and 13.2 wt.% for the best practice trials, giving supersaturation levels of -9.1 wt.% and -7.3 wt.%, respectively.

### Long-Term Trial Setup and Results

Based on the best practice trial results, proposed operating procedures were set up for the long-term trials where 200 kg of the spent fines were injected per heat, for 2 weeks at the beginning of the refining period. The slag sampling was performed at the same time points used for the short-term trials, but the frequency was reduced due to the trial length. The main objectives of these trials were to get more reliable data in terms of MgO lining pickup and to track slag foaming behaviour after injecting the fines during the refining period, using the adjusted ERS and evaluation of the FSI data.

The results of a long-term trial where MgO-C fines were injected are compared to the standard operating procedure in Table III. 130 trial heats were monitored during this proposed operating procedure, where the added MgO

**Table II.**

Comparison of the standard operating procedure and best practice trial scenarios.

| Trial scenario               | Trial heats | Additives<br>(Lime, dololime, spent MgO-C, spent doloma) |      | Slag analysis data<br>(MgO figures before tapping) |              |                |                            |           |                            |                     |
|------------------------------|-------------|--|------|--|--------------|----------------|----------------------------|-----------|----------------------------|---------------------|
|                              |             | CaO  | MgO  | B3   | MgO analysed | MgO calculated | $\Delta$ MgO lining pickup |           | MgO saturation theoretical | MgO supersaturation |
|                              |             | [kg]   | [kg] |  | [wt.%]       | [wt.%]         | [wt.%]                     | [kg/heat] | [wt.%]                     | [wt.%]              |
| Standard operating procedure | 30          | 1050   | 130  | 0.8  | 6.0          | 2.9            | 3.1                        | 150       | 15.1                       | -9.1                |
| Best practice trials         | 20          | 1180   | 270  | 0.9  | 5.9          | 5.1            | 0.8                        | 50        | 13.2                       | -7.3                |

content was approximately 60% higher than for the standard operating procedure. The specific carbon consumption figures showed that injection of carbon-containing spent refractory fines in the EAF refining period reduced the anthracite consumption by 12%. Furthermore, the analysed MgO data indicated that the spent fines reliably increased the supersaturation and the  $\Delta$  MgO figures confirmed the results of the best practice trials, in which less MgO pickup from the lining and gunning mix occurred. This was reflected in a reduced gunning mix consumption of approximately 30% and a higher residual brick thickness of up to 20 cm.

The FSI data recorded for three separate time phases during the EAF refining period, at each electrode, are shown in Table IV, as well as the average FSI for each time phase. The proposed operating procedure showed higher FSI values throughout the entire measurement period compared to the standard operating procedure. Furthermore, the EAF operators observed a less noisy EAF process and improved slag foaming.

It should be noted that interpretation of recorded FSI data is challenging. Slag viscosity, chemical composition, carbon and oxygen inputs, temperature, and the respective changes are linked to parameters such as electrical field strength and arc length. Additionally, the improvised ERS adjustment without total Level 2 parameter access plays an important role. A final point is that accurately monitoring the energy consumption was not feasible during the trial period due to a high variability of the scrap quality.

Evaluation of the different data sets to incorporate FSI figures in process optimisation tools, such as RHI Magnesita's Automated Process Optimization (APO) [30,31], is still ongoing. To further improve the slag foaming behaviour, data acquisition from additional trials with high carbon-containing spent MgO fines are planned. In these upcoming trials, the FSI results of the ERS will be compared with a sound pressure measurement system.

**Table III.**

Comparison of the results from the standard operating procedure with a proposed operating procedure, where MgO-C fines were injected.

| Trial scenario               | Trial heats | Additives<br>(Lime, dolomite,<br>spent MgO-C) |                        | Carbon consumption<br>[%] | Slag analysis data<br>(Figures before tapping) |                        |                            |           |
|------------------------------|-------------|---|------------------------|---------------------------|--|------------------------|----------------------------|-----------|
|                              |             | Total CaO<br>[kg/heat]                        | Total MgO<br>[kg/heat] |                           | B3   | MgO analysed<br>[wt.%] | $\Delta$ MgO lining pickup |           |
|                              |             |   |                        |                           |  |                        | [wt.%]                     | [kg/heat] |
| Standard operating procedure | 370         | 1050  | 130                    | 100                       | 0.8  | 6.0                    | 3.1                        | 150       |
| Proposed operating procedure | 130         | 1030  | 330                    | 87.5                      | 0.8  | 8.4                    | 1.6                        | 80        |

**Table IV.**

Comparison of the FSI data recorded for three separate time phases during the EAF refining period from the standard operating procedure and a proposed operating procedure, where MgO-C fines were injected.

| Trial scenario               | Trial heats | FSI phase 1<br>(0–120 seconds, electrode<br>number, and average) |    |    |             | FSI phase 2<br>(120–240 seconds, electrode<br>number, and average) |    |    |             | FSI phase 3<br>(240 seconds–start of tapping,<br>electrode number, and average) |    |    |             |
|------------------------------|-------------|--|----|----|-------------|--|----|----|-------------|---|----|----|-------------|
|                              |             | 1  | 2  | 3  | $\emptyset$ | 1  | 2  | 3  | $\emptyset$ | 1   | 2  | 3  | $\emptyset$ |
|                              |             | [%]  |    |    |             | [%]  |    |    |             | [%]   |    |    |             |
| Standard operating procedure | 370         | 62   | 62 | 62 | 62          | 57   | 58 | 56 | 57          | 52  | 53 | 53 | 53          |
| Proposed operating procedure | 130         | 63   | 65 | 64 | 64          | 64   | 65 | 64 | 64          | 58  | 57 | 56 | 57          |

## Conclusion

Spent refractory fines that could not be reused for refractory production were processed into a slag forming product. These materials were applied into the EAF at MHG via a big bag hopper feeding system and later with an ANKERJET pressure vessel machine. By analysing slag samples using various methods, it was shown that the spent fines dissolved well and behaved in an equivalent manner to typical MgO carriers in terms of increasing the MgO saturation level and significantly decreasing MgO pickup from the lining. The advantages of injecting spent MgO-C fines pneumatically at different process time slots included a decreased anthracite consumption, a reduced lining wear, and an improved slag foaming. As challenging as interpretation of the ERS data can be, it can provide a crucial contribution to EAF process optimisation and predictive maintenance; therefore, data analysis is still ongoing and further trials will be conducted.

## Outlook

Ideally, the target of the refractory producer and customer should be to drive a closed-loop product life cycle strategy together, namely reuse all refractory breakout material and create added value, avoid landfilling, and decrease virgin raw material use. Converting spent refractory fines into slag forming agents (e.g., offsite in RHI Magnesita's recycling

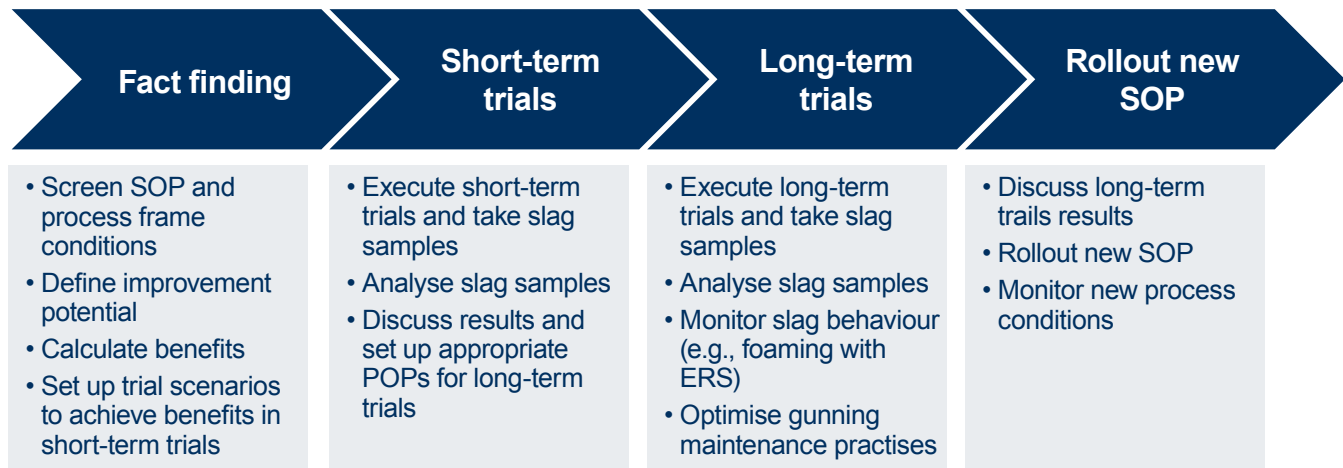
plants or directly at the customer using an appropriate crushing service) as well as optimising their application with RHI Magnesita's metallurgical expertise and software tools is one approach to support such a circular economy initiative. Furthermore, a "Slag Engineering Solution" package (Figure 4) is now available for our customers, where onsite assistance is provided in areas such as fact finding, short-term and long-term trial design, as well as implementing a new standard operating procedure to improve slag engineering through recycling spent refractory material.

## Acknowledgements

RHI Magnesita is very grateful for the successful cooperation with Marienhütte Graz, especially the EAF operators' expertise and fruitful discussions. A core understanding, evaluation, and interpretation of the ERS data was supported by Primetals Technologies.

**Figure 4.**

Slag Engineering Solution. Acronyms include standard operating procedure (SOP) and proposed operating procedure (POP).



## References

- [1] Horcksmans, L., Nielsen, P., Dierckx, P. and Ducastel, A. Recycling of Refractory Bricks Used in Basic Steelmaking: A Review. *Resources, Conservation & Recycling*. 2019, 140, 279–304.
- [2] Schutte, M. Refractory Recycling Earning Your Environmental Brownie Points. The Southern African Institute of Mining and Metallurgy Refractories 2010 Conference. Johannesburg, South Africa, March 16–17, 2010, 75–86.
- [3] <https://projekte.ffg.at/projekt/3157992>
- [4] Echterhof, T., Willms, T., Preiß, S., Omran, M., Fabritius, T., Mombelli, D., Mapelli, C., Steinlechner, S., Unamuno, I., Schüler, S., Mundersbach, D. and Griessacher, T. Developing a New Process to Agglomerate Secondary Raw Material Fines for Recycling in the Electric Arc Furnace - The Fines2EAF Project. *La Metallurgia Italiana*. 2019, 5, 31–40.
- [5] EN 13242. Gesteinskörnungen für ungebundene und hydraulisch gebundene Gemische für Ingenieur- und Straßenbau. Edition: 2008-03-01.
- [6] Cheremisina, E., Schenk, J., Viertauer, A., Nilica, R. and Roessler, R. Dissolution Behaviour of Various MgO-Containing Raw Materials in a Secondary Metallurgical Slag. *Bulletin*. 2020, 68–73.
- [7] Drissen, P. and Schrey, H. *Verbesserung der Raumbeständigkeit von Stahlwerksschlacken*. Final Report: Integrierter Umweltschutz in der Metallerzeugung. Thyssen Krupp Stahl AG, Germany, 2003.
- [8] Kwong, K.S. and Bennett, J.P. Recycling Practices of Spent MgO-C Refractories. *Journal of Minerals & Materials Characterization & Engineering* 2002, 1(2), 69–78.
- [9] Cheremisina, E., Schenk, J., Viertauer, A., Nilica, R. and Roessler, R. Dissolution Rate of Various MgO Materials in Steel and Secondary Metallurgy Slags. AISTech 2018 Conference Proceedings. Philadelphia, USA, May 7–10, 2018, 1103–1115.
- [10] Cheremisina, E., Schenk, J., Viertauer, A., Nilica, R. and Roessler, R. Evaluation of Dissolution Rate and Behaviour of MgO Carriers for Primary and Secondary Metallurgical Slags. *Metallurgical and Materials Trans. B: Process Metallurgy and Materials Processing Science*. 2021, 52(5), 2939–2950.
- [11] Krüger, K. Detektion und Regelung von Schaumslag. *VdEH Stahl Akademie Seminar Script-Elektrotechnik des Lichtbogenofens*. 2016.
- [12] Krüger, K., Ehrbar, A. and Timm, K. Schlackenabbackungen und thermische Verluste eines Drehstromofens. *Stahl und Eisen*, 1998, 118(9), 63–67.
- [13] Zapparoli Falsetti, L.O., Ferreira Muche, D.N., Santos Junior, T. and Pandolfelli, V.C. Thermodynamics of Smart Bubbles: The Role of Interfacial Energies in Porous Ceramic Production and Non-Metallic Inclusion Removal. *Ceramics International*. 2021, 47, 14216–14225.
- [14] Pretorius, E.B. and Carlisle, R.G. Foamy Slag Fundamental and Their Practical Application to Electric Furnace Steelmaking. *Iron and Steelmaker*. 1999, 26, 79–88.
- [15] Pretorius, E.B. Introduction to Slag Fundamentals. Process Technology Group, LWB Refractories. <https://etech.rhimagnesita.com/>
- [16] Pretorius, E.B., Oltmann, H. and Jones, J. Fundamentals of the EAF Process. Process Technology Group, LWB Refractories and Nupro Corporation. <https://etech.rhimagnesita.com/>
- [17] Pretorius, E.B. and Marr, R. The Effect of Slag Modelling to Improve Steelmaking Processes. 53<sup>rd</sup> Electric Furnace Conference Proceedings. Orlando, USA, Nov. 12–15, 1995, 407–415.
- [18] Pretorius, E.B. and Nunnington, R.C. Stainless Steel Slag Fundamentals: From Furnace to Tundish. *Iron & Steelmaking*. 2002, 29(2), 133–139.
- [19] Schürmann, E. and Kolm, I. Mathematische Beschreibung der MgO-Sättigung in Komplexen Stahlwerks-Schlacken beim Gleichgewicht mit Flüssigem Eisen. *Steel Research*. 1986, 57(1), 7–12.
- [20] <https://etech.rhimagnesita.com>
- [21] Souza, D., López, F., Moggee, H. and Lamare, C. A Toolbox of Slag Modelling and Metallurgy in Your Pocket. *Bulletin*. 2021, 72–77.
- [22] Kirschen, M., Hanna, A. and Zettl, K.M. Improvement of EAF Process and Refractory Consumption by Advanced Slag Modelling. *Iron and Steel Technology*. 2016, 13(1), 52–59.
- [23] Sedivy, C. and Krump, R. Tools for Foaming Slag Operation at EAF Steelmaking. *Metallurgy and Materials*. 2008, 53(2), 409–413.
- [24] [https://www.rhimagnesita.com/ram-ladle-pressure-vessel-machinery/#Request\\_info](https://www.rhimagnesita.com/ram-ladle-pressure-vessel-machinery/#Request_info)
- [25] Luz, A.P., Vivaldini, D.O., López, F., Brant, P.O.R.C. and Pandolfelli, V.C. Recycling MgO-C Refractories and Dolomite Fines as Slag Foaming Conditioners: Experimental and Thermodynamic Evaluations. *Ceramics International*. 2013, 39, 8079–8085.
- [26] López, F., Farrando, A., Disante, L. and Loeffelholz, M. Slag Modelling for Optimising the Use of Fluxes in a DRI Based Steelmaking Operation. *Bulletin*. 2019, 24–29.
- [27] Bonetti, O., Mapelli, C., Memoli, F. and Porisiensi, S. Experience and Perspectives of the Recycling of EAF and LF By-Products by Injection into the EAF. 8<sup>th</sup> European Electric Steelmaking Conference Proceedings, Birmingham, UK, May 9–11, 2005, 277–288.
- [28] Luz, A.P., Tomba Martinez, A.G., Lopez F., Bonadia, P. and Pandolfelli, V.C. Slag Foaming Practice in the Steelmaking Process. *Ceramics International*. 2018, 44, 8727–8741.
- [29] Avelar, T.C., Veiga A.F., Gueguen E. and Oliveira J.R. Recycling Practices of Crushed MgO-C Bricks and Dolomite Sinter Fines Used as a Slag Conditioning Additive in the EAF, *WIT Transactions on Ecology and the Environment*. 2012, 163, 259–270.
- [30] Lammer, G., Yaseen, A., Lanzenberger, R., Rom, A., Hanna, A., Forrer, M., Feuerstein, M., Pernkopf, F. and Mutsam, N. Advanced Data Mining for Process Optimizations and Use of AI to Predict Refractory Wear and to Analyze Refractory Behavior. *Iron and Steel Technology*. 2018, 15(9), 52–60.
- [31] Viertauer, A., Mutsam, N., Pernkopf, F., Gantner, A., Grimm, G., Winkler, W., Rössler, R., Lammer, G., Ratz, A. and Persson, M. Refractory Lifetime Prognosis for RH Degassers. *Bulletin*. 2020, 36–41.

## Authors

Florian Kek, RHI Magnesita, Vienna, Austria.

Thomas Griessacher, Stahl- und Walzwerk Marienhütte GmbH, Graz, Austria.

Christoph Bauer, RHI Magnesita, Leoben, Austria.

Barbara Zocratto, RHI Magnesita, Rotterdam, Netherlands.

Richard Krump, Primetals Technologies, Linz, Austria.

Christian Koubek, Primetals Technologies, Linz, Austria.

**Corresponding Author:** Florian Kek, [florian.kek@rhimagnesita.com](mailto:florian.kek@rhimagnesita.com)



Beat Heinrich, Jean-Daniel Cousin, Roland Bühlmann and Reinhard Ehrenguber

# New INTERSTOP Sealed Tundish Gate for Billet and Bloom Casting

The increasing demands for well-elaborated, high-strength, and quality steels are driving the industry more and more towards the production of clean steel. As undesired contact with air during the casting process can negatively affect the quality of the final steel product, INTERSTOP has developed a new sealed tundish gate incorporating an inert gas purged and sealed housing. The new tundish gate is not only the response to clean steel production, it also widens the product portfolio. Now there is an INTERSTOP system available covering both billet and bloom applications. Besides these advancements, the new tundish gate offers additional features including the possibility of a three-part refractory stack-up or a tube changer option allowing the monotube to be replaced during the casting sequence. Furthermore, the new system provides significantly improved handling and operational characteristics.

## Introduction

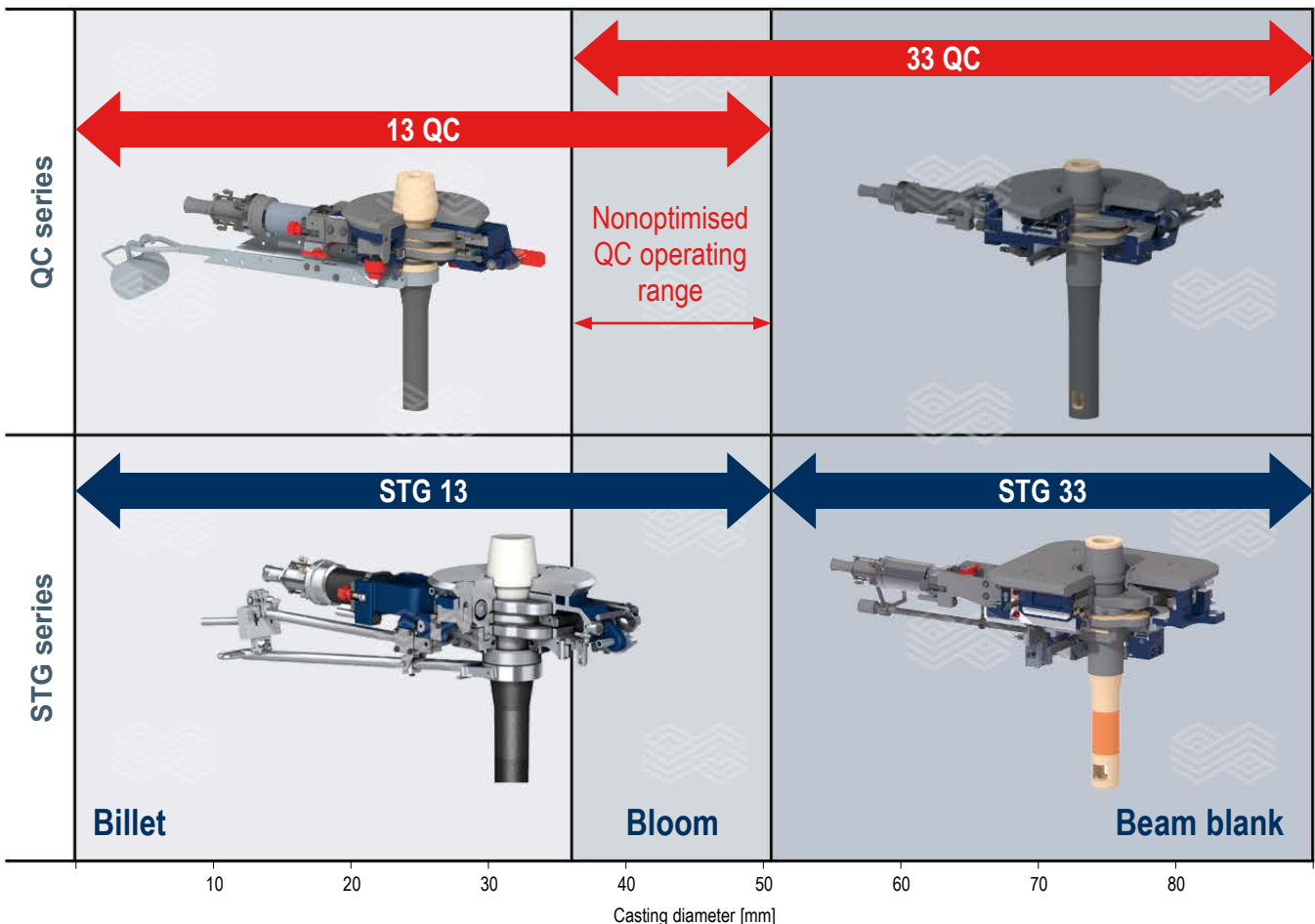
INTERSTOP tundish gates such as the 13 QC and 33 QC have been successfully operating worldwide for more than 20 years. Both products were designed for one specific format size only, namely the 13 QC for billet and the 33 QC for beam blank and slab applications; therefore, their operation for bloom applications was not optimal. As a consequence, and in response to future trends like clean steel production and long casting sequences, INTERSTOP has developed the new Sealed Tundish Gate (STG) series: The STG 13 and STG 33 (Figure 1).

With the development of the STG 13, presented below in more detail, there is now an INTERSTOP tundish gate available that is adequate for both billet and bloom applications. Therefore, in combination with the STG 33, it optimises the full range of applications including billet, bloom, and beam blank casting.

## Overview

The design of the STG 13 is modular and as a result can be configured to meet the demands and operational constraints of the customer.

Figure 1. INTERSTOP tundish gate portfolio.



The following basic options are available (Figure 2):

- Standard 4- or 5-part refractory stack-up.
- 3-part refractory stack-up for very demanding applications.
- Tube changer option enabling the customer to change the monotube during the casting sequence.

Besides the above basic options, the mechanism can be configured according to the customer requirements and operational constraints. This includes several inert gas purging options or submerged entry shroud (SES) holder solutions with a flexible mounting orientation. Furthermore, the STG 13 is designed to fit most of today's tundish and cylinder interfaces for billet and bloom applications.

In addition to the successful INTERSTOP 13 QC, the new generation tundish gate STG 13 provides further improved features and characteristics such as:

- Casting diameter up to 50 mm.
- A sealed argon-purged housing.
- Self-adjusting plate clamping mechanism.
- Full thermal compensation of the system tension.
- On-tundish refractory replacement allowing exchange of a damaged monotube in the 3-part refractory stack-up (see Figure 2b).
- Backlash-free couplings and interfaces to minimise the impact on mould level control.
- Easy and swift handling characteristics.

### Sealing Concept

The housing of the STG 13 is sealed and purged with an inert gas to prevent air contact with the liquid steel, which is known to negatively affect the final product quality.

With the presence of an inert gas atmosphere in the housing, contact with air in the critical under-pressure regions of the steel flow, typically underneath the throttling area, is excluded as inert gas is aspirated instead of air. Furthermore, for very demanding applications, the STG 13 features, besides the inert gas purging of the housing, additional connections for direct inert gas supply to (Figure 3):

- The upper nozzle.
- Lower plate.
- Interface between the lower plate and SES.

**Figure 3.**

Sealing concept.

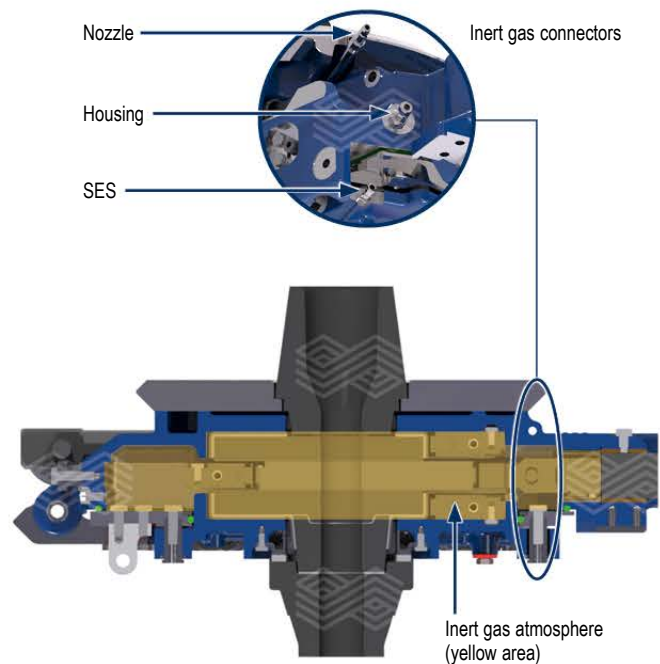
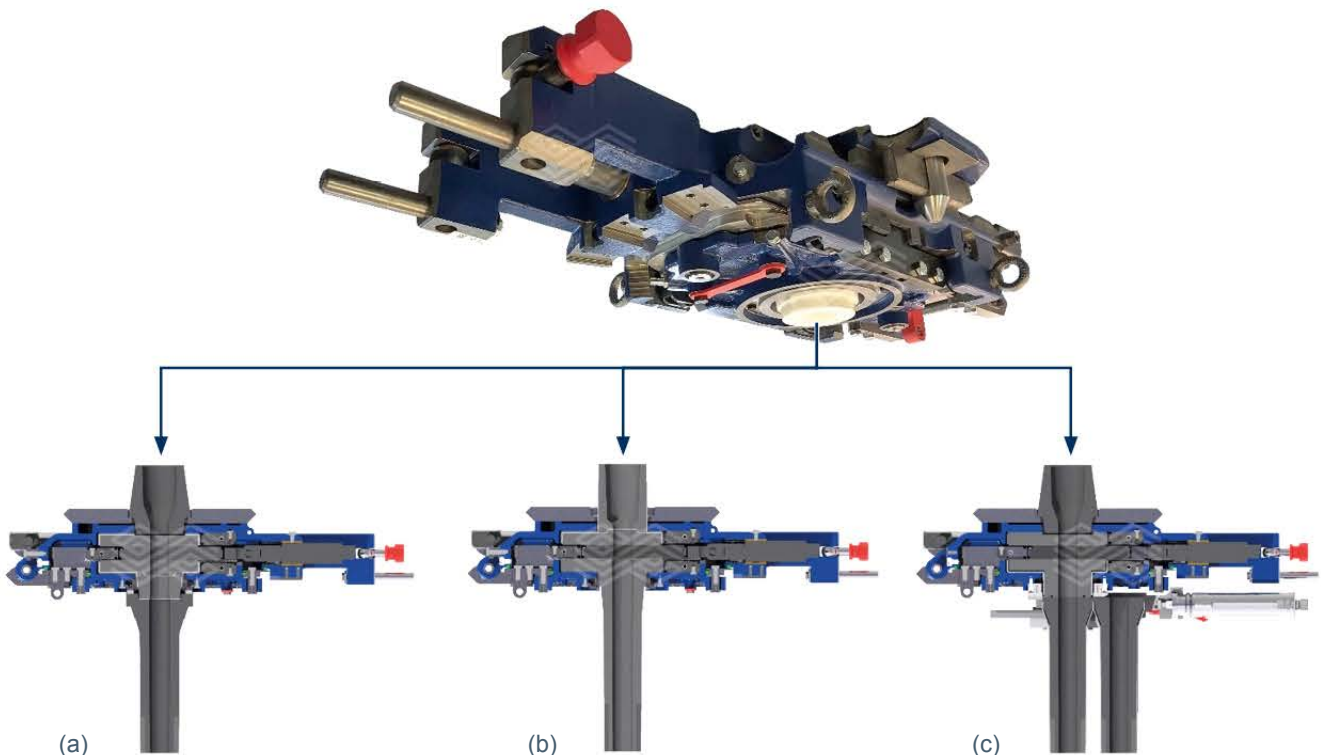


**Figure 2.**

STG 13 product configurations: (a) standard, (b) 3-part refractory stack-up, and (c) tube changer option.



Since joints provide potential passage for air ingress, their elimination in the context of clean steel production is a simple solution. Consequently, the STG 13 can be operated using a 3-part refractory stack-up to eliminate all static joints. In this configuration the refractories are composed of only three parts:

- A mononozzle combining the upper nozzle with the upper plate.
- The middle plate.
- An integral slide gate (ISG) monotube, where the plate is located inside the tundish gate.

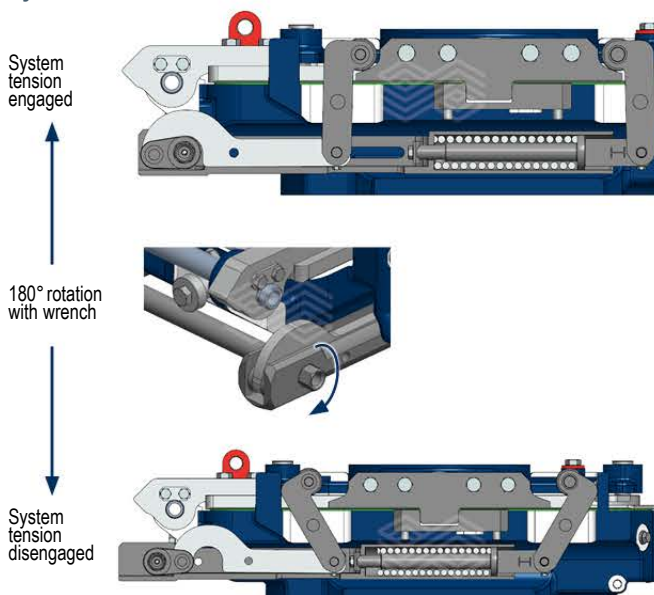
Nevertheless, depending on the steel quality produced and the operational constraints, conventional 4- or 5-part refractory stack-ups are also available.

### System Tension

Unlike previous products, where plate tensioning is achieved by bolts tightened to a well-specified torque, the system tension on the STG 13 is achieved by a spring-loaded mechanism. As shown in Figure 4, the tension force delivered by two springs is transmitted through a leverage system to the cover plate, pressing the three plates together.

By performing a half turn with a standard wrench in a clockwise direction, the system tension is engaged, namely there is no need for a specific tool or torque wrench as the required force is applied automatically. By driving the linkage back half a turn, the tension load is disengaged and the mechanism remains in the over-centre position. The levers themselves incorporate rolls that in combination with the specifically inclined contact plane of the cover plate provide a constant pressure to the refractory plates independent of thickness variations due to thermal expansion/shrinkage and/or manufacturing tolerances. Moreover, by using rolls instead of sliding contacts, the pressure loss due to friction is greatly reduced.

**Figure 4.**  
System tension.



It should also be noted that the sideways arrangement of the leverage system, parallel to the cylinder axis, allows the mechanism to be built very compactly.

Although, in general, offline replacement of the refractories is the standard process, an on-tundish replacement of the ISG monotube and middle plate is now possible due to the new tensioning system. This possibility is of particular importance as damage to the ISG monotube during the preparation work cannot be entirely excluded. Once the tension is released, the cover plate can be swivelled down using a simple tool and the ISG monotube replaced (Figure 5). This operation can be performed manually by a single person without requiring heavy and bulky equipment such as lifting trolleys.

Prior to cold and hot testing at full assembly level, the development included several functional model tests to mitigate any development risks. A functional model to test the performance of the tension system was also built as this component was identified as one of the most critical (Figure 6). The functional model underwent an exhaustive test programme including all operational process steps as well as all relevant failure modi, for example loss of a lever or a spring. Handling errors were also considered during these tests.

**Figure 5.**  
On-tundish refractory replacement.

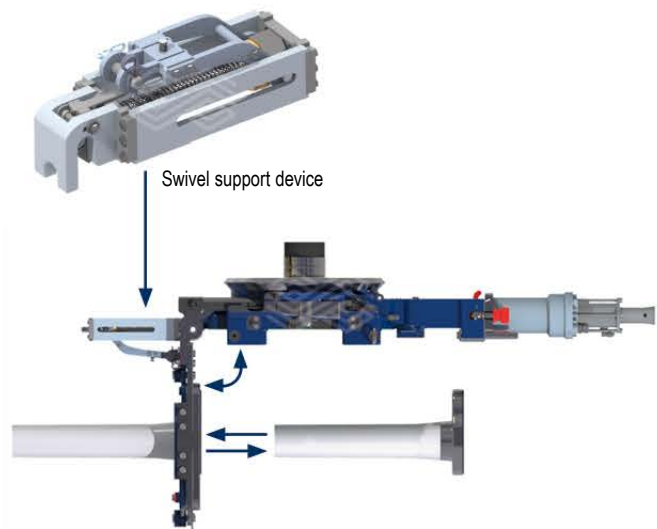


**Figure 6.**  
System tension functional model.



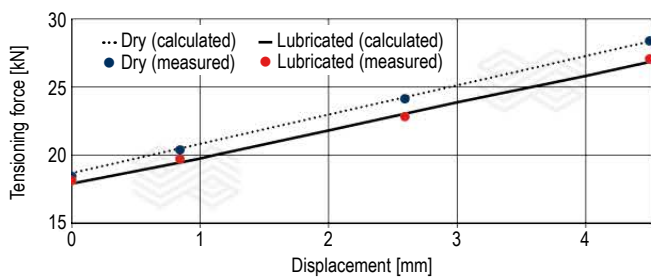
As shown in Figure 7, the tension forces measured during the functional model tests were very well within the test predictions. Even for failure cases such as loss of a lever or a spring, the tests showed that the tension system still provides a sufficiently uniform pressure to the plates.

### Plate Clamping

In most of the slide gates today, plate clamping is achieved by torqued bolts or screw spindles pushing via an interface part against the plate brick. The main drawback of this method is that in the case of larger thermal expansion of the mechanism or plate shrinking, the plates could become loose.

In addition, it is likely bolts or screw spindles can become loose due to vibrations. A loose plate clamping is particularly critical for the middle plate, as gapping between the plate brick and plate frame may likely occur due to the continuous change of the loading condition by the mould level control (MLC). Consequently, the plate brick no longer properly follows the motion given by the MLC and thus will negatively affect the stability of the mould level. By using a spring-loaded wedge, resistive forces between the plate brick are no longer exported to the clamping mechanism. Furthermore, in case of different expansions, the clamp part automatically readjusts. The plate clamping mechanism is shown in Figure 8.

**Figure 7.**  
Measured versus calculated system tension.



### Submerged Entry Shroud Holder

In the frame of further increasing the ease of use, the STG 13 provides additional new features and tools. These include a new counterweight-free SES holder and the new spring tester.

Unlike conventional SES holders, the SES loading is achieved by springs instead of weights. Thereby, heavy weights no longer have to be lifted by the operators. Moreover, the SES holder is mountable in three different orientations (in 16° steps), ensuring better accessibility for the operators (Figure 9).

**Figure 8.**  
Plate clamping mechanism in (a) clamped and (b) unclamped condition.

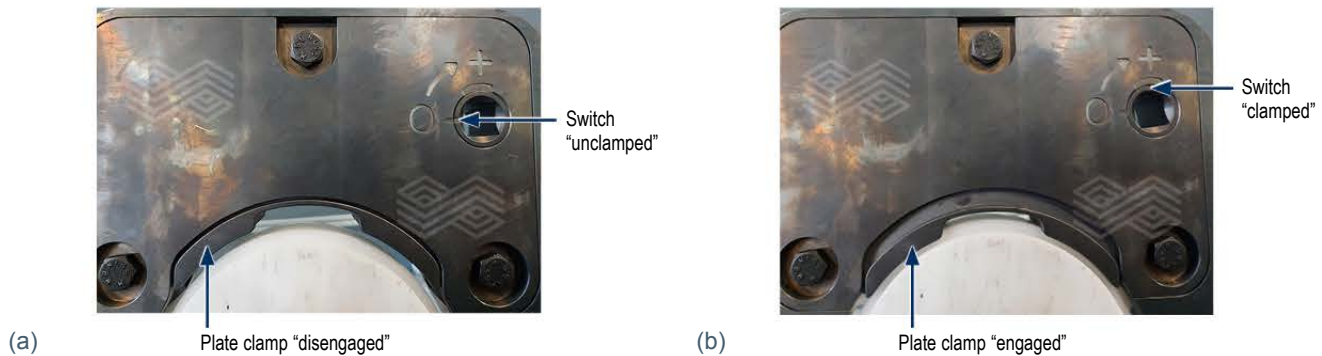
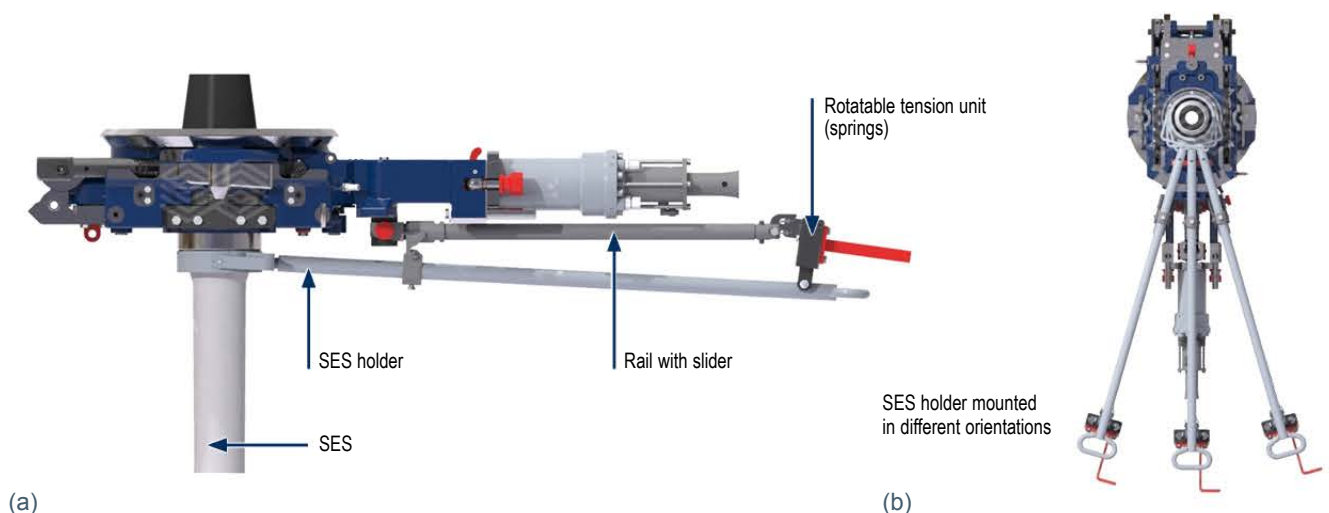


**Figure 9.**  
(a) spring-loaded SES holder and (b) SES holder mounted in different orientations.



---

## Spring Tester

The new spring tester enables the tensioning force to be measured directly. This measurement is more accurate than measuring the springs individually as the complete load path, including all resistive contributors, is considered. Furthermore, laborious disassembly to access the springs for the measurement is not required.

---

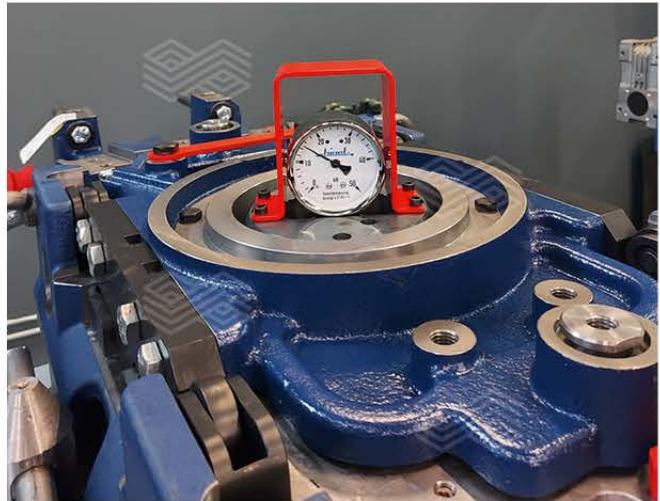
## Conclusion

The STG 13 completes the INTERSTOP product portfolio of sealed tundish gates and sets the new standard for clean steel casting of billets, blooms, or beam blanks. Due to the very failure-tolerant design, the new tundish gate is also considered a major step forward in terms of operational safety and system availability. The system performance, for example longer casting sequences, is generally improved and disturbances to the mould level are mostly eliminated by the new backlash-free couplings. In addition, the effort for maintenance and handling the STG 13 is significantly reduced.

---

**Figure 10.**

Spring testing device integrated on the STG 13 tundish gate.



## Authors

Beat Heinrich, RHI Magnesita Interstop AG, Hünenberg, Switzerland.  
Jean-Daniel Cousin, RHI Magnesita Interstop AG, Hünenberg, Switzerland.  
Roland Bühlmann, RHI Magnesita Interstop AG, Hünenberg, Switzerland.  
Reinhard Ehrenguber, RHI Magnesita Interstop AG, Hünenberg, Switzerland.  
**Corresponding author:** Beat Heinrich, [beat.heinrich@rhimagnesita.com](mailto:beat.heinrich@rhimagnesita.com)

Andreas Rief, Aloyso Oliveira Figueiredo, Markus Fasching and Markus Gruber

# Ladle Well Filler Sands for All Needs

High-quality steel production depends on a fluent flow process from the ladle to the mould. This can only be achieved when there are no interruptions in the casting sequence due to blocked casting channels or other failures. To provide a continuous flow of steel from the ladle into the tundish, the correct application and quality of well filler sand (WF) is a key factor. The article draws attention to the critical points regarding reliable ladle opening and selection of well filler grades. The function and behaviour of typical chrome ore based WF in the field and new developments to improve opening rates, like the double layer technology, are also described.

## Introduction

Well filler sand (WF) is an essential part of fluent and high-quality steel production. However, it is rarely in focus at the steel plant as long as it is functioning, namely ensuring free opening of the ladle at the caster. WF is filled in the casting channel of the ladle, seldomly also in the tundish, and inhibits steel intrusion and freezing during steel treatment. This paper provides a general overview regarding application of WF at the customer and the different qualities available on the market. The main goal is to offer the best solution for each customer and gain a deeper understanding of the mechanisms important to guarantee free opening of the ladle. It is not only about selling high-quality products to improve the customer process, for the optimal solution a holistic approach is necessary. Therefore, RHI Magnesita offers a wide range of WF from production sites all over the world, from standard grades to high tech applications, as well as providing the customer with a better service to increase opening rates at the caster through an understanding of the process going on in the casting channel [1–5].

## Application of Well Filler Sand in the Field

Free opening of the ladle is an important quality factor for steel production and a major wish of all steel plant staff at the caster. Furthermore, there are health and safety issues for staff if they have to use oxygen lances to start casting and often the steel quality must be downgraded, or even complete loss of the steel batch can result from a blocked casting channel. There are many factors affecting free opening of the casting channel. As shown in Table I, a number are related to the design of the steel plant equipment, some are linked to operational conditions at the customer, and others pertain to the WF itself [1–9].

Our experience has shown that the WF quality plays a minor role compared to the other factors. Several examples from the past have shown that the opening rate increased significantly after customers installed a proper cleaning procedure or increased the amount of sand used.

If everything has been done at the customer to ensure optimal handling, the final approach is to select the best fitting product quality. Here, RHI Magnesita offers a wide range of WF grades for any purpose, which will be described in detail later. Typical WF consists of chrome ore, quartz sand, and a carbon carrier. Besides the chrome ore based sands, zircon sand containing grades are also common in some regions like North America. However, the following paper will only refer to standard chrome ore containing WF grades.

**Table I.**  
Variables affecting casting channel free opening rates.

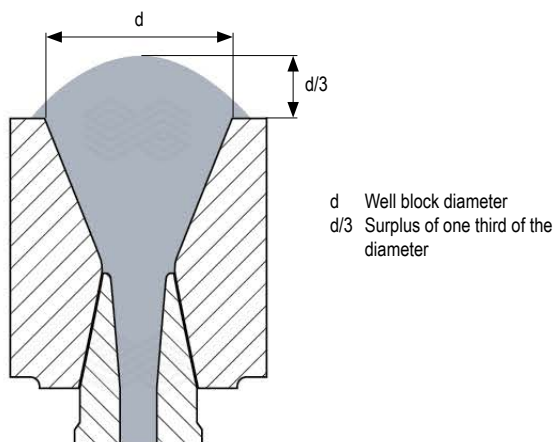
| Steel plant related variables          | Operational conditions   | Well filler sand quality    |
|--|--|-----------------------------|
| Ladle size—ferrostatic pressure        | Efficiency of the casting channel cleaning process                     | Flowability                 |
| Geometry of the well block             | Method used to place the sand in the well block                        | Thermal expansion           |
| Bore diameter of the nozzle and plates | Applied amount of WF   | Wettability by molten steel |
|  | Well block repair method and frequency                                 | Sintering rate              |
|  | Number of ladles in cycle—average temperature of the refractory lining | Permeability                |
|  | Average casting temperature  | Moisture content            |
|  | Average steel residence time in the ladle                              |                             |
|  | Type of steel produced   |                             |
|  | Easy segregation of WF by excessive handling                           |                             |

But what is known about the correct handling and mechanism of WF, as well as the process happening in the casting channel after tapping? Unfortunately, it's not possible to have a close look in the casting channel during operation and laboratory trials can only give a rough assumption of the things happening. However, the many experiments described in the literature and those performed in RHI Magnesita's laboratories provide an overall picture [2–4,7–10].

The WF process can be divided into four steps (Figure 1 and Figure 2). Firstly, the right amount of WF must be considered when filling the casting channel. It must be ensured that the channel is completely filled and that a heap with a height of at least  $1/3$  the well block diameter (at the uppermost point) is formed (see Figure 1). The amount of "over-filling" the casting channel is based on RHI Magnesita's experience and is also similarly described in the literature [4,5,11]. An excess amount of 30% related to a fully filled casting channel has been reported as optimum by our customers. Depending on the exact well block geometry, this 30% corresponds to approximately the  $1/3$  minimum filling height given as our advice.

**Figure 1.**

Minimum filling height of the casting channel.



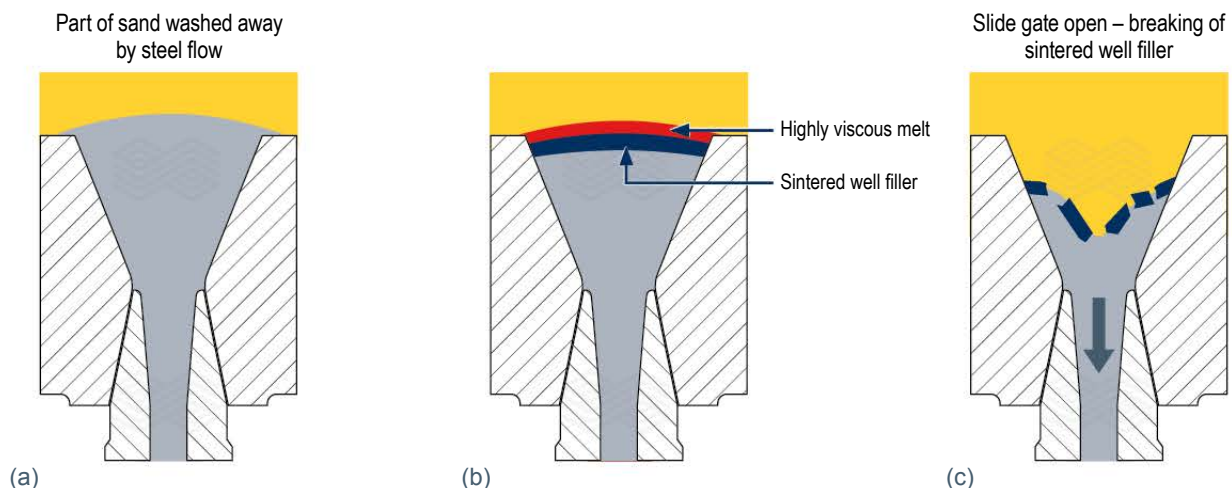
During a typical ladle preheat of up to  $1000\text{ }^{\circ}\text{C}$ , only decarburisation of the upper most sand layers occurs and no sintering or even melting of standard sands happens at these temperatures. Simple tests performed by heating WF in quartz tubes with air have shown oxidation rates of  $3\text{--}14\text{ mm/hour}$  depending on the carbon content and grain size. While in the field this factor may play a minor role regarding the opening rate as typically WF is applied only shortly before casting, our experience suggests that decarburised sand has a negative impact on opening rates. In contrast, the literature reports a worse opening rate associated with a higher carbon content; however, this was with blast furnace iron rather than steel [1] and indicates that further research is required to fully understand this topic.

During steel tapping into the ladle some of the WF heap is washed away depending on the tapping position and speed; however, ideally the sand heap survives the tapping process (see Figure 2). It is assumed that during steel treatment a highly viscous melt forms above a thin sintered WF layer. Subsequently, when the slide gate is opened the ferrostatic pressure of the steel bath above breaks the sintered layer and casting starts [4–6,9,11]. The loose sand below the sintered layer flows unhindered through the channel and into the ladle shroud.

From laboratory experiments we have seen that above  $1250\text{ }^{\circ}\text{C}$  the WF quartz components begin to sinter and form a highly viscous melt containing solid chrome ore grains. Published FactSage simulations of WF with different chrome ore content indicate the formation of melts above  $1300\text{ }^{\circ}\text{C}$ , interestingly widely independent of the silica content [2]. However, our team calculated slightly higher temperatures for the first melt appearance, for example  $1390\text{ }^{\circ}\text{C}$  for a 70% chrome ore containing WF. The chrome ore grains themselves are slowly reduced by the carbon carrier to metals and partly degenerate by a diffusion process. As the limited carbon is quickly consumed, only the grain surface degenerates to a glassy phase supporting sintering of the chrome ore grains. The thickness of the sintered layer and amount of melt formed correspond to the WF composition. With short treatment times below 1 hour, sintered layers are

**Figure 2.**

Ideal behaviour of WF during application.



usually thin and can be easily broken by the steel pressure and the WF quality plays a minor role. However, the longer the treatment time the more important correct selection of the sand composition becomes. Nevertheless, above a steel treatment duration of 4–5 hours it is rather unlikely to achieve high opening rates with standard WF grades. For these cases special solutions like the double layer technology or coated WF have been developed [4,9].

The thickness of the WF sintered layer and reaction zones can be estimated using temperature simulations of the casting channel. Field temperature measurements described in the literature [1] fit very well with the simulations performed (Figure 3). For the simulation described below thermal parameters of a ladle bottom used at an American customer were used. The ladle had an alumina well block and inner nozzle, and the calculations were performed with a dwell time of 200 minutes. The ladle was preheated to 900 °C and the steel temperature was set at 1700 °C. The measured thermal conductivity of the WF was 0.6 W/mK at 1000 °C. The simulations showed that the temperature gradient in the filled casting channel was quite high. Three different filling levels were used as a starting point, namely optimal overfilling and two cases of insufficient filling. These starting points are shown with the temperature distribution after 200 minutes steel treatment in Figure 3. The temperature range of 1250–1390 °C, in which the WF sinters with only a thickness of 3–4 cm, is indicated in Figure 3 as a solidus line. These temperatures were selected according to the first quartz sintering and the first melt formation. In the best case (see Figure 3a) the area with sintered WF is above the casting channel and easily broken by the ferrostatic pressure. In the cases where the casting channel is insufficiently filled there is either a sintered layer in the channel which has a suboptimal thickness to area ratio (see Figure 3b) or the steel is already frozen with more than a 16 cm thick solid layer of steel formed (see Figure 3c) [1,4].

As steel treatment can sometimes last several hours, the solidus line moves down the casting channel. As seen in the above simulation, the opening rate is then expected to drop significantly. This is widely confirmed by observations in the

field. To tackle such demanding conditions special solutions have been developed. One common option offered to customers is WF containing zircon sand or coated WF, but these only slightly increase the opening rates [11]. Therefore, to tackle long treatment times more effectively, RHI Magnesita developed the double layer technology described later in this paper.

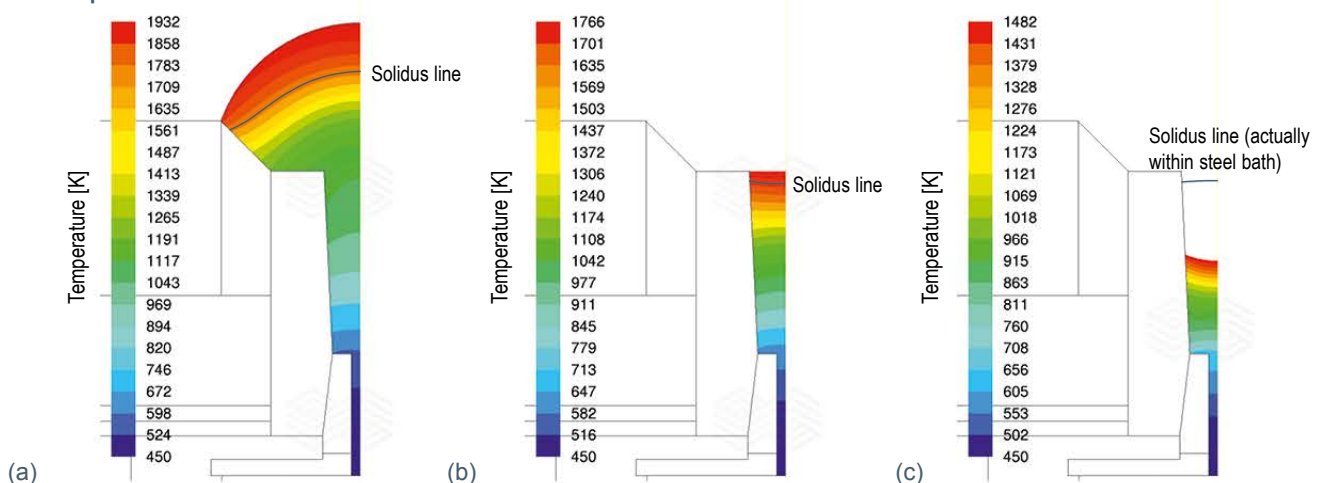
The correct handling or addition of WF is as important as cleaning the casting channel and WF quality. In the past several different methods for filling sand into the casting channel were developed. In general, these can be split into two groups, namely manual and automatic feeding as shown in Figure 4.

Figure 4a depicts one of the manual methods where bags containing WF are thrown into the ladle by caster staff aiming to hit the casting channel. However, it is not only difficult to hit the best position using this approach but also the ideal filling level with the characteristic sand cone cannot be achieved. Furthermore, by throwing the whole bag the packaging material is also introduced. This can influence the sintering behaviour negatively, especially when plastic bags or foiled paper bags are used. In the second manual case, a tube or chute is used for filling (see Figure 4b). Thereby, the ideal filling level as well as the characteristic sand cone can be achieved. However, pouring the sand through the funnel leads to segregation of the different components due to differences in density and grain size, which has a negative influence on the opening rate. In both manual cases the employee is exposed to the heat of the ladle.

Automated addition of WF can be performed using a funnel or basket that is lowered down to the bottom of the ladle (see Figures 4c and 4d). However, like manual filling with a funnel the automated version also has the disadvantage of segregation. This does not occur in the version where the container is lowered. In both cases the employee can operate the machines from a safe position and is not exposed to the heat of the ladle. It is also possible to adjust the necessary WF amount due to the combination of different optical systems incorporated in the handling machine [5,6].

**Figure 3.**

**Simulation of the temperature distribution in the casting channel filled with WF at three different filling levels. (a) optimal filling and (b–c) insufficient filling with expected low opening rates. The representative temperature colours are not equivalent in the three examples.**



Ideally all these filling options go hand in hand with proper casting channel cleaning and even a camera-supported check of the cleaning. RHI Magnesita can offer a semi-automated system as depicted in Figure 4d and a corresponding prototype is in operation at a South American customer.

Segregation of WF should be avoided as much as possible. However, due to the huge difference in density between chrome ore and silica sand suboptimal application of WF can occur and even sampling for quality control can lead to false results and discussions with the customer as well as production plant.

### Well Filler Sand Raw Materials and Properties

WF is mainly composed of three raw materials types, namely chrome ore, silica sand, and a carbon carrier. These can significantly influence the behaviour of the WF, depending on the raw material properties and also the way in which the WF is designed. The WF should be designed with a focus on the following final properties [2–10]:

#### Flowability

Flowability is a very important property of WF as it affects free flow of the sand when the slide gate is opened [10]. This property is strongly related to the packing efficiency of the grains and therefore, when creating a WF recipe, it is very important to guarantee a low packing efficiency.

One of the ways to achieve this is using raw materials with a controlled grain size distribution, usually in the range of 0–1 mm. Another important point to increase flowability is the use of natural raw materials. These raw materials are often found in sand deposits and are exposed to chemical

and physical attack over the years enhancing formation of spherical shaped grains (Figure 5). This enables easy movement of the grains against each other and a low friction process.

**Figure 5.**

Typical natural (a) silica sand grains and (b) chrome ore grains.

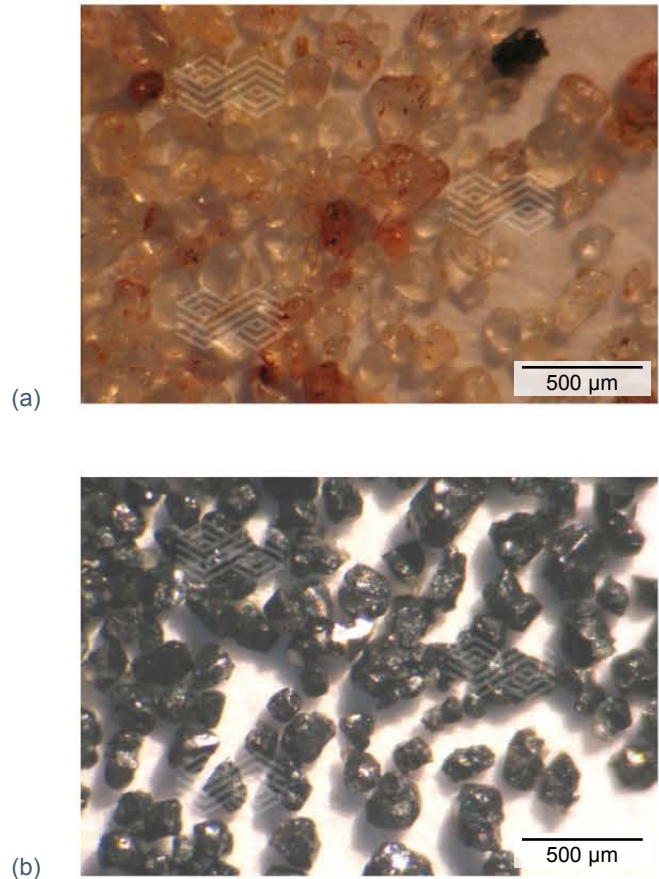
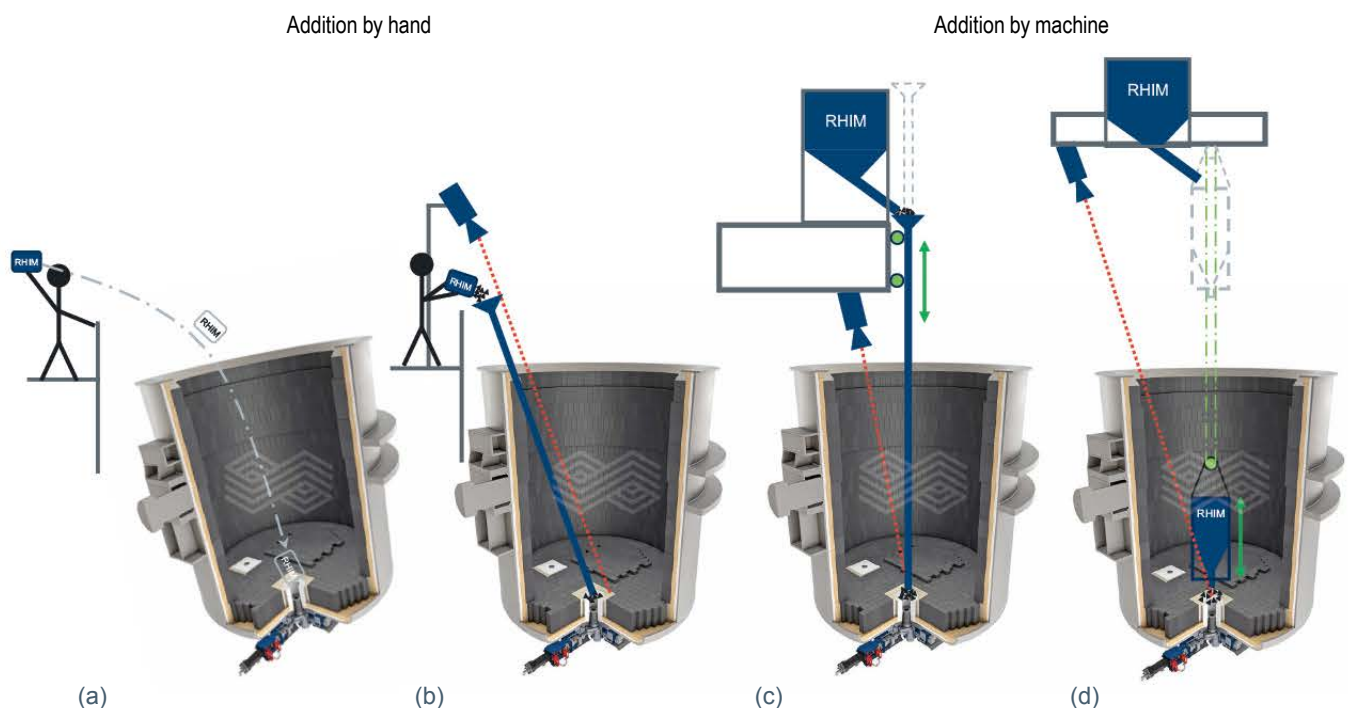


**Figure 4.**

Different sand filling methods. (a) manual throwing of bags, (b) manual filling with a funnel, (c) automatic filling with a funnel, and (d) automatic filling with a basket.



Artificial man-made raw materials, normally originating from a grinding and sieving process, tend to have grains with a rough and multi-faceted surface. This impairs the movement of the grains against each other and reduces flowability.

Another variable to increase the flowability of WF is including a carbon source in the formulation. Carbon can act as a lubricant and supports movement of the grains against each other.

### Thermal expansion

The thermal expansion behaviour of WF is a property that influences the flowability and as a consequence the free opening rate. If a given WF has a high thermal expansion, it will exert a high pressure against the well block and nozzle walls when it is heated. As a result, the WF is under a high compression force that will impair its free flow out of the casting channel. As silica sand has a higher thermal expansion than the chrome ore, silica sand rich WF will tend to present a higher thermal expansion and consequently a lower free opening rate. This is especially valid for steel shops with a small bore diameter.

### Low wettability by molten steel

The introduction of a carbon source in the WF promotes a decrease in the wettability of the sand by molten steel. This decreases the likelihood of steel penetration into the open pores of the sand structure [1,2].

### Sintering rate

As already mentioned, the WF should have a controlled sintering process. Nevertheless, the sintering rate should not be too intense, otherwise the ferrostatic pressure will be insufficient to break it down so it can flow through the bore of the nozzle and plate [7,9]. In order to control the sintering rate, two important points should be considered:

- Sieve analysis of the WF: It is advisable to reduce the fines in order to minimise the number of grain-to-grain contacts; thereby, decreasing the sintering rate [2,8].

- Purity and homogeneity of the raw materials: Close attention should be paid to the presence of contaminants in the raw materials as they might increase the sintering rate of the WF and negatively impact the free opening rate of the ladle.

### Permeability

To decrease the WF permeability and decrease the chance of steel infiltration, one of the best approaches is to reduce the pore size of the WF. This is achieved by using as much fine raw material as possible. However, this contradicts what was described in the previous point regarding the WF sintering rate. Therefore, it is necessary to balance all the variables in order to develop a WF that best fits the customer needs.

### Moisture content

It is important to mention that most of the natural raw materials used to produce WF go through a washing process with water to remove by-products and impurities. After contact with water, it is essential to dry the raw materials, thereby guaranteeing the lowest moisture content in the product.

According to observations at customer sites, with an increased moisture content above 0.5% a greater tendency towards lower free opening rates is observed. The explanation for this behaviour is related to the water vaporisation when the WF is added to the ladle, which causes a dislocation of the WF and possible penetration of steel into the well block [7]. Therefore, not only the moisture of the raw materials is important, but also the WF packaging system and storage conditions at the customer's site [7].

## RHI Magnesita's Well Filler Sand Portfolio and Production

RHI Magnesita offers a wide range of WF grades (Table II). The production sites are in Europe, South America, and Mexico with resale partners in South Africa and China.

**Table II.**

RHI Magnesita WF portfolio (excluding China).

| Grade                                 | Chrome ore [%] | Silica [%] | Zirconia [%] |
|---------------------------------------|----------------|------------|--------------|
| ANKERFILL WF0-BR*                     | 0.0            | 95.4       | -            |
| ANKERFILL WF10                        | 10.0           | 76.5       | -            |
| ANKERFILL WF20                        | 20.0           | 55.0       | -            |
| ANKERFILL WF32                        | 32.0           | 30.0       | -            |
| ANKERFILL WF33RB (coated well filler) | 33.0           | 28.0       | -            |
| ANKERFILL WF34                        | 34.0           | 25.0       | -            |
| ANKERFILL WF34-BR*                    | 33.7           | 25.5       | -            |
| ANKERFILL WF37                        | 37.0           | 19.0       | -            |
| ANKERFILL WF37-BR*                    | 37.3           | 16.7       | -            |
| ANKERFILL WF40                        | 39.0           | 14.0       | -            |
| ANKERFILL WF45-BR*                    | 41.3           | 10.6       | -            |
| ANKERFILL WF9ZR                       | 9.0            | 33.0       | 45.5         |
| ANKERFILL WF15ZR                      | 15.0           | 27.0       | 39.5         |

\* South American production site

Packaging options range from 5 kg paper bags up to 1.5 tonne big bags. As described above, the correct grade selection depends on many factors that should be discussed in advance with our experts.

### Double Layer Technology

As a special solution for long treatment times, RHI Magnesita developed the double layer technology to tackle low opening rates (Figure 6).

This technology can be described as follows:

- The top part of the WF, that forms the so-called “mushroom” covering the well block, exhibits a controlled sintering process in the preheating stage, to avoid steel penetration into the sand.
- The middle and lower region of the sand are not supposed to sinter, enabling free opening of the ladle when the slide gate opens.

The points above represent the ideal situation to obtain the highest possible free opening rate of the ladle and avoid the need for oxygen lancing. This means not exposing the worker to a high-risk operation, as well as avoiding any negative impact on the steel quality.

Based on the aforementioned points, the idea was to develop two types of sand used in combination, or what is called the double layer sand. The following combination of sands is available in the RHI Magnesita portfolio:

- ANKERFILL WF0-BR: One third of this material is used for the upper layer with sintering occurring at around 1000 °C (preheating temperature).
- ANKERFILL WF45-BR: This material has a high refractoriness and two thirds are used for the lower layer. Round shaped silica sand grains are added to help the flowability of the sand. A carbon source is also included to increase the flowability.

Some characteristics of this two-layer WF technology include:

- It should be used at customers with special needs and high demands on opening rates.
- The sand must be added in the correct sequence and amount. This requires special filling equipment (see Figures 4b–4d) and careful attention from the plant staff. Any incorrect filling must be strictly avoided to guarantee free opening.
- The two sands should look like Figure 6 after application.
- This two-sand technology should be used at customers with low opening rates due to their harsh operational conditions, namely high tapping temperature, long ladle treatment time (> 2 hours), and nozzle bore diameters smaller than 60 mm.

### ANKERFILL 33RB Coated Well Filler Sand

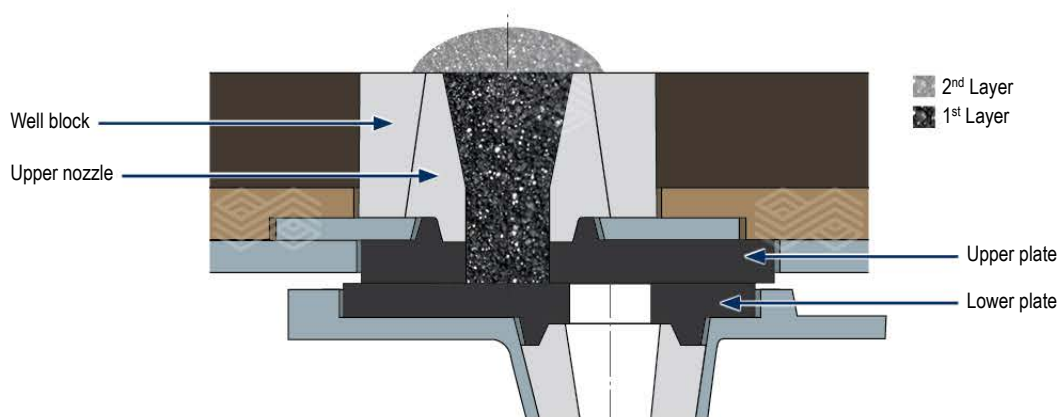
Among the types of WF supplied by RHI Magnesita, there is one special product where the grains are coated with a carbon layer. The basic raw materials (i.e., chrome ore and silica sand) are the same as in common grades. However, the applied carbon layer offers a better surface protection to reduce sintering and also increases flowability by giving the grains a spherical shape. This sand is recommended for customers that work with long ladle treatment times, usually > 2 hours, and also with a plate bore diameter below 60 mm.

Figure 7 shows the different appearance of the carbon-coated ANKERFILL WF 33RB compared to a standard WF with carbon black addition. The standard sand is only partially covered by the carbon black or micro graphite used as the carbon carrier. This leads to an inhomogeneous carbon distribution.

In contrast, the coated sand has a shiny homogeneous surface covering all the chrome ore and silica grains (Figure 7b). According to microscopic evaluations, the entire surface of the grains is covered, which makes the sintering process of the sand more difficult. Therefore, this WF behaves well in very aggressive operational conditions where other types of WF would not provide a good free opening rate.

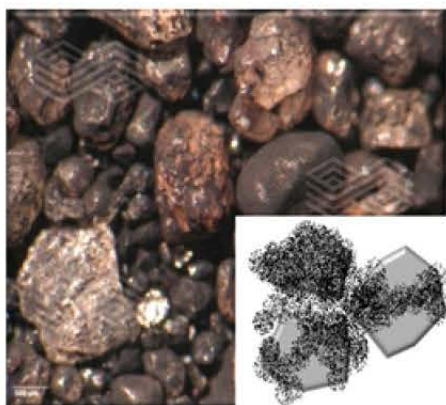
Figure 6.

Schematic drawing of the double layer technology.

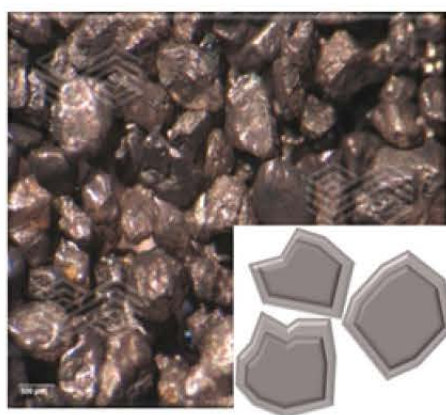


**Figure 7.**

(a) traditional WF with carbon black addition and (b) WF where the grains are coated with a carbon layer.



(a) ANKERFILL WF34-BR



(b) ANKERFILL WF33RB

## Conclusion

Worldwide, the ideal situation for any steel plant is to operate with a 100% free opening rate in their ladles. If the casting channel is blocked shop floor staff have to use an oxygen lance to remove the blockage, which exposes them to unsafe conditions and reduces the steel quality being cast. In order to help steelmakers work according to the ideal situation, RHI Magnesita offers a broad portfolio of WF, from where the most suitable grade can be selected to best fit the operational conditions at the steel plant. Since there are many variables involved in this process, it is very important to have a close discussion between the RHI Magnesita technicians and the customer to fully understand the operational conditions and thereby define the best WF to fulfil the needs.

It must be highlighted that the best quality WF will not guarantee a high free opening rate due to the numerous factors influencing a free flow. The steelmaker should ensure that the correct procedure is being followed on their shop floor to provide a good well block and nozzle channel cleaning process, as well as guarantee that the WF is being handled and applied in the right way without any segregation. Since there are many variables involved in the process, none of them must be neglected to assure a high free opening rate.

## References

- [1] Bombeck, M., Janssen, M., Breitzmann, M., Deinet, T. and Dannert, C. Ladle Well Filler – The Key to High Free Opening Rates. *2015 UNITECR Conference Proceedings (Proceeding 100)*, Vienna, Austria, 15–18 Sept., 2015.
- [2] Da Cruz, R., Pelisser, G., Bielefeldt, W. and Bragança, S. Free Opening Performance of Steel Ladle as a Function of Filler Sand Properties. *Materials Research*. 2016, 19(2), 408–412.
- [3] Vitlip, C. Evaluation of Ladle Free Open Performance. *Iron & Steelmaker*. 1996, 6, 55–59.
- [4] Bombeck, M., Janssen, M., Dannert, C., Deinet, T. and Izaskun Alonso, O. Fundamental Research on the Functionality of Well Fillers. *Stahl und Eisen*. 2016, 136(8), 35–44.
- [5] Morais, F., Costa Neto, J., Amaral, E., Penna, L., Bosco, M., Ramalho, J. and Almeida, J. An Overview of Ladle Free Open Performance at ArcelorMittal Monlevade. *Rev. Met. Paris*. 2008, 105, 115–120.
- [6] Tajik, R., Holke, C. and Nugin, J. *The Influence of Placement and Sintering Time of the Steel Ladle Filler Sand*, Thesis, KTH Royal Institute of Technology, Sweden, 2018.
- [7] Seixas, M., Lavinhas, A., Bezerra, M., Valadares, C., Noma, K., Emi, M. and Uchiyama, H. Moisture Influence on Performance of Nozzle Filler for Continuous Casting of Steel. XXXIX Steelmaking Seminar – International. 2008, May 12–16. Curitiba, Brazil.
- [8] Zhiyin, D., Glaser, Bombeck, M. and Sichen, D. Mechanism Study of the Blocking of Ladle Well Due to Sintering of Filler Sand. *Steel Research International*. 2016, 87(4), 484–493.
- [9] Kuo, C.H., Chen, K.M., Chen, L.H., Wu, C.H. and Hsiao, C.K. Improvement in Free Opening Performance of Ladle Filler Sand. *China Steel Technical Report*. 2020, 33, 36–42.
- [10] Farshidfar, F. and Kakroudi, M. Effect of Chromite-Silica Sands Characteristics on Performance of Ladle Filler Sands for Continuous Casting. *Journal of Iron and Steel Research*. 2012, 19(3), 11–13.
- [11] Bombeck, M., Janssen, M., Deinet, T. and El Gammal, A. Verhalten von Schiebersanden bei Kontakt mit flüssigem Stahl. *Stahl und Eisen*. 2019, 139(4), 46–50.

## Authors

Andreas Rief, RHI Magnesita, Leoben, Austria.  
 Aloyso Oliveira Figueiredo, RHI Magnesita, Contagem, Brazil.  
 Markus Fasching, RHI Magnesita, Vienna, Austria.  
 Markus Gruber, RHI Magnesita, Leoben, Austria.  
**Corresponding author:** Andreas Rief, andreas.rief@rhimagnesita.com

Rodrigo Ribeiro, Alexandre Resende, Carlos Lares and Marcos Manso

# Numerical Simulation as a Tool to Improve Energy Efficiency During Operation of a Continuous Casting Tundish

## Introduction

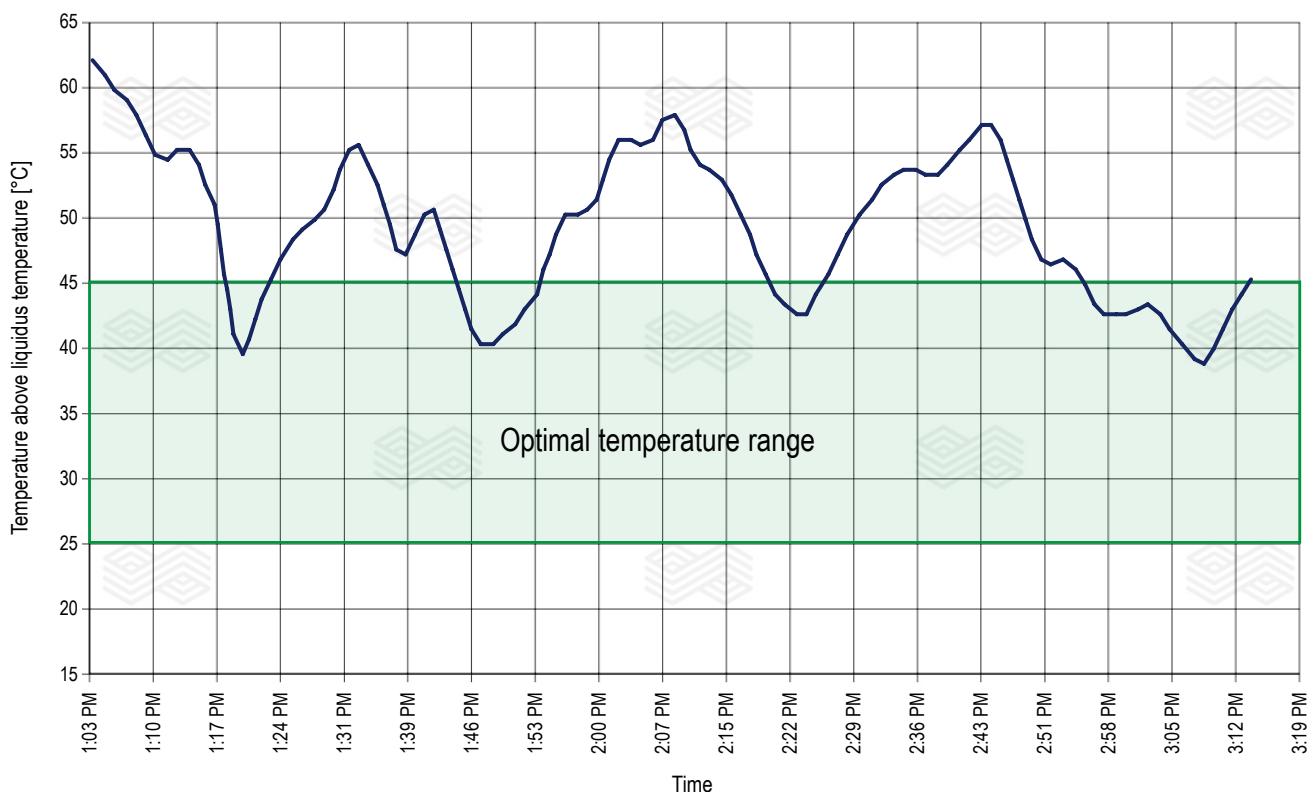
The tundish is a metallurgical vessel with the main role to maintain a reservoir of molten steel to feed the casting machine during ladle exchange. It also contributes to steel cleanliness through inclusion capture by the slag, and together with suitable refractory furniture, it can improve the kinetic energy dissipation of the incoming jet and help in temperature conservation and homogenisation, avoiding freezing and providing similar temperatures to the strands. As the refractory design and furniture directly influence the fluid dynamics and heat losses in a tundish, they are critical to prevent undesired phenomena. Due to the harsh environment of steelmaking processes, numerical simulations [1–4] are an alternative way to study and improve heat transfer and molten steel flow in a tundish. In this paper, a case study is presented where the tundish refractory design was optimised to reduce heat losses and enhance energy savings, while preserving the other flow characteristics. The suggested modifications were adopted in a steel mill and the effects were measured at the plant.

## Steel Mill Operation

The steel mill’s tundish where this study was conducted had a thermal cycle that varied from 40 °C to 65 °C above the steel liquidus temperature during continuous casting. Figure 1 shows the inlet tundish temperature variability and illustrates that most of the time the tundish operated outside the optimal temperature range of between 25 °C and 45 °C above the liquidus temperature.

Before being distributed among the strands through the tundish, the molten steel is subjected to secondary refinement, which occurs in the ladle. One of the steps of this secondary refinement is at the ladle furnace, which heats the steel using graphite electrodes with the intense use of electrical energy. By reducing the ladle furnace operating temperature, the tundish can operate within the optimal temperature range and a considerable amount of electrical energy can be saved. A new tundish refractory design was proposed to support this temperature reduction without freezing occurrence, and its effects in terms of fluid dynamics and heat transfer were analysed through numerical simulations to provide a theoretical basis for the field modifications.

**Figure 1.** Tundish temperature above the steel liquidus temperature during continuous casting.



## Refractory Lining Configurations

All simulations were performed using the two different tundish configurations shown in Figure 2 (i.e., Configuration #1 and Configuration #2). Configuration #1 was the reference and Configuration #2 was proposed to reduce molten steel heat losses to the refractory lining by removing the refractory mortar around the impact pot. Both configurations were analysed to verify the effect of the refractory lining change on the tundish thermal field.

Configuration #1 comprised:

- RISAIMPACT impact pot (520 mm x 510 mm; height: 277 mm).
- Dams installed on the impact pot laterals.
- Mortar covering to fill the space between the dams and the impact pot.
- Impact brick installed below the impact pot.

Configuration #2 comprised:

- RISAIMPACT impact pot (354 mm x 347 mm; height: 188 mm).
- Impact brick installed below the impact pot.

The refractory lining of the tundish walls was the same for both configurations.

## Description of the Transient Thermal Model

To obtain the thermal profile of the refractory lining and heat flow at the internal walls of the refractory over time, transient thermal simulations were performed for both configurations. They included four steps:

- Step 1: First stage of the lining preheating—linear increase in temperature for 1 hour, reaching 1200 °C by the end.
- Step 2: Second stage of the lining preheating—temperature maintained at 1200 °C for 2 hours.
- Step 3: Waiting time between the end of preheating and the beginning of continuous casting—15 minutes.
- Step 4: Continuous casting—1645 minutes (35 heats x 47 minutes per heat).

The boundary conditions for each step were: Natural convection and radiation to ambient for the cold faces during the four process steps. Hot faces were subjected to the preheating conditions in Steps 1 and 2, to convection and radiation to ambient in Step 3, and molten steel temperature (mean operation temperature) in Step 4.

## Fluid Dynamics Model Description

For the molten steel analysis during continuous casting, a computational fluid dynamics (CFD) simulation was performed using Ansys CFX. The numerical model had the following characteristics:

- Steady-state flow, nonisothermal.
- 2400000 element mesh.
- Turbulence model: k- $\epsilon$ .

For the temperature field of the molten steel, the numerical model considered:

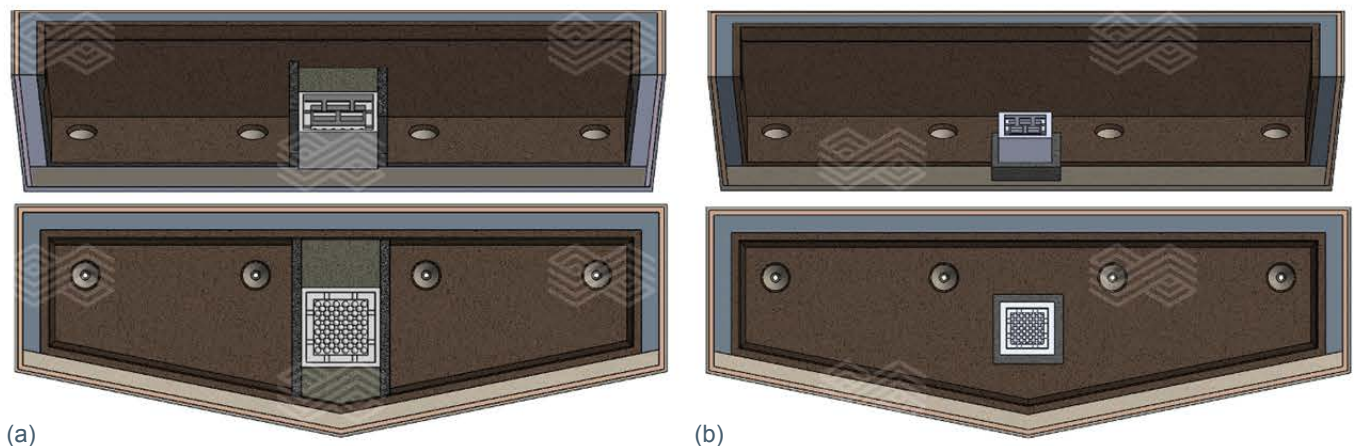
- An intake temperature of the molten steel jet. Field measurements provided inlet temperature values of  $1552.6 \pm 6.9$  °C.
- Molten steel heat losses to the refractory walls as boundary conditions. Values used were obtained from the thermal transient simulations at different instants of the sequence.
- The heat flow of the molten steel to the slag was calculated with an in-house, steady-state, one-dimensional heat flow calculator, using the measured thickness and thermal conductivities of the slag and rice husk ash layers.

CFD simulations were realised for both configurations and for two different thermal states of the refractory lining:

- Critical thermal transient regime (first heat—highest heat losses).
- Steady state (heat flow values used in the walls were the steady-state thermal values).

With CFD results it is possible to estimate the cold steel mass in the tundish by using a reference liquidus temperature. In the case of not having the cold steel mass, according to each criterion, it is possible to estimate how

**Figure 2.**  
Tundish (a) Configuration #1 and (b) Configuration #2.



much the inlet temperature can be reduced without freezing occurring using the difference between the minimum molten steel temperature and the liquidus temperature. For the liquidus temperature calculations, literature models were used to estimate its value [5,6]. The chosen model was Schürmann and Stišović, since it provided the highest value for the liquidus temperature (1517 °C) among the literature models investigated, thus taking a conservative approach.

**Figure 3.** Temperature field in the central plane of the (a) Configuration #1 and (b) Configuration #2 tundishes at the beginning of continuous casting.

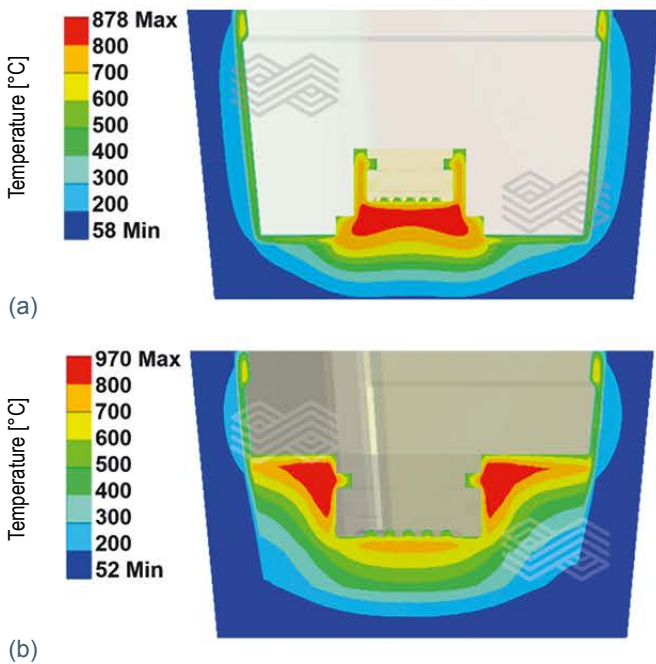
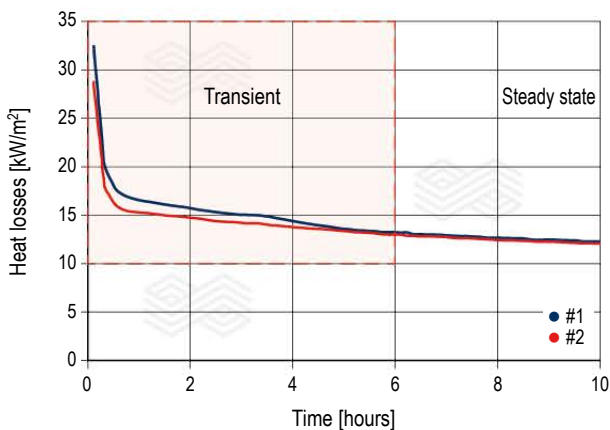


**Figure 4.** Total heat losses of the molten steel to the tundish with operational time.



### Transient Thermal Simulation Results

Figure 3 shows the refractory lining temperature field for both tundish configurations at the beginning of continuous casting. The presence of mortar in Configuration #1 increased the time required to reach a steady temperature field compared to Configuration #2, since a higher amount of energy was required to heat a higher refractory mass. Consequently, this led to higher molten steel heat losses in the initial heats for Configuration #1.

The total heat losses of the molten steel to the refractory walls over time are presented in Figure 4. A peak was observed right at the beginning of the continuous casting, caused by the hot molten steel in sudden contact with the tundish walls. As the temperature field developed, the heat losses decreased with time, reaching steady state at approximately the 8<sup>th</sup> heat.

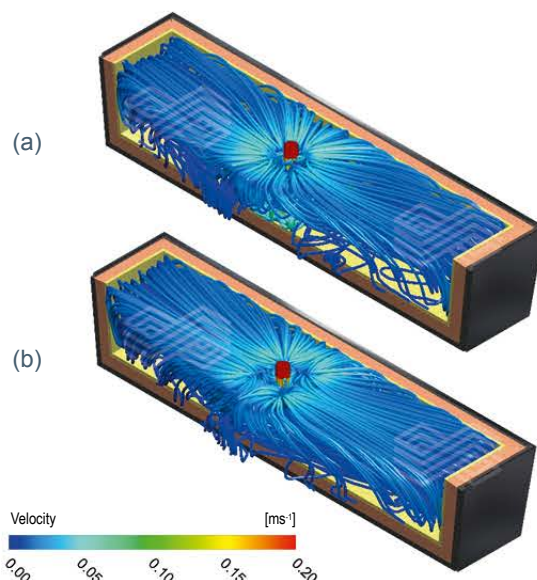
While in a transient thermal state, Configuration #1 presented higher heat loss values than Configuration #2, due to its higher refractory mass (i.e., presence of dams and mortar in the furniture) absorbing more heat to increase its temperature. On the other hand, both configurations reached similar heat loss values at steady state.

### Fluid Dynamics Simulations

Observing the streamlines (Figure 5) obtained from the CFD simulations showed a similar flow pattern for both configurations indicating the tundish furniture modifications would not cause significant differences in the molten steel flow pattern.

In order to evaluate the mixing and residence time of the molten steel, two tracers were injected at the inlet, one continuously to evaluate mixing and the other as a pulse to examine the residence time distribution (RTD). The results in Figure 6 show the continuous tracer spreading over time for

**Figure 5.** Streamlines representing the molten steel flow in the (a) Configuration #1 and (b) Configuration #2 tundishes.



both tundish configurations and the RTD curves obtained by measuring the pulse-injected tracer concentration at the outlets. The tracer spreading and the RTD curves corroborate what was observed in the streamlines: The general flow is similar for both configurations and only slight differences were noticed, such as slightly longer residence times in the internal strands of Configuration #1.

**CFD Simulations—Thermal Transient Regime**

To simulate the tundish flow patterns regarding the refractory thermal field under a transient regime, molten steel heat losses for the first heat were considered to represent the most critical scenario. Figure 7 shows the temperature field at the bottom and at the plane of the intake jet for the first heat, with lower temperatures observed near the bottom of the tundish. This is related to higher heat losses to the refractories in the bottom, compared to the walls, and too low velocities near the bottom. Higher temperatures were observed for Configuration #2 as a consequence of the lower molten steel heat loss at the beginning of continuous casting.

For the three representative temperature values measured in the field (i.e., lower bound, mean, and upper bound), Figure 8 shows values of the cold steel mass and minimum temperatures in the tundishes provided by the CFD simulations for the first heat. For the three inlet

temperatures, Configuration #2 showed a lower cold steel mass (it only occurred for an inlet temperature of 1545.7 °C), and higher minimum temperature values in comparison to Configuration #1. These results corroborate with the temperature fields (see Figure 7) where lower temperatures were observed for Configuration #1 in the bottom region compared to Configuration #2. The regions of cold steel mass estimated by the simulations for the first heat are presented in Figure 9 for both configurations. The criterium used was to consider the volumes with temperatures below the liquidus temperature.

**Figure 7.** Molten steel temperature field of the first heat for (a) Configuration #1 and (b) Configuration #2.

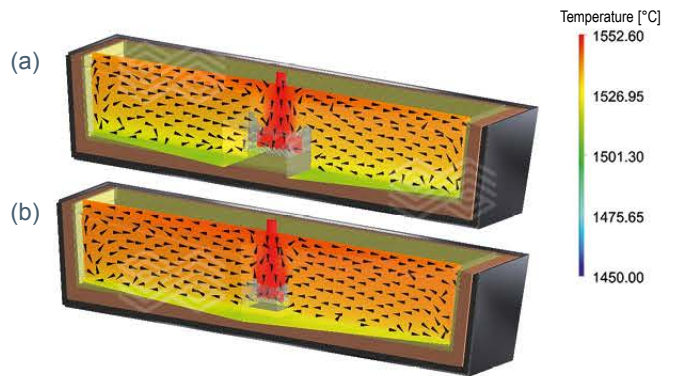
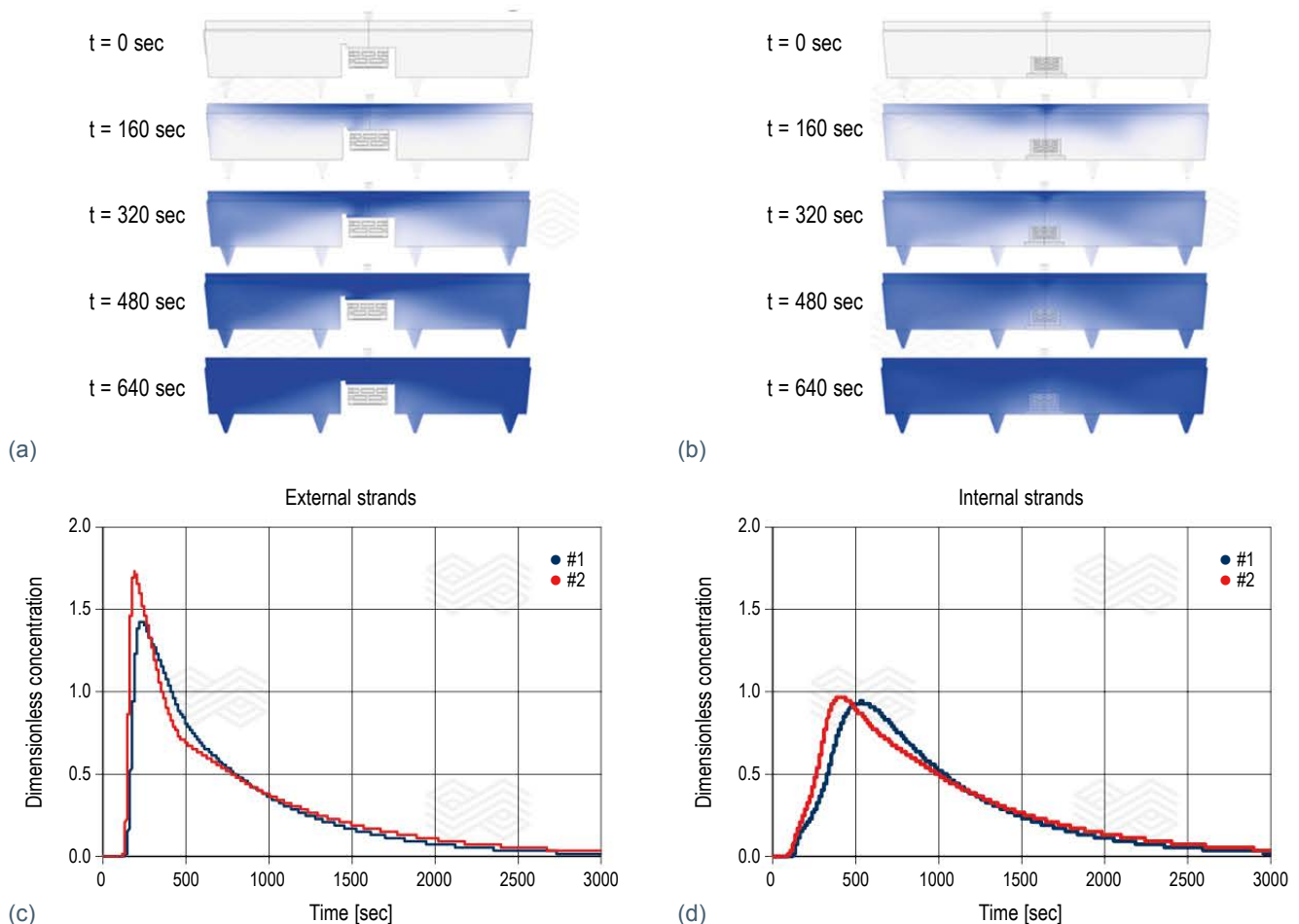


**Figure 6.** Tracer spreading for (a) Configuration #1 and (b) Configuration #2. RTD curves for the (c) external and (d) internal stands of both configurations.



### CFD Simulations—Steady-State Thermal Regime

Figure 10 shows the temperature field for the molten steel in the intake jet plane, under a steady-state thermal regime. The molten steel temperature fields under a steady-state thermal regime were similar for both configurations. This similarity is due to a similar flow pattern associated with similar molten steel heat loss values at steady state. The minimum temperatures for the two tundish configurations obtained from CFD simulations under a steady-state thermal regime are provided in Figure 11. The graph shows that the minimum temperature is above the liquidus temperature

(1517 °C) in all scenarios, which would lead to no cold steel mass, allowing a reduction in the inlet steel temperature and consequently in the ladle furnace operation temperature.

From the simulation results, it can be concluded that once the tundish has reached a steady-state thermal regime, it is possible to safely reduce the inlet temperature without jeopardising the process. The results indicate that a steady-state thermal regime is reached after approximately 8 heats. Furthermore, it was observed that Configuration #2 results in less heat loss than Configuration #1, mainly during the initial heats.

**Figure 8.**

(a) cold steel mass and (b) minimum molten steel temperatures in the Configuration #1 and #2 tundishes for the first heat.

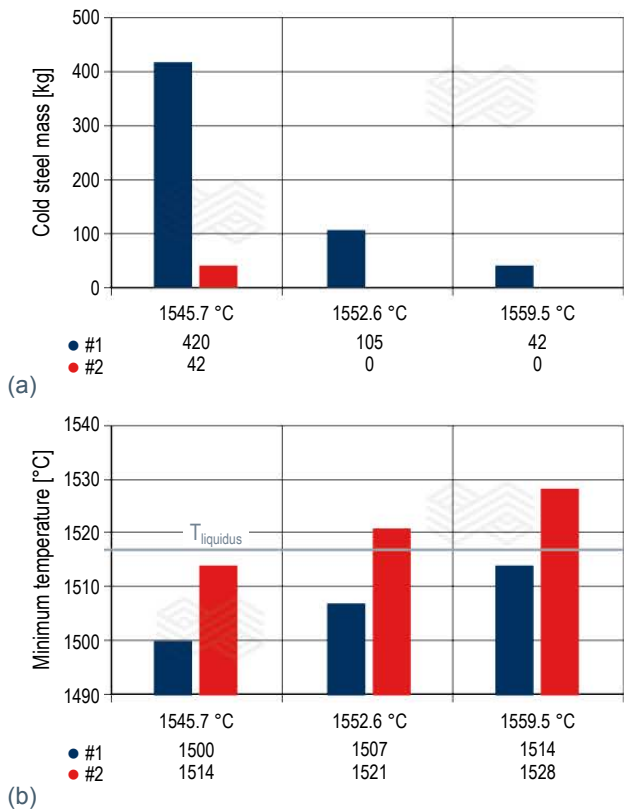
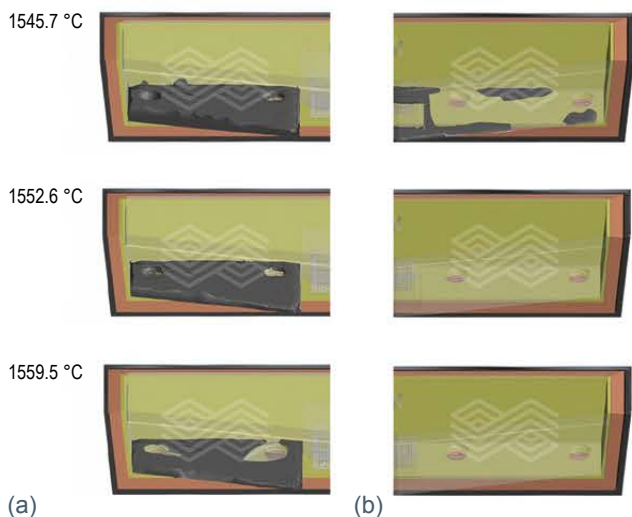


**Figure 9.**

Cold steel mass depicted in brown for (a) Configuration #1 and (b) Configuration #2 at different inlet temperatures.



### Field Results

By using the technical basis provided by the numerical simulations and modifying the tundish configuration from #1 to #2, a reduction in temperature was implemented in the field and significant improvements were observed, mainly during secondary refining in the ladle furnace, such as the power-on reduction, temperature reduction, and energy cost savings shown in Table I.

The reduction in power-on was about 20%, while the ladle furnace temperature decreased by 12 °C. As a result of both reductions in the power-on and temperature, the ladle furnace energy consumption dropped by approximately 10%, leading to representative savings in production costs.

**Figure 10.**

Molten steel temperature field under a steady-state thermal regime for (a) Configuration #1 and (b) Configuration #2.

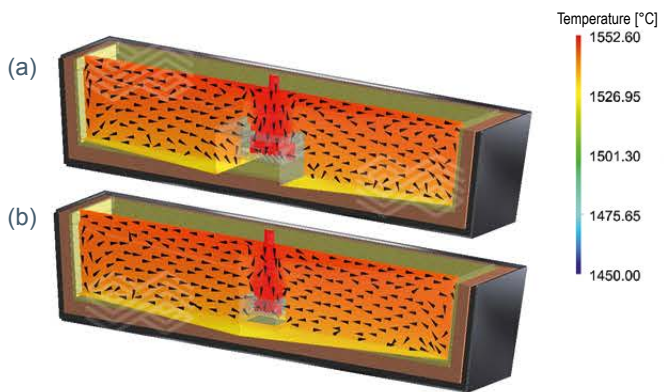


**Figure 11.**

Minimum molten steel temperatures in the Configuration #1 and #2 tundishes under a steady-state thermal regime.

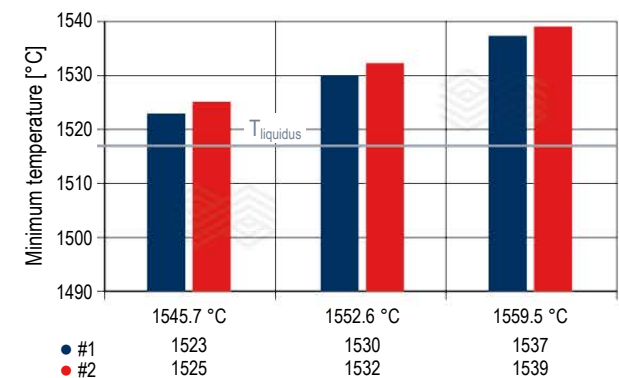


**Table I.**

Improvements in the ladle furnace due to implemented modifications.

| Ladle furnace improvements          | Power-on | Temperature | Energy consumption |
|-------------------------------------|----------|-------------|--------------------|
| Reduction during implementation     | 4.9%     | 5°C         | 3%                 |
| Reduction after full implementation | 19.5%    | 12°C        | 9.7%               |

Furthermore, by operating at a lower temperature, these modifications could increase the refractory lifespan and consequently decrease refractory consumption in the steel ladle.

### Safety and Environmental Aspects

Regarding contributions to environmental aspects, the field implementations described in this work were able to:

- Reduce the specific refractory consumption by increasing the refractory lining lifespan and optimising resources.
- Reduce energy consumption.

Both aspects are directly related to a more sustainable steelmaking operation and reduced carbon footprint. The carbon footprint savings can be estimated using publicly available data [7]. A typical ladle furnace average energy consumption of 22 kWh for each degree temperature increase was considered. Thus, for a reduction of 12 °C (see Table I) an estimated saving would be approximately 260 kWh, or 5.9 kWh per tonne of steel, as the ladle in question has a capacity of 45 tonnes. By applying this estimation to various energy sources' carbon footprint data provided by the World Nuclear Association [7], it is possible to estimate the potential carbon emission saving per tonne of steel that the field implementations could bring regarding typical energy sources (Figure 12). Furthermore, the implementations assured that besides continuous process improvement due to a more stable operation, a failure mitigation could be achieved, avoiding human interventions and out-of-routine worker exposure, thereby enhancing operational safety.

### References

- [1] Pardeshi, R., Basak, S., Singh, A.K., Basu, B., Mahashabde, V., Roy, S.K. and Kumar, S. Mathematical Modeling of the Tundish of a Single-Strand Slab Caster. *ISIJ International*. 2004, 44(9), 1534–1540.
- [2] Liu, S. X., Yang, X. M., Du, L., Li, L. and Liu, C. Z. Hydrodynamic and Mathematical Simulations of Flow Field and Temperature Profile in an Asymmetrical T-Type Single-Strand Continuous Casting Tundish. *ISIJ International*. 2008, 48(12), 1712–1721.
- [3] Merder, T. Numerical Simulation of Liquid Flow and Mixing Steel in Multi-Strands Tundish. *Journal of Achievements in Materials and Manufacturing Engineering*. 2012, 55(2), 561–566.
- [4] Sowa, L. Numerical Modelling of Fluid Flow and Thermal Phenomena in the Tundish of CSC Machine. *Archives of Foundry Engineering*. 2014, 14(1), 103–106.
- [5] Kagawa, A. and Okamoto, T. Influence of Alloying Elements on Temperature and Composition for Peritectic Reaction in Plain Carbon Steels. *Materials Science and Technology*. 1986, 2(10), 997–1008.
- [6] Miettinen, J. and Howe, A. Estimation of Liquidus Temperatures for Steels Using Thermodynamic Approach. *Ironmaking & Steelmaking*. 2000, 27(3), 212–227.
- [7] <https://www.world-nuclear.org/information-library/energy-and-the-environment/carbon-dioxide-emissions-from-electricity.aspx>

### Authors

Rodrigo Garcia Ribeiro, RHI Magnesita, Contagem, Brazil.  
 Alexandre Dolabella Resende, RHI Magnesita, Contagem, Brazil.  
 Carlos Alberto Rodrigues Lares, RHI Magnesita, Contagem, Brazil.  
 Marcos Pereira Manso, RHI Magnesita, Contagem, Brazil.

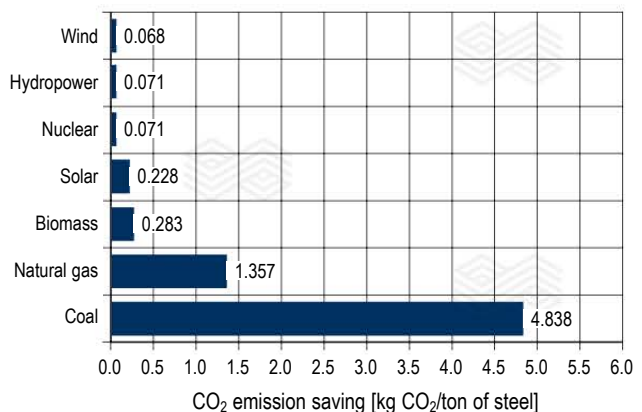
**Corresponding author:** Rodrigo Garcia Ribeiro, [rodrigo.ribeiro@rhimagnesita.com](mailto:rodrigo.ribeiro@rhimagnesita.com)

### Conclusion

Numerical simulation results indicated that with the proposed refractory design modification, a lower operating temperature could be adopted in the tundish without cold steel spots, highlighting this as a valuable tool to provide the technical basis for field modifications. After the modifications were implemented, field results showed significant energy and cost savings and an improved operation in terms of safety and environmental aspects. This illustrates how RHI Magnesita can provide solutions backed by numerical simulations to support our customers' initiatives related to more sustainable operations and a reduced carbon footprint.

**Figure 12.**

Potential CO<sub>2</sub> emission savings resulting from the 12 °C temperature reduction observed in the field.



Christine Wenzl and Heinz Telser

# RHI Magnesita as a Technology Partner and Solution Provider for our Industrial Customers—We Thrive on Complexity

As the world’s leading refractory supplier, RHI Magnesita has been supporting customers for well over a century. High-quality refractories, expert knowledge, and longstanding industry experience enable optimisation of production processes, for example reducing maintenance times, managing refractory wear, and proactively advising on material quality improvements. However, “Taking innovation to 1200 °C and beyond” also means including additional technologies and tools in our portfolio, to offer attractive, value-adding technology packages and solutions for the customer. This paper provides an overview of some of these new and digital technologies and how they generate customer benefits, with particular emphasis on our Industrial sector that includes cement, lime, nonferrous, glass, as well as environment, energy, and chemistry.

## Introduction

Traditionally, RHI Magnesita has been known for its high-quality refractory products and services, as well as continuous product improvement based on its research and development activities, industry knowledge, and close customer contact. As a result of the changing requirements of our customer industries, aiming for better process understanding and insights to further optimise processes and output as well as reduce furnace downtimes, RHI Magnesita has focused on new and digital technologies to support our customers “beyond refractories”.

The recent, sudden, and pronounced increase in demand for metals and construction materials after the COVID-related downturn highlights even more the importance of efficient and smooth production processes to meet the market demands of our Industrial customer industries. Plant optimisation and high production utilisation are therefore key factors, as greenfield projects require a longer time and higher investments for realisation. RHI Magnesita’s new technologies provide essential tools for such plant optimisations and technology updates, namely to help improve process and cost efficiency, prolong refractory and furnace lifetime, optimise maintenance scheduling, reaching CO<sub>2</sub> as well as health and safety targets—ensuring a competitive advantage for our Industrial customers.

## “Beyond Refractories”

To meet the demanding requirements and environmental regulations, as well as guarantee operator safety, it is of utmost importance to invest in plant modernisation as well as new technologies. Recent examples of plant closures showed and confirmed the importance of plant modernisation and low-cost production. Environmental regulations are a global topic—we only have one planet and regulations are becoming stricter, even in countries where this was not the main priority in the past.

The term Industry 4.0 is omnipresent—however, automation requires a solid data basis and respective tools for data collection and analysis. Only after establishing this basis, models and processes can be set up to automate operations and finally introduce Industry 4.0.

Even though the individual customer processes are quite different, there are some common issues that require adequate solutions in the areas of safety, sustainability, total cost of ownership (TCO), process and data, as well as technical service and support. It is important to recognise these common challenges and investigate suitable approaches for tackling them. Here it is important to understand processes and requirements, identify similarities, choose suitable technologies, and apply technologies that are common in one industry to other industries where they have not been used before. This mutual learning and experience exchange between various industries, based on new ideas and cross-industrial thinking, enables faster and more efficient problem solving.

Regarding process optimisation, RHI Magnesita has been providing detailed engineering, simulation and modelling, as well as process-based lining recommendations for several decades. State-of-the-art simulation tools (e.g., finite element method and computational fluid dynamics) and thermodynamic calculations (e.g., FactSage) are RHI Magnesita’s standard tools for furnace and process optimisation (Figure 1). However, not only are such tools effectively applied but development of simulation software is proactive conducted, for example by developing new models for industrial processes together with international academic partners. RHI Magnesita also experimentally determines important refractory physical parameters for simulations, which generates more accurate results.

Furthermore, technologies like gas purging are already well-established, especially in copper and aluminum production, to enhance the process kinetics. However, also here further developments are being made:

The COPKIN EX technology now enables reactive gases to be introduced through purging plugs—this becomes very interesting when considering CO<sub>2</sub> reduction and the use of hydrogen as a reductant. It also makes sense to consider and discuss gas purging for other industries, for example glass and foundry.

Collaboration and learning from best practices are decisive factors for improvement and competitiveness—not only when learning about customer processes, but also internally. Slide gate technology is a very common technology in the steel industry, providing significant improvements regarding tapping control and safety. RHI Magnesita has already successfully transferred this technology to Industrial customer processes, so far mainly for metal tapping. The newest development in this area is a slide gate for slag tapping (i.e., S-TAP). Implementing slide gates allows the tapping operations to be performed remotely, thereby avoiding operators having to be near this potentially hazardous area and process. Additionally, it is a first step for tapping automation: In combination with sensors for metal or slag detection, the slide gate can be activated automatically based on the sensor signals.

These types of sensor technologies for metal and slag detection are one part of RHI Magnesita's new technology portfolio. The use of sensors is generally always linked to safety—on the one hand process safety (i.e., providing process-related data as a basis for decisions) and on the other hand operator safety (i.e., removing operators from hazardous areas and processes). One of the most dangerous situations in industrial plants—especially when handling hot liquid phases—is furnace or ladle breakouts. Such events are a critical safety risk for operators and additionally are associated with high costs due to equipment damage and lost production time. The formation of hot spots is a suitable indicator to detect issues with vessel integrity; however, such hot areas on the steel shell need to be detected at an early stage (i.e., before they become visible to the human eye) to implement respective measures. Therefore, it is important to monitor the vessel steel shell and take maintenance decisions based on reliable, objective data. The VISIR LadleSafe (Figure 2) and VISIR FurnaceSafe systems monitor the steel shell temperature and provide information as well as warnings in case of temperature abnormalities at an early stage [1].

**Figure 1.**

(a) heat transfer simulation of a furnace sidewall with cooling panels and (b) FactSage example of the interaction between a refractory material and process phase (i.e., slag).

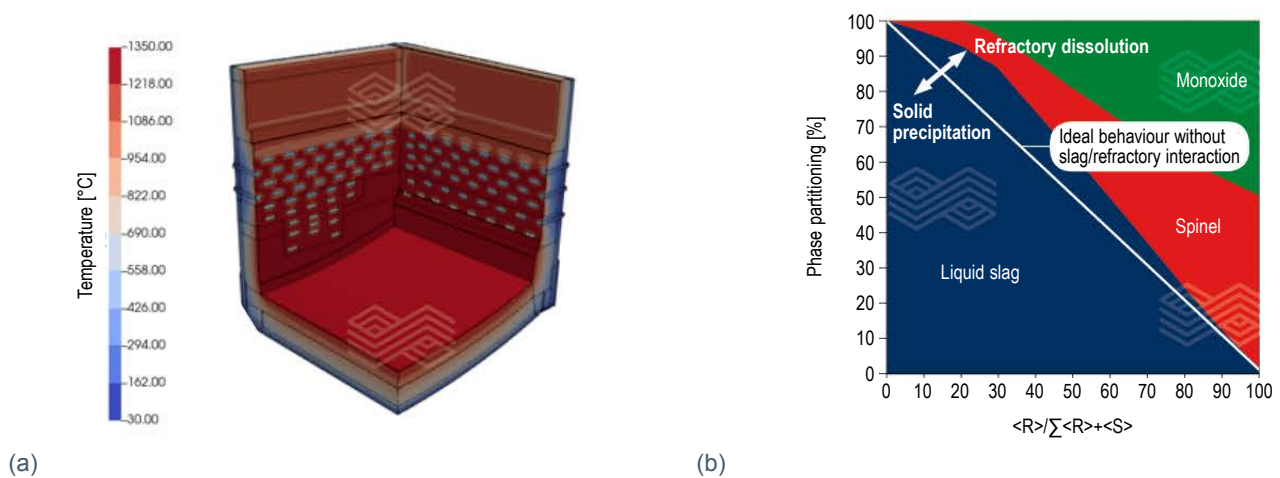
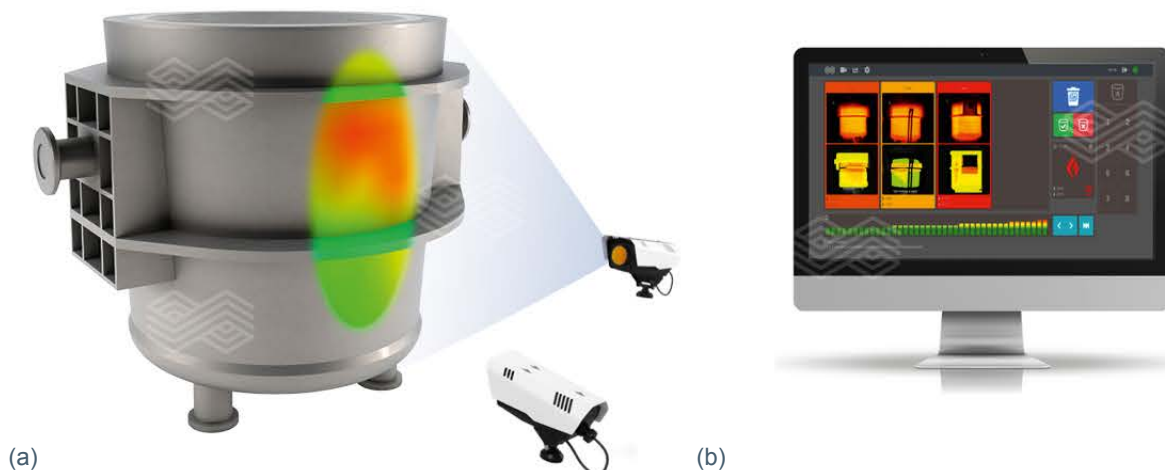


**Figure 2.**

VISIR LadleSafe. (a) steel shell temperature monitoring and (b) data evaluation.



Sensors not only help with safety topics, but also in daily operations, process efficiency optimisation, and sustainability: Level measurement (i.e., EMLI FurnaceProfile, EMLI SmelterLevel (Figure 3), EMLI TundishLevel, and EMLI MouldLevel) and slag/metal detection during deslagging or tapping operations (i.e., EMLI MetalSlag, VISIR LadleDeslag, and VISIR MetalDetect) ensure smooth operations and improved process efficiency.

All the aforementioned sensor technologies can be used as stand-alone solutions or integrated in the plant PLC system to automatise processes. The collected data can be used for data analysis and subsequent optimisation. Furthermore, it can be used in RHI Magnesita's artificial intelligence (AI)-based technologies. For example, APO (Automated Process Optimization) uses AI to model and predict refractory lifetime and wear based on process data and measured lining data (e.g., laser scan measurement data). This system is already successfully in use at several steel plants [2–4] and is currently also being introduced at nonferrous customers.

A similar technology is under development for further Industrial applications to provide automated refractory optimisation and predictive maintenance. Generally, APO is applicable to every industrial process that fulfils the minimum requirements: Process data is available and a connection between the process and refractory geometry can be established (e.g., laser scan of the refractory lining).

Laser scan technology is also the cornerstone of the LES technology, namely Lining Evaluation Service (Figure 4). Such LES data provides a valuable basis for lining repair decisions, indicating kiln areas with a critical remaining lining thickness. Besides detailed pdf reports this technology also provides the possibility of virtual kiln tours and virtual furnace inspections. This technology was first introduced and used in cement rotary kilns but is applicable to basically every furnace with some first experiences in the nonferrous and environment, energy, and chemistry (EEC) sectors.

**Figure 3.**

(a) EMLI FurnaceProfile and (b) EMLI SmelterLevel.

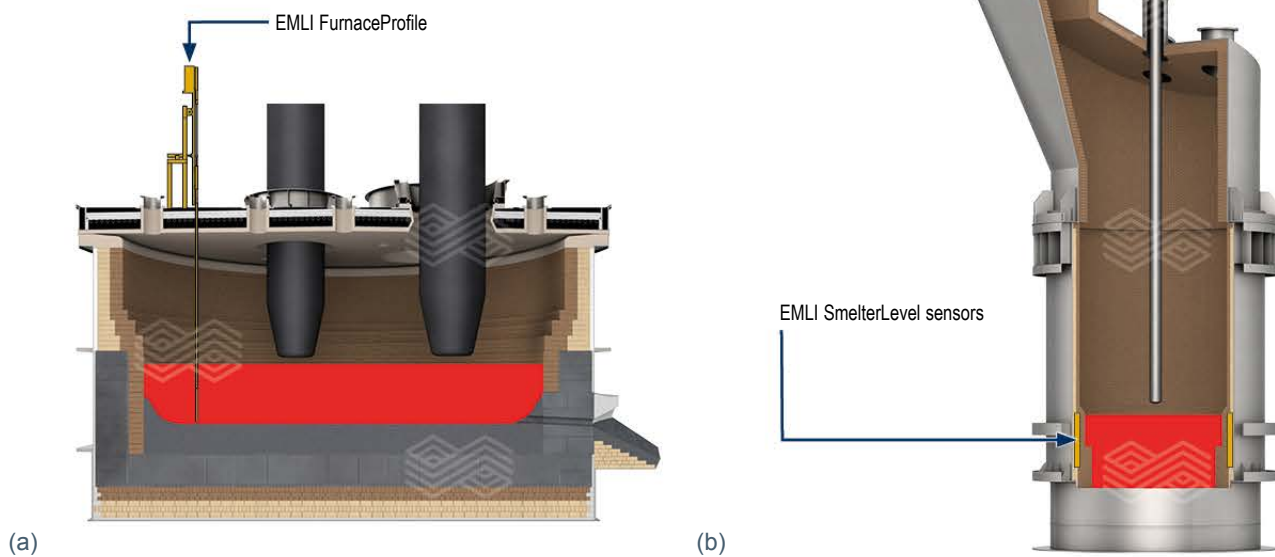


**Figure 4.**

(a) laser scanning process and (b) Lining Evaluation Service (LES) scan data of a lime shaft kiln.



While LES is optimal for vessel inspection under cold conditions, the new QCK (Quick Check) technology is used for hot vessel measurements. This technology is based on stereoscopic cameras and is a very interesting alternative to laser scans in hot conditions, being much faster and more accurate (Figure 5).

**Figure 5.**  
(a) QCK schematics and (b) QCK measurement data.



(a)



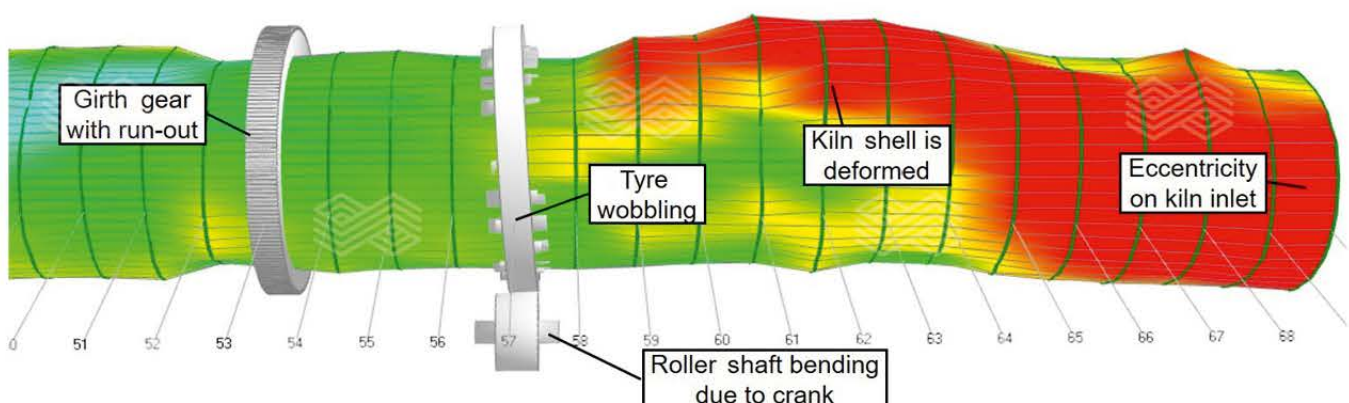
(b)

Another digital tool to monitor the mechanical condition of rotary kilns is the Mechanical Kiln Audit (MKA) (Figure 6). This technology is used to measure ovality and deformations, which have a major influence on refractory performance. Based on the MKA findings, adequate actions can be taken (i.e., refractory material changes or mechanical kiln repairs) to avoid mechanical refractory damage or even more severe unplanned kiln stoppages. The MKA has typically been used for rotary kilns in the cement and lime industries; however, it can also be applied to rotary kilns in other industries (e.g., nonferrous and EEC) and even other rotating furnace types.

Sensor technology and the application of digital tools all have the same target, namely to optimise the process and furnace utilisation. Digitalisation will not only increase our customers' competitiveness and profitability, it will also deliver the required input data to optimise energy usage and minimise CO<sub>2</sub> emissions. Therefore, digitalisation and sustainability go hand in hand.

RHI Magnesita is focusing on the reduction of CO<sub>2</sub> in the refractory industry's entire supply chain, benefiting from its global production network to minimise transport-related emissions. The reduction of the raw materials' carbon footprint is one of the main focus areas. RHI Magnesita is actively contributing to closing the material cycle and enhancing the circular economy from raw materials to brick production and installation, as well as recycling used refractory materials. Based on our Industrial customers' processes, the used materials are contaminated with various elements and compounds so that further processing is required to enable reuse of secondary raw materials in the production of new refractories. For the cement industry we have already established processes and offer a product line based on sustainable technology, namely the ANKRAL LC series characterised by a significantly reduced carbon footprint (Figure 7). This sustainable customer solution supports our customers' initiatives towards zero waste [5].

**Figure 6.**  
Mechanical Kiln Audit (MKA).



Similar developments are under investigation and ongoing for other Industrial areas and vessels. Recycling is a crucial step in fully establishing RHI Magnesita's circular economy: Starting with our mines and raw materials, extending over brick production and installation in the customers' vessels, up to taking back the spent materials and processing these adequately to produce new bricks.

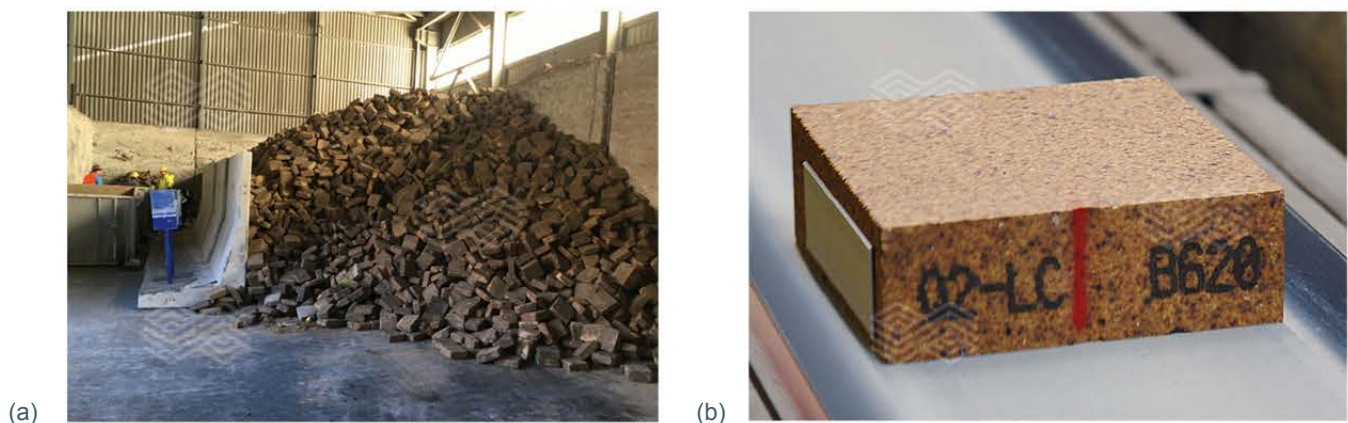
The COVID-19 crisis accelerated and pushed RHI Magnesita's actions regarding remote assistance as the need for adequate assistance tools increased with the pandemic-related travel restrictions. Using remote assistance technology (e.g., Microsoft Dynamics 365 and HoloLens) we can connect our local onsite engineers and customers with our remote specialists, providing expert knowledge to our customers without the need for travel and associated delays.

## Conclusion

Refractories have been RHI Magnesita's core business and competency for many decades. To meet the changing customer demands and requirements, new technologies "beyond refractories" have been added to the portfolio and provide comprehensive customer solutions for various requirements and needs—with the target of being a 360° heat-management partner for our customers. Even though there are differences in the specific Industrial processes and vessels, there are some overarching issues and challenges. Close collaboration with our customers is a key factor for successful technology implementation, from initial discussions to planning and after-sales support. Comprehensive solution packages, for example high-quality refractory products, technical services, and additional new technologies provide maximum customer benefit regarding safety, process and plant efficiency, as well as CO<sub>2</sub> and sustainability targets.

**Figure 7.**

(a) used bricks for recycling and (b) ANKRAL LC brick with a reduced product carbon footprint.



## References

- [1] Persson, M., Nilsson, J.P., Adolfsson, K., Sjöstedt, A. and Höck, M. Ladle Fleet Monitoring for Safety and Lifetime Evaluation. *Bulletin*. 2019, 18–23.
- [2] Lammer, G., Lanzenberger, R., Rom, A., Hanna, A., Forrer, M., Feuerstein, M., Pernkopf, F. and Mutsam, N. Advanced Data Mining for Process Optimizations and Use of A.I. to Predict Refractory Wear and to Analyze Refractory Behavior. *2017 AISTech Conference Proceedings*, Nashville, USA, 8–11 May, 2017; pp. 1195–1207.
- [3] Viertauer, A., Mutsam, N., Pernkopf, F., Gantner, A., Grimm, G., Winkler, W., Lammer, G., Ratz, A. and Persson, M. Refractory Lifetime Prognosis for RH Degassers. *2019 UNITECR Conference Proceedings*, Yokohama, Japan, 13–16 Oct., 2019; pp.154–157.
- [4] Steiner, R., Lammer, G., Spiel, C. and Jandl, C. Refractories 4.0. *BHM*. 2017, 162(11), 514–520.
- [5] Telser, H., Klitzsch, M. and Krischanitz, R. Brick by Brick. *World Cement*. October 2020, 37–43.

## Authors

Christine Wenzl, RHI Magnesita, Vienna, Austria.

Heinz Telser, RHI Magnesita, Vienna, Austria.

**Corresponding author:** Heinz Telser, heinz.telser@rhimaginesita.com



Paulo Souza, Celso Freitas, Gregor Arth, Gustavo Penido, Karl Zettl, Jose Bolognani, Carlos Lamare, Gregor Lammer, Gerry Moser and Antonio Hoffert

# Next Level of Digital Refractory Contracts

The Fourth Industrial Revolution has been changing the way companies interact and do business, blurring the lines between physical and digital worlds. Connectivity, intelligence, and flexible automation are megatrends observed nowadays in the industry to optimise the shop floor, producing more goods with less waste at lower cost. However, early adopters are the only ones who are fully benefiting from the industry transformation, followers will just see a minor impact on their business. Being global leader of the refractory industry, RHI Magnesita is changing the way customer and supplier interact, offering a full digital customer experience, from opportunity to continuous business. In this paper we will elucidate our digital solution contracts. Starting with SAR+, the fully automated refractory consumption and performance tracker, then going through artificial intelligence for refractory optimisation (e.g., Automated Process Optimization) and blockchain smart contracts for month-end financial reports, and finally describing our unique Customer Portal—the one stop solution for all customers’ needs. All this managed by experts using analytical methodologies, having on hand a unique product portfolio to support continuous improvements. This paper intends to give an overall view of our digital solutions, showing how they integrate among themselves, maximising the benefits.

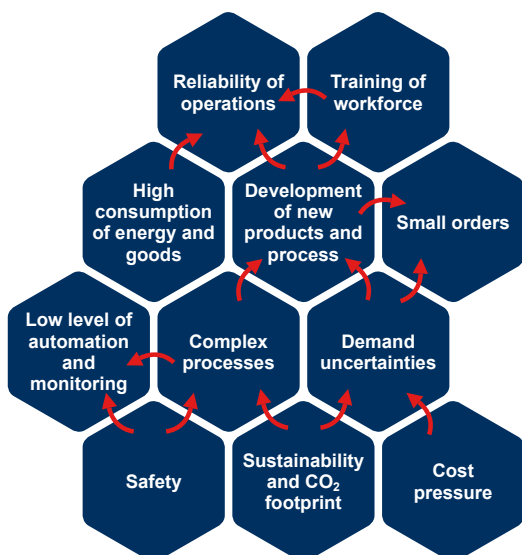
## Introduction

“Businesses will do better in the end if they concentrate on meeting customers’ needs rather than selling products” [1]. This was the view Theodore Levitt presented more than 60 years ago in his award-winning paper “Marketing Myopia” [2] and it is still highly relevant. From 1960 up to now we have gone through the Third Industrial Revolution and the Fourth is happening as we speak. Nuclear power, programmable logic circuits, robots, quantum computers, and the Internet of Things (IoT) are just a handful of examples of disruptive technologies that in the end should support the most important need—the customer’s. A number of businesses failed in the past and will keep failing in the future because they were not able to be, in this changing and challenging environment, customer oriented instead of product oriented [2]; because there is no guarantee against product obsolescence. If a company itself does not make a product obsolete, another one will. It is easy to find some very

famous examples such as Kodak, Nokia, and Xerox where new solutions were developed by others to fulfil customers’ needs. And normally a new solution does not even come from companies in the same industry segment. Why? They are too occupied with producing products. Electric cars might be one of the reasons why the oil industry could significantly decline in the next decades and none of those companies who are now developing electric cars belong to the oil and gas industry sector. If we look back a long time ago, the same oil and gas industry benefited a lot from the internal combustion engine development, which again did not come from any of the oil companies. So, the question one might need to answer is: What business am I really in? Is it the oil and gas industry or the energy business? Was Nokia in the mobile phone business or in the “connecting people” business? Was Kodak in the photographic film business or in the “visual recording” business? The way a business is defined, will tell how innovative the company will be.

Figure 1. Customer challenges and value proposition.

### Our customers face many interlinked challenges



### But value our help on five key pain points

- 1 **AVAILABILITY**  
of products and equipment ready to run
- 2 **PREDICTABILITY**  
of downtimes and maintenance stops
- 3 **SUSTAINABILITY & EFFICIENCY**  
Savings of energy, ferroalloys, yield, less CO<sub>2</sub> emissions, and quality assurance
- 4 **HEALTH & SAFETY**  
and less manpower on the shop floor
- 5 **DATA TRANSPARENCY & TRUST**  
Highly efficient digital sales processes and compliance

At RHI Magnesita, a completely new and innovative way of doing business started in the mid-1990s: Offering the steel industry a complete solution-oriented package. Refractory products bundled with laser scanners, machinery, sensors, automation, mechanisms, and installation services to optimise the customer's total cost of ownership (TCO), making their steel production cheaper, safer, and more sustainable. In addition, a unique financial model of sharing gains and losses was introduced, sealing the goodwill with a symbiotic model that elevates the customer-supplier relationship to the next level, all fine-tuned by our onsite experts.

The Fourth Industrial Revolution is building on top of the Third, the digital revolution, that was already happening. However, this is taking place at exponential speed due to emerging new technologies such as IoT, artificial intelligence (AI), computer processing, 3D printing, and 4–5G internet, disrupting all industries globally. According to Jupiter Research [3], in 2020 38.5 billion devices were connected to the internet, generating data that is shaping human life.

RHI Magnesita is present worldwide in the steelmaking market, with more than 1000 people in daily contact with our customers' employees and processes. This makes the company in a unique position to map our current and future customers' challenges. At the end of the day, we need to capture the main values our solution packages must have to get the job done (Figure 1). Because they are interlinked and in constant change, new digital solutions, embedded in a single platform for contract management have been developed and will be the topic of the following discussion.

## Challenges—Availability

The post-COVID-19 logistic challenges have shown how important it is to have full control and understanding of the refractory inventory. Despite being mandatory to always keep the vessels available for production at every step of steelmaking, refractory products still have their consumption and inventory levels controlled in a very old fashion way—manual counting and pencil/paper. For more than 20 years and with over 50 customers around the globe, our Refractory Application System (SAR+) was revamped to incorporate a tracking system using radio frequency identification (RFID) (Figure 2). This technology was invented during the Second World War to differentiate enemy from allied aircraft when returning to base [4]. However, only after 2000, when the technology cost dropped significantly, did it start to be widely used at a pallet or even item level. One example is Walmart, which required their top 100 suppliers to be RFID ready by 2005 as a strategy to improve their supply chain management (SCM) [5]. A RFID system basically consists of 3 parts: The RFID tags, which are divided in two big families—passive and active. The passive draws its operational power from the electromagnetic field generated by the RFID transmitter while the active ones are self-powered by an internal battery. The other two parts are the transmitter and receiver. The first sends a signal to the environment and the second receives the signal emitted by the RFID tag, reads it, and sends it to the computer to be processed. For several reasons passive RFID tags were chosen to develop this digital product.

**Figure 2.**  
SAR+ cockpit.

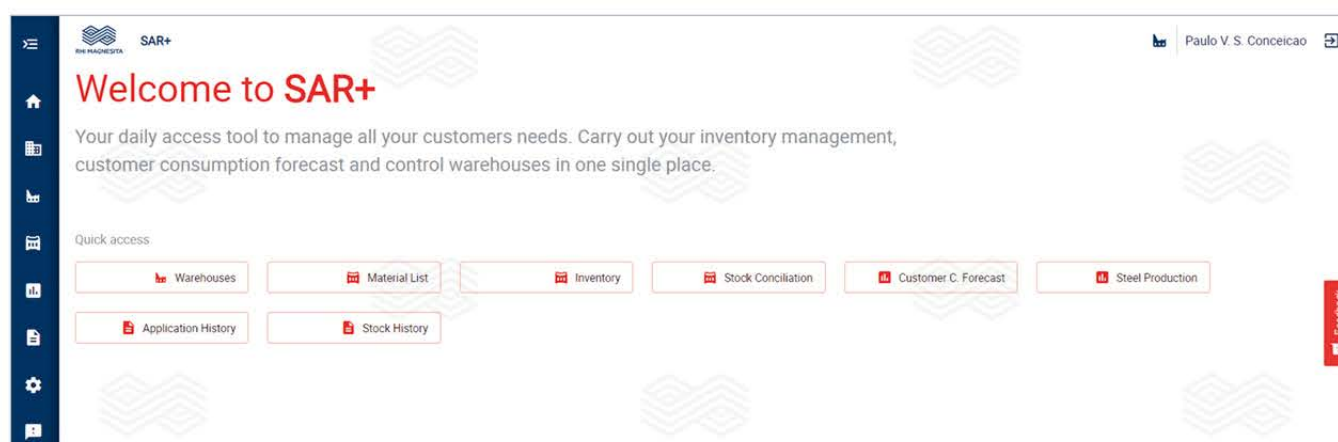


Figure 3 presents how the automated SCM system works. Pallets are produced in our facilities and shipped to the customer site with RFID tags specifying the handling unit (HU), which is a unique international number. When the pallets enter the warehouse for storage, “RFID gates” installed at the entrance detect each pallet individually and load this information into the SAR+ system as an inbound movement. When the pallet leaves the warehouse, the gates detect an outbound movement, which means that the material is leaving to be consumed in the melt shop, represented by the “Lining area”. During the refractory installation, each pallet is individually assigned to specific equipment and a specific shell number, for example “Steel Ladle—Shell 05”. The bricklayers have a handheld sensor that can identify the RFID tags and using a human machine interface (HMI) they can easily select in which part of the ladle the material will be applied. The benefits include:

- **Traceability:** If any issue arises, all refractories applied to a specific shell can be traced back. This provides full traceability and process reliability, which can be very important particularly for special steel producers who need to be accredited by their customers’ quality process.
- **Automation:** Time savings of up to 65% on manual tasks with regards to SCM. An entire warehouse inventory audit can be done in just minutes.
- **Reliability:** RFID technology developed by RHI Magnesita is 100% failure proof.
- **Working capital:** Online and reliable information gives authority to reduce working capital.
- **Reporting:** All information is available online for process analysis and improvement.

**Challenges—Predictability**

On the one hand customers want to keep vessels running for as long as possible; however, on the other hand it would be ideal to know in advance when to stop for refractory

maintenance, to enable better production planning. Because refractories are so intimately linked to the whole steelmaking process, being the only barrier between liquid steel at 1600°C, millions in CAPEX investments, and much more importantly priceless human lives, it is essential to avoid unexpected refractory-related events. For some equipment, as illustrated in Figure 4, there are several methods to elucidate how refractory wear is behaving, starting from human visual inspection up to laser measurements.

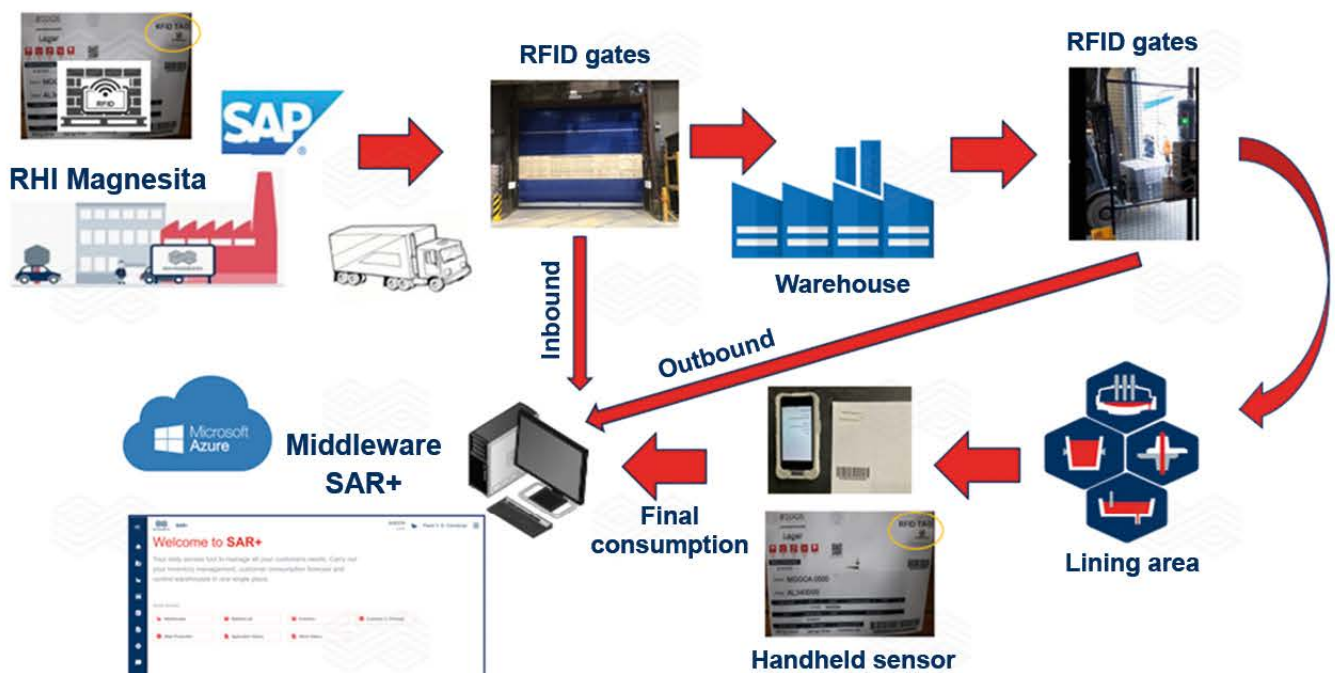
However, for certain vessels like the RH degasser there is no effective way to judge the refractory lining conditions. Therefore, the solution designed by RHI Magnesita, already in operation at several steel plants, is to combine historical process big data with a historical refractory wear protocol to build a model using machine learning techniques powered by AI [6]. This model has a unique capability to predict refractory wear, providing a lifetime prognosis. Therefore, steelmakers have the chance to make data-driven decisions to better manage upstream and downstream processes. It was shown that this solution can provide refractory cost reductions of around 15% in the steel plant [7]. It also enabled the melt shop to better schedule refractory maintenance, increasing process predictability and safety (Figure 5).

**Challenges—Efficiency**

It is well known that refractory products can play a very important role when it comes to steelmaking processes and the related product quality. As a solution provider, RHI Magnesita has an ever-increasing portfolio that targets steelmaking process efficiency. Listed below are just a few published examples:

- Efficient hot metal desulphurisation in the ladle [8].
- Implementation of BOF gas purging technology and successful operation at Severstal Cherepovets after one year [9].

**Figure 3.** Automated SCM system using SAR+ and RFID technology.



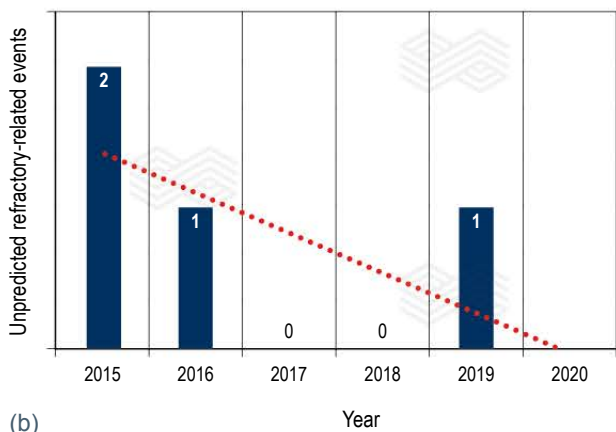
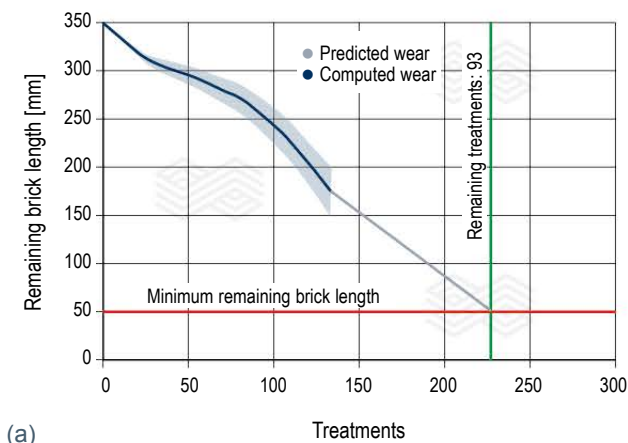
- Efficient value-added steel production with a low mix maintenance level at JSW Steel in India [10].
- Slag modelling to optimise the use of fluxes in a DRI-based steelmaking operation [11].
- Development and application of a slag model to increase ladle life in an integrated steel mill in Brazil [12].
- Improving surface quality as well as decreasing rhombohedral occurrence and breakout on billets casted using PROIL as a mould flux [13].
- Studying the intermix in a six-strand billet caster [14].

Refractory hot maintenance is one of the most successful ways to prolong the refractory lifetime of many different vessels in the steel shop. For the EAF, a fully automatic gunning robot called TERMINATOR has been implemented in several shops with a built-in laser system to measure refractory thickness and determine the most critical regions that need to be maintained. Decreasing specific refractory consumption and reducing repair time were just some of the results achieved using this approach [15]. The next level was achieved when the TERMINATOR data was connected

**Figure 4.** Refractory monitoring and maintenance for different vessels.

|             | Direct inspection                               | Direct measurement | Indirect  | Repair method                          |
|-------------|---|--------------------|---|--|
| BOF         |   |                    | Not common. Fixed to monitor shell temperature    |  |
| Ladle       |   |                    |   |  |
| EAF         |   |                    | Fixed thermocouples to control bottom temperature |  |
| RH Degasser | Just outside (direct) or top cameras (indirect) | Not available      | <br>Being investigated                            | <br>Just snorkels (inside and outside) |

**Figure 5.** (a) prediction of the remaining brick length over the number of treatments [6] and (b) number of RH degasser unpredicted refractory-related events [7].



to a Cloud centre via IoT and now the information is processed and transformed into value for our customers. Figure 6 details some of the valuable information our customers have access to. By knowing online and in real time the region of the furnace that is maintained with hot repair/gunning—which results in a higher power-off time—steelmakers can make data-based decisions such as changing parameters of the electrodes, burners, scrap charging/quality, and flux additions to minimise production impacts.

### Challenges—Data Transparency and Trust

Blockchain is a list of records, called blocks, that are linked together using cryptography. Each block contains basic transactional data, a time stamp, and all the information of the previous blocks. Therefore, all blocks are connected as an immutable data storage, because changing any record would lead to changing all the others, which is virtually impossible with the existing computer processing power. It was first invented in 2008 to serve as a public transaction ledger for the bitcoin cryptocurrency and is considered one of the most secure ways to make public transactions. The

Refrac Chain is a smart contract based on blockchain technology. A consensus mechanism establishes a state-of-the-art corporate governance to our solution contracts. The Refrac Chain methodology implements a workflow to reach consensus, based on cross validation by two or more parties, namely RHI Magnesita and the customer. There are executives, as representatives from both parties, for each level of the knowledge domain such as quality control, technical, sales, and legal. Every user has a personal private key associated with their identity. Every action of approving or reproving a measurement, alongside every informational input in any data format is recorded in a distributed ledger. In a straightforward scenario the parties reach an organic consensus without external influences, which is expected from the strategic nature of RHI Magnesita’s commercial relations. On rare occasions when the participants cannot agree upon the truth of the current situation, a previously elected arbiter can be invoked to secure consensus. Given the explanation of business rules of the consensus mechanisms, it can be stated that the Refrac Chain platform is an innovative interface for technical, sales, legal, and financial governance regarding performance contracts.

**Figure 6.**  
Connected Machine dashboards.

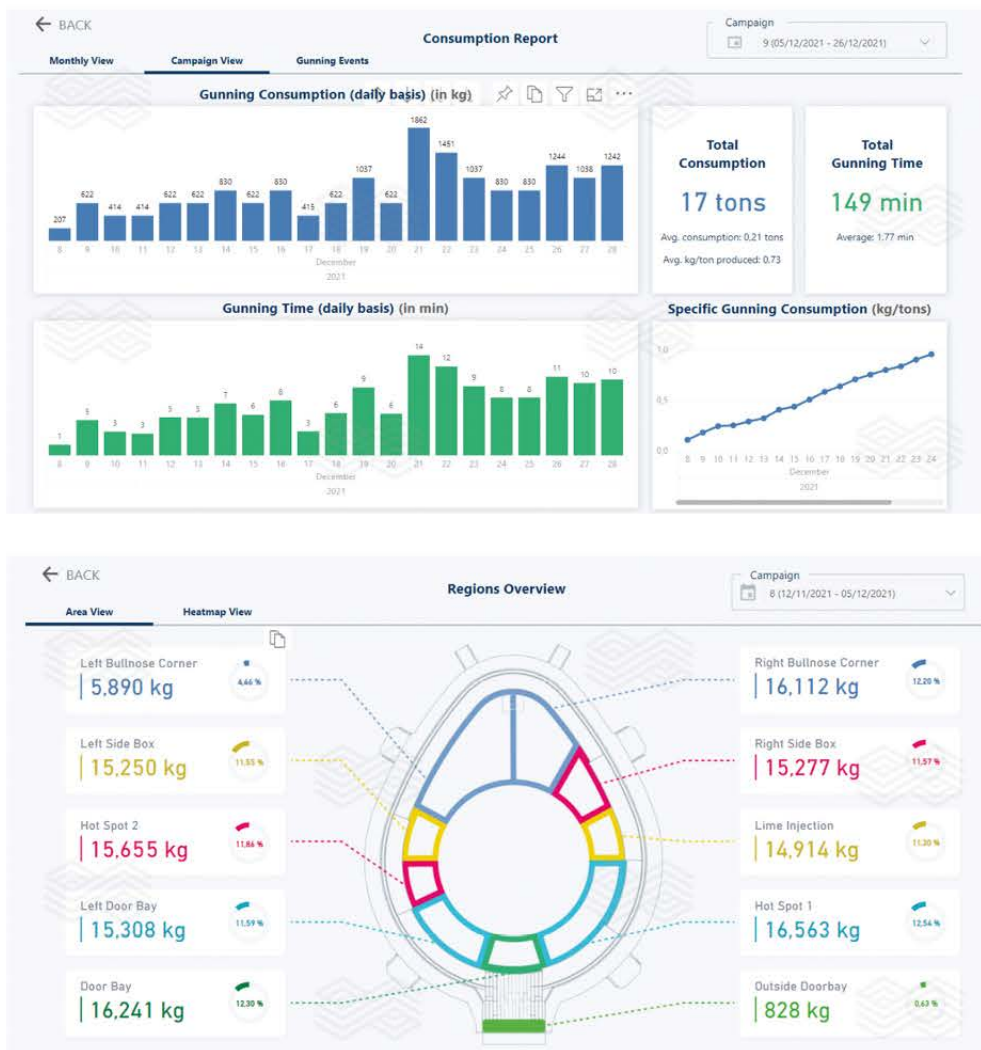




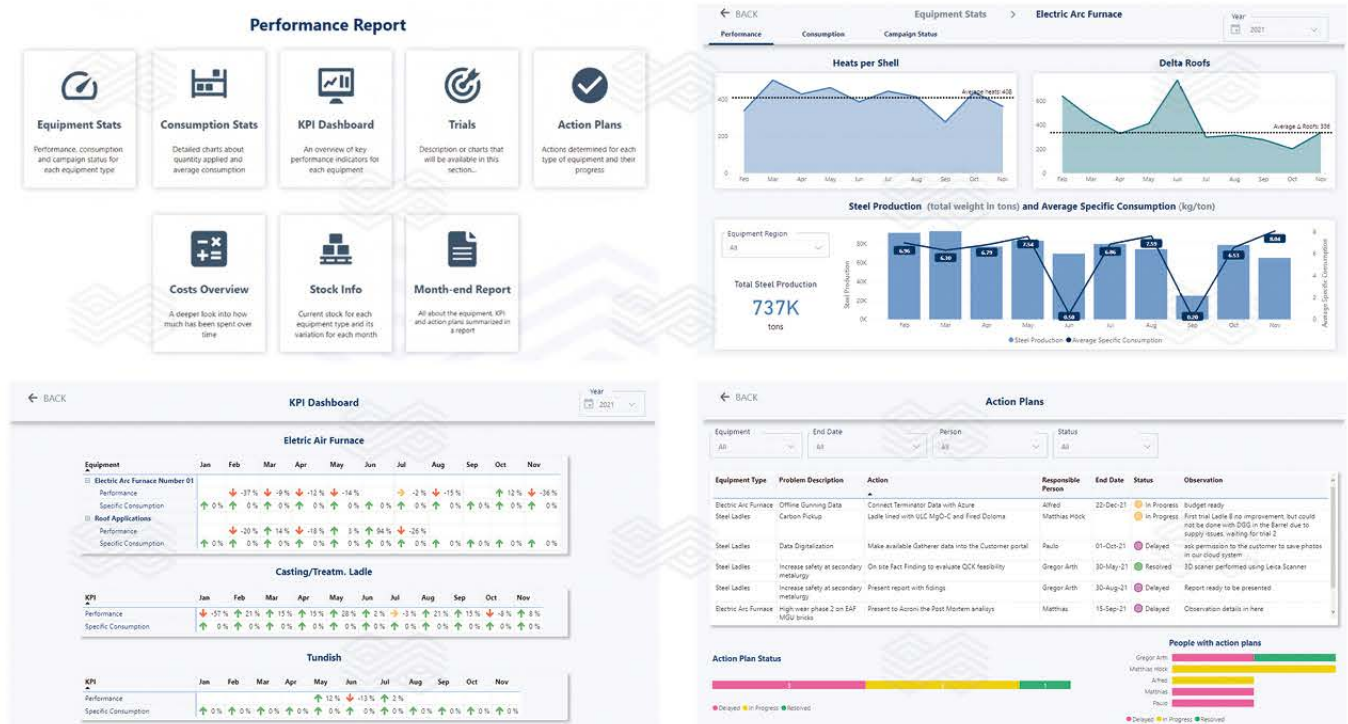
Figure 8 presents the refractory consumption and performance data available: From year-month, to a very specific region inside a specific ladle shell for a defined ladle campaign.

From one side RHI Magnesita provides in real time, online, and in a very transparent way big data analysis reports that cover the whole RHI Magnesita/customer network, while from the other side RHI Magnesita has a very strong onsite technical support team to make the best of it, using process improvement and problem-solving methodologies to build a 4 hands action plan to improve customer results.

### Conclusion

The next level of digital contracts provided by RHI Magnesita brings even more transparency to an already seamless relationship between a high-temperature solutions provider and steelmakers, increasing agility and automating processes, allowing both companies to make, more and more, data driven decisions for a more sustainable and efficient future.

**Figure 8.** Customer Portal refractory performance reports, KPIs, tracking, and action plan.



## References

- [1] <https://www.carlajohnson.co/why-b2b-suffers-from-marketing-myopia/>
- [2] Levitt, T. Marketing Myopia. *Harvard Business Review*. 1960, 38, 24–47.
- [3] <https://www.juniperresearch.com/whitepapers/industrial-revolution-4-the-future-of-iiot>
- [4] Landt, J. The history of RFID. *IEEE Potentials*. 2005, 24, 8–11.
- [5] Siew, N.L. *A Reliability Study of the RFID Technology. Thesis*. Naval Post Graduate School. Monterrey, California. 2006.
- [6] Viertauer, A., Mutsam, N., Pernkopf, F., Gantner, A., Grimm, G., Winkler, W., Rössler, R., Lammer, G., Ratz, A. and Persson, M. Refractory Lifetime Prognosis for RH Degassers. *Bulletin*. 2020, 36–41.
- [7] Souza, P., Oliveira, S., Almeida, E., Campos, M., de Paula, A., Hugo, T., Gomes, G., Lammer, G., Baitz, R. and Berganholi, J. Automated Process Optimization at the RH Degasser in Gerdau Ouro Branco—Results After 2 Years of Operation. *Bulletin*. 2021, 42–47.
- [8] Viertauer, A., Christmann, K., Schütz, J., Gruber, M., Spiess, B. and Bloemer, P. Efficient Hot Metal Desulphurization Ladle. *Bulletin*. 2019, 12–17.
- [9] Viertauer, A., Schacher, M., Ulitsky, S., Scheibmayr, M., Röllin, E., Ehrenguber, R., Stalzer, M., Dolzer, O., Staicu, T., Kollmann, T., Trummer, B., Orlov, A., Papushev, A., Razgulyaev, S., Kirschen, M. and Zhuravlev, S. Implementation of BOF Gas Purging Technology and Current Process Results After One-Year of Successful Operation at Severstal Cherepovets. *Bulletin*. 2021, 78–82.
- [10] Sarkar, A., Joshi, H., Schretter, A., Gutschier, G. and Mitterer, T. Efficient Value Added Steel Production with Low Mix Maintenance Level at JSW Steel in India. *Bulletin*. 2019, 30–33.
- [11] Lopez, F., Farrando, A., Disante, L. and Loeffelholz, M. Slag Modelling for Optimising the Use of Fluxes in a DRI Based Steelmaking Operation. *Bulletin*. 2019, 24–29.
- [12] Lopez, F., Souza, P., Garzon, de Souza, D. and Dettogne, R. Development and Application of a Slag Model for Increasing Ladle Life at Integrated Steel Mill – Brazil. *Bulletin*. 2018, 48–52.
- [13] Giacobbe, A., Tomas, M., Haynes, B., Spulin, K., Dudley, C., Lawrence, M., Kuehne, R. and Alloni, M. PROILTM: Value Innovation for Mid American Steel & Wire Inc. *Bulletin*. 2019, 34–38.
- [14] Amorim, L., Silva, C., Resende, A., Silva, I. and Oliveira, M. A Study of Internix in a Six-Strand Billet Caster. *Metallurgical and Materials Transactions A*. 2018, 49, 6308–6324.
- [15] Emadi, Y., D'Souza, J., Reiterer, R. and Sauer, G. Increased Electric Arc Furnace Availability at Qatar Steel Company Through the Fully Automatic TERMINATOR Gunning Robot. *RHI Bulletin*. 2008, 18–21.
- [16] <https://www.forbes.com/sites/theyec/2020/04/21/why-b2b-e-commerce-is-a-top-growth-sector-today/?sh=1da9ac0b3043>
- [17] <https://www.gartner.com/en/sales/insights/b2b-buying-journey>

## Authors

Paulo Souza, RHI Magnesita, Vienna, Austria.

Celso Freitas, RHI Magnesita, Vienna, Austria.

Gregor Arth, RHI Magnesita, Leoben, Austria.

Gustavo Penido, RHI Magnesita, Vienna, Austria.

Karl Zettl, RHI Magnesita, Vienna, Austria.

Jose Bolognani, RHI Magnesita, Vienna, Austria.

Carlos Lamare, RHI Magnesita, Rotterdam, Netherlands.

Gregor Lammer, RHI Magnesita, Vienna, Austria.

Gerry Moser, RHI Magnesita, Vienna, Austria.

Antonio Hoffert, Criptonomia, Belo Horizonte, Brazil.

**Corresponding author:** Paulo Souza, paulo.souza@rhimagnesita.com



Patrick Seitz, Daniel Lüftner, Raghunath Rana and Klaus Reinwald

# Material Characterisation and Product Analysis of Refractories Using X-Ray Computed Tomography and Radioscopy

X-ray analysis is a standard approach to investigate all kinds of materials and is well established for refractory analysis (e.g., X-ray diffraction, X-ray fluorescence, and X-ray adsorption). By collecting X-ray absorption images during the rotation of a sample, a three-dimensional (3D) density distribution can be obtained using X-ray computed tomography (CT), which offers the possibility to look inside a sample in 3D with a resolution down to the sub-micron range. In this article, the capabilities of the new CT system at RHI Magnesita’s Technology Center Leoben (Austria), which enables detailed information of the inner structure of a sample to be obtained, are demonstrated using investigations in the area of flow control products. In particular, the importance of the device for postmortem analyses is shown for a used submerged entry nozzle as well as a slide gate plate. A further application presented in the paper is where the CT data was used for product and process development, as well as the quality improvement of a thin slab submerged entry nozzle.

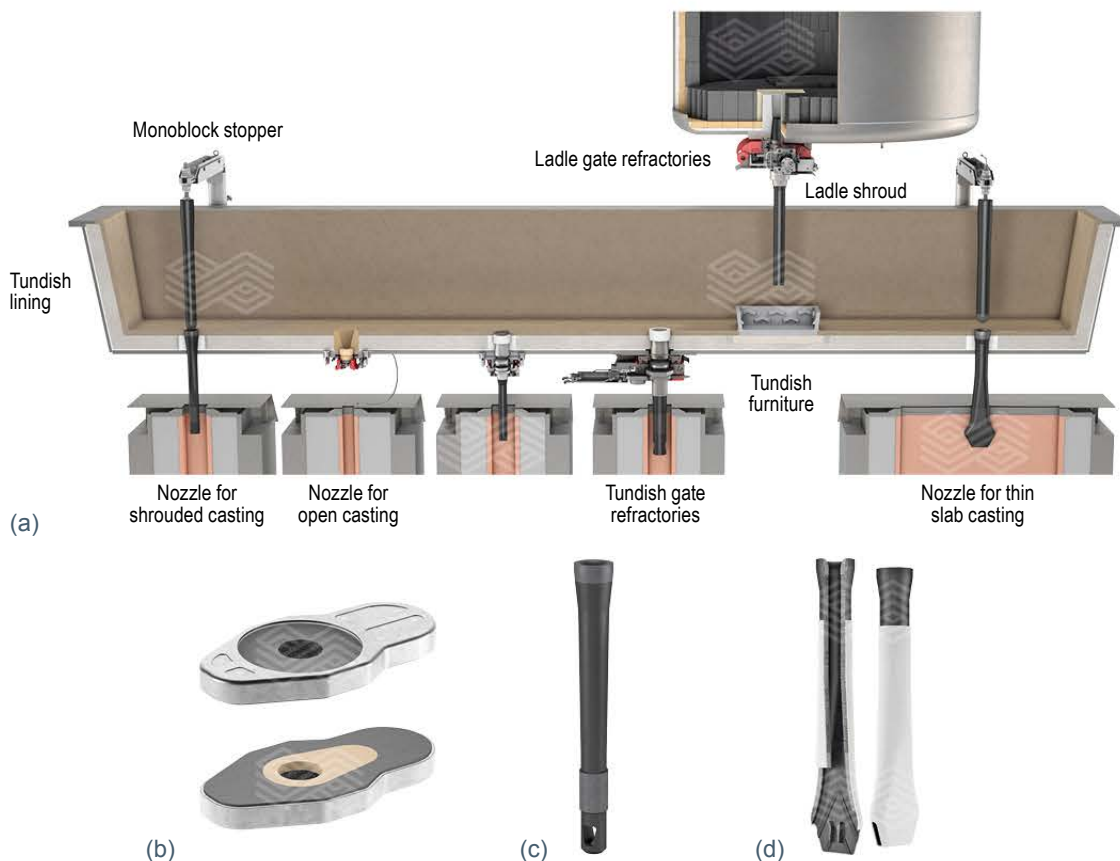
## Introduction

X-ray radioscopy is an indispensable tool for many industrial applications, especially in the field of quality control and has been in use at RHI Magnesita for many years. However, because it produces a two-dimensional (2D) representation of a three-dimensional (3D) object, it is often difficult to interpret [1]. In the last two decades the field of industrial computed tomography (CT) has been steadily increasing [2]. During an industrial CT scan several thousand X-ray

transmission measurements of a rotating object are performed and then this data is converted into a 3D representation of the object using various reconstruction algorithms. As such, the drawbacks of pure X-ray radioscopy can be overcome because firstly, CT provides a map of the radiation absorption coefficient (i.e., density) for each point in space. Secondly, the dimensions are absolute values and the 3D tomogram represents the real shape of the object [1]. Therefore, defects or flaws can be detected with high accuracy and their dimensions can be extracted.

Figure 1.

(a) refractories used for flow control in the steel continuous casting process from the ladle to mould, (b) slide gate plates, (c) submerged entry nozzle, and (d) thin slab submerged entry nozzle.



In this paper, the capability of CT in the world of refractories is demonstrated using various flow control product examples ranging from postmortem investigations of a submerged entry nozzle (SEN) and slide gate plate to the development and quality control of a 1500 mm long thin slab submerged entry nozzle (TS-SEN).

### Flow Control Products

In the area of flow control, products such as refractory slide gate plates, ladle shrouds, monoblock stoppers, and SENs are used in the continuous casting process to transfer molten steel from the ladle to the tundish and then into the mould (Figure 1) [3,4]. These products are used to regulate the steel flow and protect the molten metal stream from reoxidation. Due to their direct contact with the high-velocity liquid steel stream, they need to resist elevated temperatures, corrosive and abrasive attack by steel and slags, as well as high-temperature gradients during application.

To fulfil the rising customer demands (e.g., clean steel and anticlogging), these refractories are becoming more and more complex. Consequently, improving the product performance is challenging and time consuming. Hence, there is an increasing demand for innovative technologies to support product development in the flow control area. CT, which gives the opportunity to have a detailed look inside

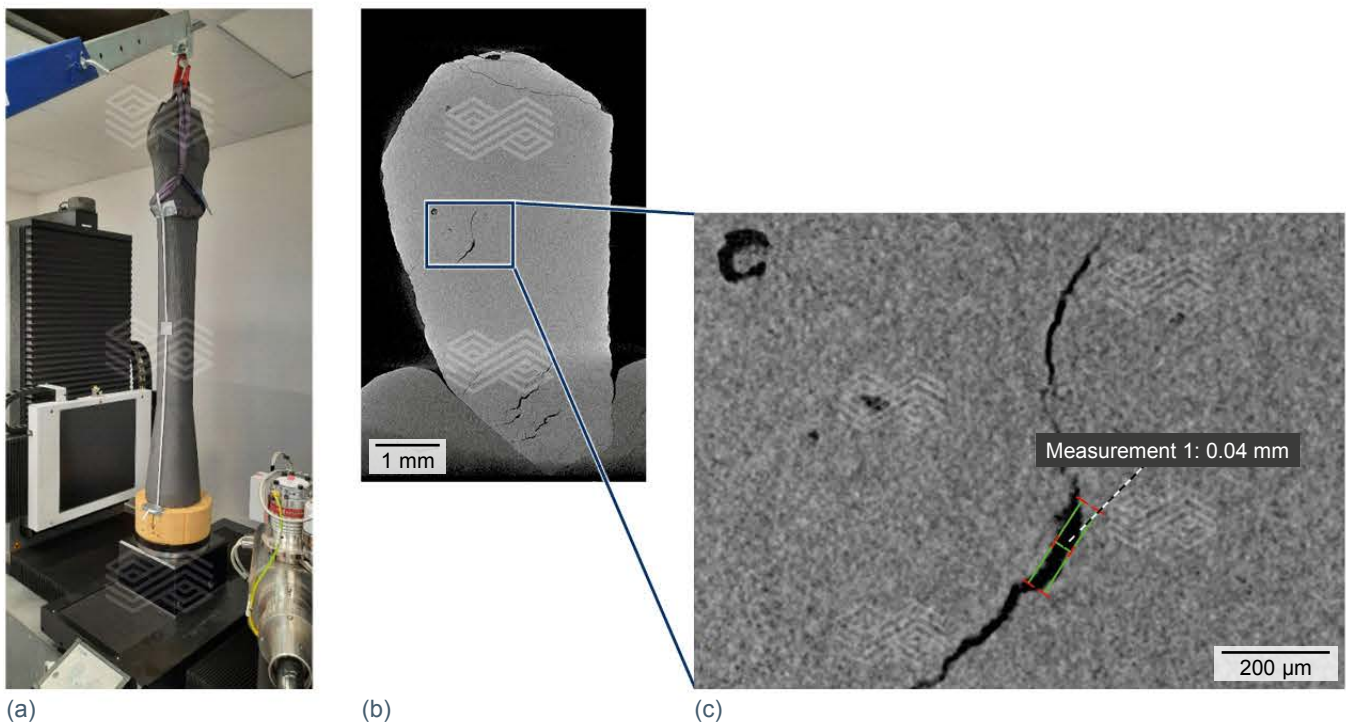
the full volume of an uncut product, enables fast optimisation of the manufacturing process, product design, as well as excellent quality control.

### New X-Ray Computed Tomography Device at the Technology Center Leoben

The new tailor-made CT device at RHI Magnesita's Technology Center Leoben (TCL) is depicted in Figure 2. It is a dual X-ray source device, equipped with a 225 kV direct beam and a 190 kV transmission beam source. While the former has a higher penetration depth and may be used for larger samples, the latter is limited in power but with a focus spot size in the sub-micron range, which enables high-resolution measurements of small samples. As an example, the result of scanning a single MgO grain is shown in Figure 2b, where the light colour corresponds to higher density material and the dark regions are low density areas. A voxel size resolution of approximately 2  $\mu\text{m}$  offers a precise determination of a crack's thickness (i.e., 40  $\mu\text{m}$  in this case) and length (Figure 2c). Furthermore, the system is comprised of a 3000 x 3000-pixel flat panel detector with a pixel pitch size of 150  $\mu\text{m}$ , a manipulator with seven independent axes of movement, a maximum focus detector distance of more than 1400 mm (necessary to achieve the geometrical magnification for high resolutions), and a vertical travel distance of the X-ray source and detector of about 800 mm.

**Figure 2.**

(a) TS-SEN standing upright on the system's rotating table and (b) vertical cut through the 3D CT data set of a single MgO grain with a detailed dimensional measurement of the crack (i.e., 40  $\mu\text{m}$ ).



## Application of X-Ray Scanning Technology

### Postmortem analyses

The first postmortem example described in this section is the analysis of a used SEN that showed rather high wear after use. A full 3D CT measurement of the piece was accomplished and an image of the sample surface is shown in Figure 3a. A slice through the 3D data at the position indicated by the red line in Figure 3a is depicted in Figure 3b. The slag band area, which has a high amount of  $ZrO_2$  and therefore a higher density, was easily identified at the bottom of the sample. In addition, the following conspicuous regions were observed in the data.

Inside the bore remaining droplets of steel could be detected (whitish because of their high density). Furthermore, changes to the body material above the slag band during operation of the product were also identified. Firstly, local densification of the product due to steel and/or slag infiltrating pores was observed in the CT measurements, with the infiltrations leading to a brighter colour that can be seen in the regions indicated with a green arrow (see Figure 3b). Secondly, at the elevated temperatures during casting,

oxidation (i.e., decarburisation) of the body material can occur that locally lowers the density and therefore appears darker in the CT data. In this case, it was evident that a large part of the sample above the infiltrations had undergone oxidation. Thirdly, and most importantly, the nozzle was affected by chemical attack from the mould powder above the meniscus, which caused material wear. The wear is clearly visible in Figure 3c, where the red-purple horizontal lines show deviation of the surface of the used SEN from the CAD drawing of an unused product. It can be concluded from the CT images that the root cause of the high product wear was a too deep immersion of the product during casting and/or an insufficiently long slag band.

For certain flow control products a 3D CT measurement may not be applicable, for example in the case of slide gate plates. This is primarily due to the aspect ratio of the piece as well as the metal can covering a proportion of the refractory surface. However, the CT device at TCL can also be used to perform 2D radioscopy measurements and this was the approach used in the following postmortem investigation. In this example, a slide gate plate showed cracks on its surface after application (Figure 4a). The

**Figure 3.**

(a) 3D view of the SEN surface obtained by CT, (b) vertical cut through the SEN CT data, and (c) difference between the used SEN's surface and the CAD drawing of the product. The inner bore profile of the used SEN is indicated in green.

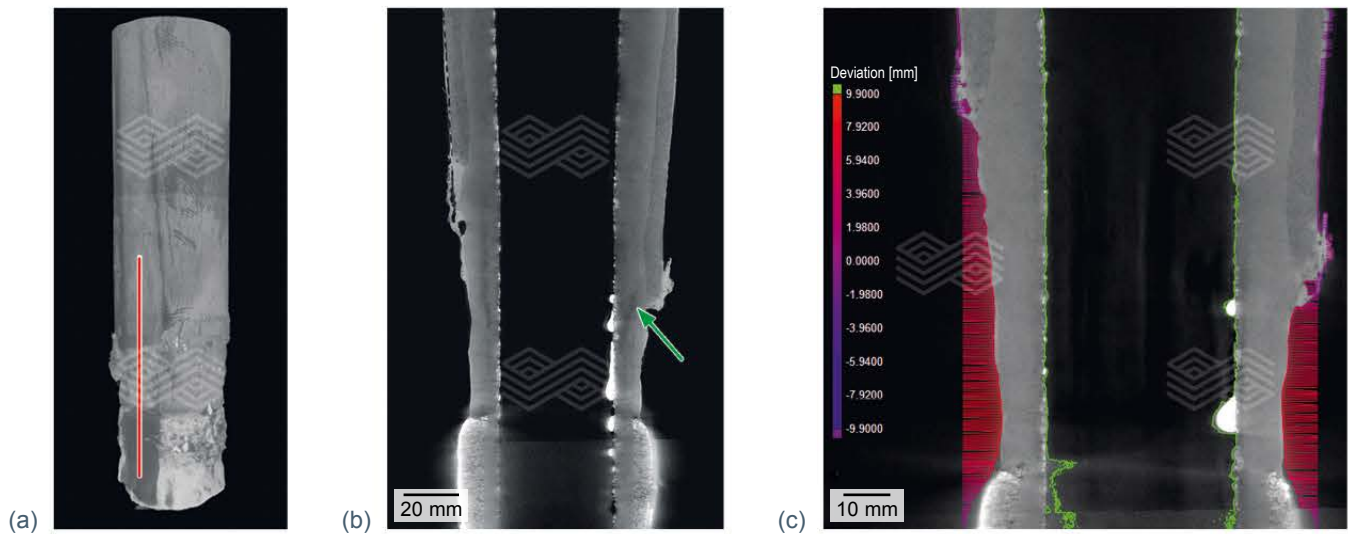
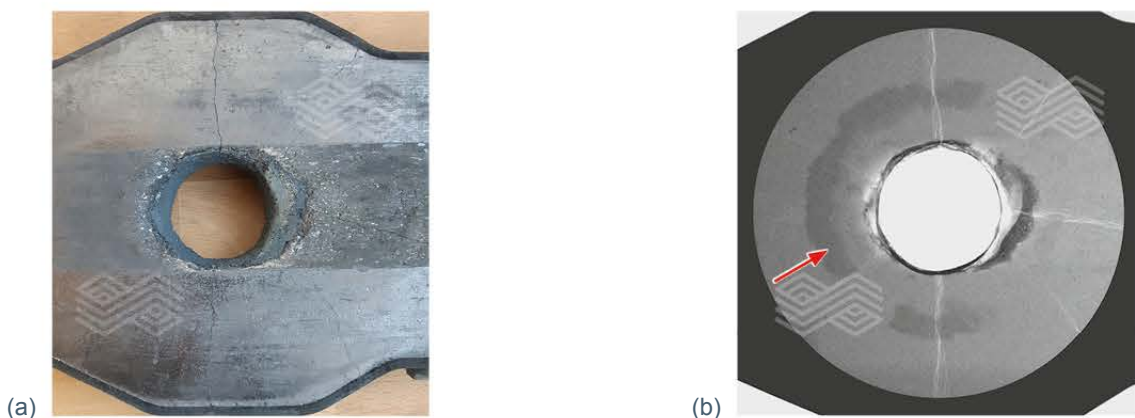


**Figure 4.**

(a) image of the used slide plate and (b) 2D radioscopy measurement of the corresponding slide gate plate.



question in this case was whether the cracks occurred during cool down or if they had formed at an earlier stage during application. The 2D radiography image of the used slide gate plate is shown in Figure 4b. It should be noted that the radiography images directly show the information from the detector, meaning that light grey values correspond to a high radiation intensity and hence a low linear absorption, while dark values indicate a higher density/thickness. Thus, the black area surrounding the grey circle is the steel jacket around the slide plate and the bore hole appears white. The cracks can be seen as white lines radiating from the bore hole. Because there are no visible steel infiltrations, which would have appeared dark, it can be concluded that the cracks formed during cool down of the product due to thermal shrinkage of the material. The darker areas indicated by the red arrow are due to the remaining mortar located on the backside of the plate.

In addition to these examples, the CT equipment has been pivotal for the postmortem analysis of many other flow control products such as monoblock stoppers and ladle shrouds. Furthermore, if the root cause of a sample failure cannot be determined directly from the CT scan, the images can be used to identify the ideal location for sampling so that further analyses can be performed, such as microscopic investigations.

### Product development and process improvement

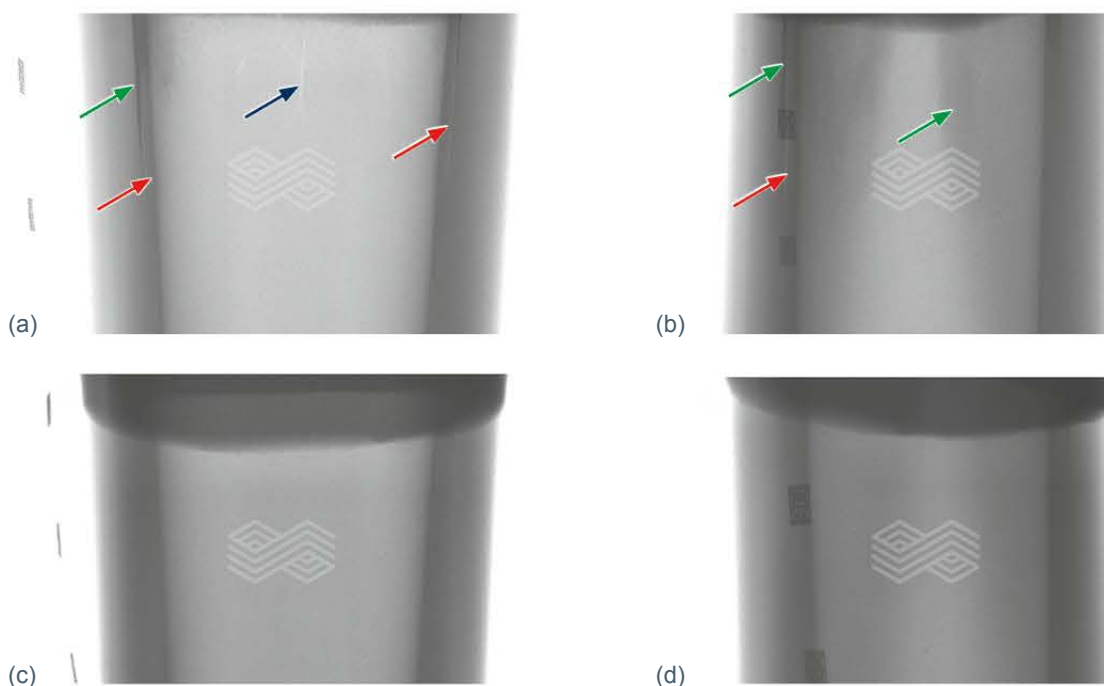
Another important application for the CT technology is supporting new product developments or improving existing ones. This is particularly important for flow control products with an elaborate design, consisting of multiple different materials, and/or a complex shape and therefore requiring an expensive production process. One example for which these criteria hold true are TS-SENS, which are used for thin

slab casting where a well-controlled steel flow from the tundish to the mould is essential. The image of a typical TS-SEN can be seen in Figure 1. For this case, the potential of CT lies in a fast analysis of any change in the production process and/or material recipe for the whole volume of a piece in a nondestructive way. This enables a direct link to be established between implemented changes and their effect on the product in terms of defects or imperfections. As such the CT can significantly reduce the development time for this kind of product in the prototype stage.

The following is an example of how the CT equipment was used to expedite the development of a TS-SEN design. Due to the large size of the TS-SEN, a full 3D CT scan of the whole volume would have been more time consuming and expensive compared to a 2D scan. Therefore, this example also demonstrates how in many cases a 2D scan is sufficient for a proportion of the analysis and only the most critical parts, namely the slag band and port area are 3D scanned. Because of the TS-SEN's rotational symmetry along a high proportion of the shape, it was sufficient to measure these sections three times in 2D with a 60° rotation selected between each image. Thereby any defect could be detected in the entire sample volume. The results of such investigations are depicted in Figure 5. The images show the interface between the high-density slag band (upper dark grey region clearly visible in Figure 5c and 5d) and the lower density body material (light grey). The dark dashes on the left-hand side of the samples in Figures 5a and 5c derive from a lead ruler and were used as reference points for measurements. While in Figures 5a and 5b, several anomalies can be recognised, Figures 5c and 5d show the evolution to a flawless TS-SEN after several improvement measures were implemented. The sample in Figure 5b is rotated by 60° compared to Figure 5a and while there is a crack clearly visible in the centre of the piece in Figure 5a

**Figure 5.**

2D radiography images of two TS-SENS before and after production improvements were implemented. (a) TS-SEN with anomalies, (b) TS-SEN with anomalies, rotated by 60°, (c) TS-SEN with flawless slag band/body material interface, and (d) TS-SEN with flawless slag band/body material interface, rotated by 60°.



(blue arrow) this crack cannot be identified in Figure 5b, thereby indicating the importance of 2D measurements in various orientations. In addition, a dark vertical line is visible on the left-hand side of Figure 5a and 5b (green arrows). This was due to contamination of the body material by the zirconia slag band located above, which occurred during the production process. In the image of the rotated TS-SEN, the slag band material can also be identified as a dark veil (green arrow in the centre of Figure 5b). Finally, a delamination of the body material could be recognised as vertical light lines (red arrows).

The remaining TS-SEN volume, namely a proportion of the slag band region and the nozzle outlet, was investigated using 3D CT measurements and a number of anomalies were identified that occurred while trying new production routes or recipe alternatives. For example, Figure 6a shows the outcome of a new production approach that led to scratches and zirconia contamination at the outlet and Figure 6b depicts the results of a trial where significant intermixing of the slag band and body material occurred. Only with the fast and direct feedback from the CT measurements could such trials be done efficiently and economically. The images in Figure 6c, which show vertical cuts in three orientations (i.e., top, front, and side view), demonstrate two more imperfections. Firstly, there are white lines which are, as already discussed above for the 2D

measurements, due to the zirconia material migrating down from the slag band area. This indicates an improper filling of both the alumina graphite and zirconia graphite materials. Secondly, a crack is visible in all three Figure 6c images, which can be identified from the typical nonlinear shape and the sharp contrast to the surrounding material. Based on these results the necessary improvements were made.

## Conclusions

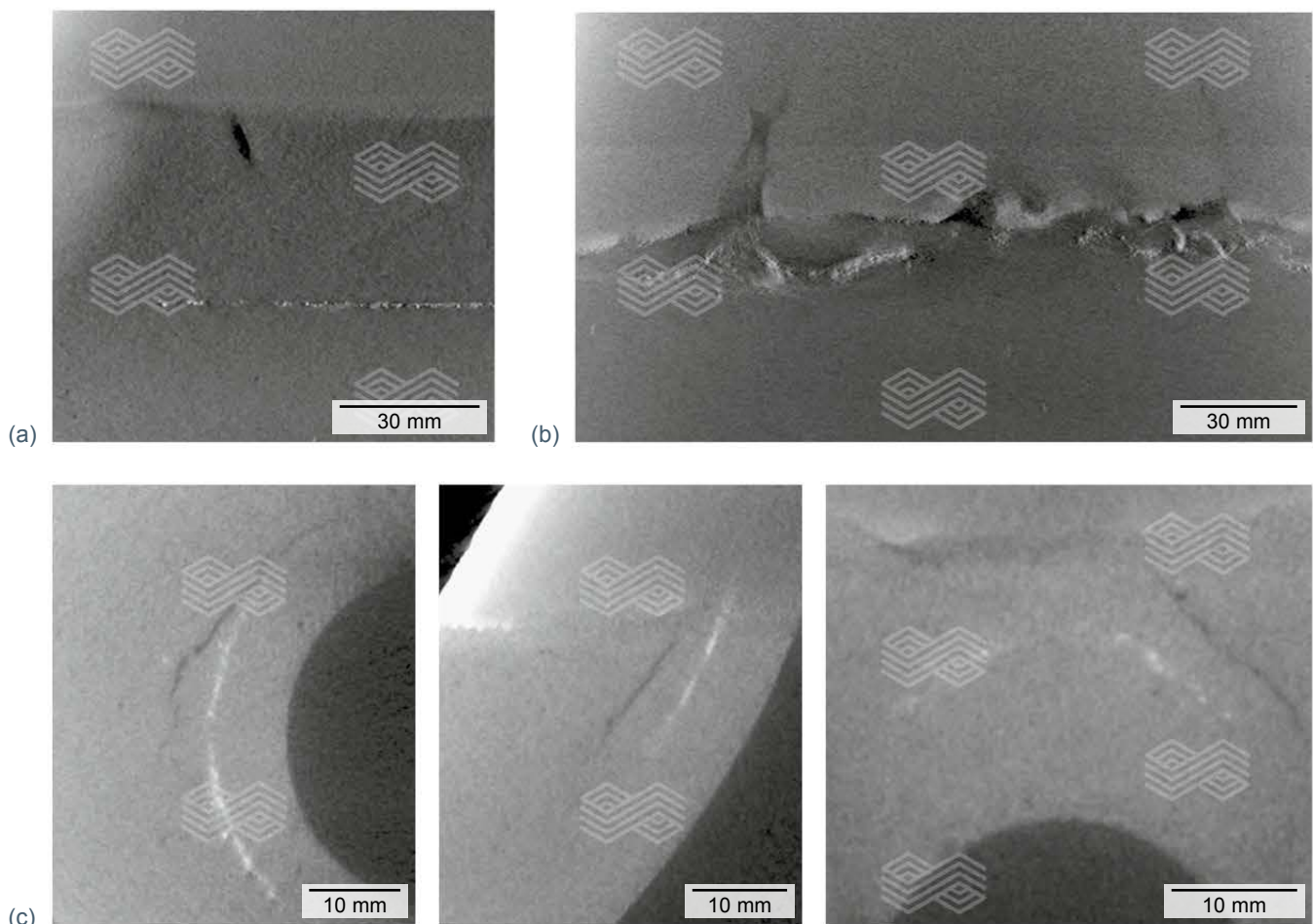
In conclusion, with the possibility to get a rapid and complete picture of a sample's inner structure, ranging from a single grain to the full dimensions of a complex product in a nondestructive way, CT is an indispensable tool for refractory investigations. In this article the following uses of an industrial CT system were discussed:

- Raw material characterisation.
- Postmortem analysis.
- Dimensional measurement/wear measurement.
- Quality control.
- Process optimisation.
- Product development.

Besides these applications, there are several other possibilities for the CT system within the world of refractories. Among them are 3D microstructure

**Figure 6.**

**Compilation of anomalies found in TS-SENs. The images show vertical and horizontal cuts through the 3D CT data. (a) scratch on the inner surface and zirconia contamination at the outlet, (b) intermixing of slag band and body material, and (c) crack close to the slag band material in three orientations (top, front, and side view) and zirconia material migration (white).**



characterisation, for example the geometric and size distribution of pores or inclusions (i.e., material characterisation), use as a reference method for other nondestructive testing methods, and generating input data for subsequent mechanical or thermomechanical simulations such as finite element method and discrete element method. In the future, it is planned to perform in-situ measurements at elevated temperatures or with applied stresses. Finally, it can be concluded that the new X-ray equipment significantly supports refractory developments, especially in the area of flow control. It has become a key technology for detecting all kinds of anomalies and leads to a better understanding of their origin, thereby increasing the product and process quality and hence refractory performance.

## References

- [1] Carmingnato, S., Dewulf, W. and Leach, R. *Industrial X-Ray Computed Tomography*; Springer International Publishing AG: Switzerland, 2018.
- [2] De Chiffre, L., Carmingnato, S., Kruth, J.P., Schmitt, R. and Weckermann, A. Industrial Applications of Computed Tomography. *CIRP Annals-Manufacturing Technology*. 2014, 63(2), 655–677.
- [3] Routschka, G. and Wuthnow, H. *Praxishandbuch Feuerfeste Werkstoffe (5. Auflage)*; Vulkan-Verlag GmbH: Germany, 2011.
- [4] Hackl, G., Nitzl, G., Tang, Y., Eglsäer, C. and Chalmers, D. Innovative Flow Control Refractory Products for the Continuous Casting Process. *AISTech 2015 Proceedings*, Cleveland, USA, 4–7 May, 2015; pp. 2436–2442.

## Authors

Patrick Seitz, RHI Magnesita, Leoben, Austria.

Daniel Lüftner, RHI Magnesita, Leoben, Austria.

Raghunath Rana, RHI Magnesita, Leoben, Austria.

Klaus Reinwald, RHI Magnesita, Leoben, Austria.

**Corresponding author:** Patrick Seitz, patrick-paul.seitz@rhimagnesita.com



# bulletin

2022

**Copyright notice:**

The texts, photographs and graphic design contained in this publication are protected by copyright. Unless indicated otherwise, the related rights of use, especially the rights of reproduction, dissemination, provision and editing, are held exclusively by RHI Magnesita N.V. Usage of this publication shall only be permitted for personal information purposes. Any type of use going beyond that, especially reproduction, editing, other usage or commercial use is subject to explicit prior written approval by RHI Magnesita N.V.

